Revision 2, July 2004

NATIONAL ENRICHMENT FACILITY

SAFETY ANALYSIS REPORT

TABLE OF CONTENTS

Page

3.2 SITE DESCRIPTION 3.2-1

3.2.1 Site Geography 3.2-1
3.2.1.1 Site Location 3.2-1
3.2.1.2 Public Roads and Transportation 3.2-2
3.2.1.3 Nearby Bodies of Water 3.2-3
3.2.2 Demographics and Land Use 3.2-3
3.2.2.1 Population Information 3.2-3
3.2.2.2 Population Centers 3.2-4
3.2.2.3 Public Service Facilities 3.2-5
3.2.2.4 Industrial Areas 3.2-6
3.2.2.5 Land Use 3.2-7
3.2.2.6 Water Use 3.2-7
3.2.3 Meteorology 3.2-8
3.2.3.1 Local Wind Patterns and Average and Maximum Wind Speeds 3.2-9
3.2.3.2 Annual Amounts and Forms of Precipitation 3.2-10
3.2.3.3 Design Basis Values for Snow or Ice Load 3.2-10
3.2.3.4 Type, Frequency, and Magnitude of Severe Weather 3.2-11
3.2.4 Hydrology 3.2-13
3.2.4.1 Surface Hydrology 3.2-14
3.2.4.2 Major Surface and Subsurface Hydrological Systems 3.2-14
3.2.4.3 Floods 3.2-16
3.2.4.4 Groundwater Hydrology 3.2-16
3.2.4.5 Groundwater Chemistry 3.2-18
3.2.5 Geology 3.2-18
3.2.5.1 Regional Geology 3.2-18
3.2.5.2 Site Geology 3.2-20
3.2.5.3 Geotechnical Investigations 3.2-22
3.2.6 Seismology 3.2-23
3.2.6.1 Seismic History of the Region and Vicinity 3.2-23
3.2.6.2 Correlation of Seismicity with Tectonic Features 3.2-25
3.2.6.3 Earthquake Recurrence Models 3.2-26
3.2.6.4 Probabilistic Seismic Hazard Analysis 3.2-27
3.2.6.5 Selection of the Design Basis Earthquake 3.2-30
3.2.7 Stability of Subsurface Materials 3.2-32
3.2.7.1 Liquefaction Susceptibility 3.2-33
3.2.8 References 3.2-35

LIST OF TABLES

Table 3.2-1 Population and Population Projections, 1970-2040
Table 3.2-2 Educational Facilities Near the Site
Table 3.2-3 Land Use Within 8 km (5 mi) of the Site
Table 3.2-4 Agriculture Census, Crop, and Livestock Information
Table 3.2-5 Midland-Odessa, Texas, Wind Data
Table 3.2-6 Roswell, New Mexico, Wind Data
Table 3.2-7 Midland-Odessa Five Year (1987-1991) Annual Joint Frequency Distribution For All Stability Classes Combined
Table 3.2-8 Midland-Odessa Five Year (1987-1991) Annual Joint Frequency Distribution Stability Class A
Table 3.2-9 Midland-Odessa Five Year (1987-1991) Annual Joint Frequency Distribution Stability Class B
Table 3.2-10 Midland-Odessa Five Year (1987-1991) Annual Joint Frequency Distribution Stability Class C
Table 3.2-11 Midland-Odessa Five Year (1987-1991) Annual Joint Frequency Distribution Stability Class D
Table 3.2-12 Midland-Odessa Five Year (1987-1991) Annual Joint Frequency Distribution Stability Class E
Table 3.2-13 Midland-Odessa Five Year (1987-1991) Annual Joint Frequency Distribution Stability Class F
Table 3.2-14 Hobbs, New Mexico, Precipitation Data
Table 3.2-15 Midland-Odessa, Texas, Precipitation Data
Table 3.2-16 Roswell, New Mexico, Precipitation Data
Table 3.2-17 Midland-Odessa, Texas, Snowfall Data
Table 3.2-18 Roswell, New Mexico, Snowfall Data
Table 3.2-19 Straight Wind Hazard Assessment
Table 3.2-20 Location of Recorded Earthquakes Within a 322 km (200 mi) Radius of the NEF Site
Table 3.2-21 Earthquakes of Magnitude 3.0 and Greater Within 322 km (200 mi) Radius of the NEF Site
Table 3.2-22 Earthquake Data Sources for New Mexico and West Texas
Table 3.2-23 Modified Mercalli Intensity Scale
Table 3.2-24 Comparison of Parameters for the January 2, 1992 Eunice, New Mexico Earthquake
Table 3.2-25 Earthquake Recurrence Models for the NEF Site Region
Table 3.2-26 Earthquake Recurrence Models for the Central Basin Platform (CBP)in the Waste Isolation Pilot Project (WIPP) Safety Analysis Report (SAR)
Table 3.2-27 Attenuation Model Formulas and Coefficients
Table 3.2-28 Seismic Hazard Results at NEF Site From Rio Grande Rift Seismic Source Zones

LIST OF TABLES

Table 3.2-29 Seismic Hazard Results at NEF Site From Local Source Zones
Table 3.2-30 Peak Acceleration Seismic Hazard Summary for the NEF Site
Table 3.2-31 Regulatory Guide 1.60 Ratio of Vertical to Horizontal Component Design Response Spectra
Table 3.2-32 Horizontal Response Spectrum for the 10,000-Year Design Earthquake
Table 3.2-33 Vertical Response Spectrum for the 10,000-Year Design Earthquake

LIST OF FIGURES

Figure 3.2-1 County Map
Figure 3.2-2 Plot Plan (1 Mile Radius)
Figure 3.2-3 Site Plan
Figure 3.2-4 Average Lightning Flash Density
Figure 3.2-5 Site Boring Plan and Profile
Figure 3.2-6 Water and Oil Wells in the Vicinity of the NEF Site
Figure 3.2-7 Permian Basin Geologic Structures and Profile
Figure 3.2-8 Site Topography
Figure 3.2-9 Surficial Geologic Map of the NEF Site Area
Figure 3.2-10 Soil Test Boring Record B-1
Figure 3.2-11 Soil Test Boring Record B-2
Figure 3.2-12 Soil Test Boring Record B-3, Sheet 1
Figure 3.2-12 Soil Test Boring Record B-3, Sheet 2
Figure 3.2-12 Soil Test Boring Record B-3, Sheet 3
Figure 3.2-13 Soil Test Boring Record B-4
Figure 3.2-14 Soil Test Boring Record B-5
Figure 3.2-15 Soil Test Boring Key to Symbols and Descriptions
Figure 3.2-16 Site Soils Map
Figure 3.2-17 Tectonic Subdivisions of the Permian Basin
Figure 3.2-18 Seismicity Map for 322 Kilometers (200Mile) Radius of the NEF Site
Figure 3.2-19 Seismicity in the Immediate Vicinity of the NEF Site
Figure 3.2-20 Regional Seismicity and Tectonic Elements of the Permian Basin
Figure 3.2-21 Earthquake Frequency Contours and Tectonic Elements of the Permian Basin
Figure 3.2-22 Seismic Source Areas for Earthquake Frequency Statistical Analyses
Figure 3.2-23 Earthquake Recurrence Models for the 322 km (200-mile) Radius Composite Catalog
Figure 3.2-24 Earthquake Recurrence Models for Region 1 –(161 km (100mile) Radius of the NEF Site)
Figure 3.2-25 Earthquake Recurrence Models for Region 2 (CBP Higher Density Earthquake Cluster)
Figure 3.2-26 Alternate Seismic Source Geometries Used in the WIPP Seismic Hazard Study
Figure 3.2-27 Comparison of PGA Attenuation for a Magnitude 5.0 Earthquake
Figure 3.2-28 Seismic Hazard at the NEF Site From Rio Grande Rift Seismic Sources
Figure 3.2-29 Seismic Hazard at the NEF Site From Local Seismic Source Zones
Figure 3.2-30 Zoom of Seismic Hazard at the NEF Site From Local Seismic Source Zones
Figure 3.2-31 Horizontal Response Spectra for the 10,000-Year Earthquake Bedrock and Soil Class C for the NEF Site
Figure 3.2-32 Horizontal and Vertical Response Spectra for the 10,000-Year Earthquake Soil Class C for the NEF Site

LIST OF FIGURES

Figure 3.2-33 Quaternary Faults in New Mexico
Figure 3.2-34 Quaternary Faults in Texas
Figure 3.2-35 Quaternary Faults within 322 km (200 mi) of NEF Site
Figure 3.2-36 Locations of Nearest Faults to the NEF Site

3.2 SITE DESCRIPTION

This section provides an overall description of the National Enrichment Facility (NEF) site and its environment, including regional and local geography, demography, meteorology, hydrology, geology, seismology, and stability of subsurface materials. Significant portions of the information presented in this section were derived from the NEF Environmental Report (LES, 2003).

This section also provides a characterization of natural phenomena (e.g., tornadoes, hurricanes, floods, and earthquakes) and other external events (e.g., explosions and aircraft crashes) in sufficient detail to assess their impact on facility safety and to assess their likelihood of occurrence.

3.2.1 Site Geography

Site features are well suited for the location of an uranium enrichment facility as evidenced by favorable conditions of hydrology, geology, seismology and meteorology as well as good transportation routes for distributing feed and product by truck.

3.2.1.1 Site Location

The proposed NEF site is located in Southeastern New Mexico near the New Mexico/Texas state line, in Lea County. This location is about 8 km (5 mi) east of Eunice and about 32 km (20 mi) south of Hobbs. The site comprises about 220 ha (543 acres) and is within county Section 32, Township 21 South, Range 38 East. The approximate center of the NEF is at latitude 32 degrees, 26 min, 1.74 sec North and longitude 103 degrees, 4 min, 43.47 sec West (see Figure 3.2-1, County Map).

Section 32 is currently owned by the State of New Mexico. The State of New Mexico has granted a 35 year easement to LES for site access and control.

The NEF site is relatively flat with slight undulations in elevation ranging from 1,033 to 1,045 m (3,390 to 3,430 ft) above mean sea level. The overall slope direction is to the southwest. Except for a gravel covered road which bisects the east and west halves of Section 32, the property is undeveloped and utilized for domestic livestock grazing (see Figure 3.2-2, Plot Plan).

Figure 3.2-3, Site Plan, shows the site property boundary and the general layout of the buildings.

3.2.1.2 Public Roads and Transportation

3.2.1.2.1 Public Roads

The site lies along the north side of New Mexico Highway 234. New Mexico Highway 234 intersects New Mexico Highway 18 about 4 km (2.5 mi) to the west. (See Figure 3.2-1). To the north, U.S. Highway 62/180 intersects New Mexico Highway 18 providing access from the city of Hobbs south to New Mexico Highway 234. To the east in Texas, U.S. Highway 385 intersects Texas Highway 176 providing access from the town of Andrews west to New Mexico Highway 234. To the south in Texas, Interstate 20 intersects Texas Highway 18 which becomes New Mexico Highway 18. West of the site, New Mexico Highway 8 provides access from the city of Eunice east to New Mexico Highway 234.

Potential adverse impact to NEF from chemical releases or explosions from trucks on nearby highways was evaluated. Due to the distance of the highway from the facility boundary, a chemical release from a passing vehicle will not have a safety impact on facility operations. Detailed probabilistic analyses show the annual probability of an explosion adversely impacting the plant is less than 1.0 E-5 per year.

3.2.1.2.2 Railroads

The nearest active rail transportation (the Texas-New Mexico Railroad) is in Eunice, New Mexico to the west about 5.8 km (3.6 mi) from the site. This rail line is used mainly by the local oil and gas industry for freight transport. There is also a rail spur to the Waste Control Specialists (WCS) facility along the northern boundary of the NEF site about 1 km (0.5 mi) from the Separations Building. This spur does not transport explosive materials or chemical shipments which could have a safety impact on facility operations. As such, there is no railroad traffic within proximity to the facility which poses a safety concern.

3.2.1.2.3 Water Transportation

There are no navigable waterways in the vicinity of the site.

3.2.1.2.4 Air Transportation

The nearest airport facilities are located just west of Eunice and are maintained by Lea County. The airport is about 16 km (10 mi) west of the proposed NEF and consists of two runways measuring about 1,000 m (3,280 ft) and 780 m (2,550 ft) each. Privately owned planes are the primary users of the airport. There is no control tower and no commercial air carrier flights (DOT, 2003). The nearest major commercial carrier airport is Lea County Regional Airport in Hobbs, New Mexico, about 32 km (20 mi) north.

An aircraft hazard analysis has been performed for the facility site, following the methodology of NUREG-0800 (NRC, 1981). Airports and airways in the vicinity of the site have been identified. Based on the published number of operations and distance to the proposed site, it is concluded that the presence of these airports does not pose any risk to the site with regard to aircraft hazard. For the identified airways, the probability of aircraft along these airways crashing onto the proposed site has been conservatively calculated to be less than 1.0 E-6 per year.

3.2.1.3 Nearby Bodies of Water

The climate in southeast New Mexico is semi-arid. Average precipitation at the site is calculated to be 33 to 38 cm (13 to 15 in) per year. Evaporation and transpiration rates are high. This results in minimal, if any, surface water occurrence.

The NEF site contains no surface drainage features. The site topography is relatively flat. Some localized depressions exist due to eolian processes, but the size of these features is too small to be of significance with respect to surface water collection.

The closest water conveyance is Monument Draw, a typically dry, intermittent stream located several miles west of the site.

Baker Spring, an intermittent surface water feature, is situated a little over 1.6 km (1 mi) northeast of the NEF site.

There are also three “produced water” lagoons for industrial purposes on the adjacent quarry property to the north.

There is also a manmade pond at the Eunice golf course approximately 15 km (9.5 mi) west of the site.

3.2.2 Demographics and Land Use

This section provides the census results for the site area, specific information about nearby population areas with respect to proximity to the site, specific information about nearby public facilities (schools, hospitals, parks, etc.) with respect to proximity to the site, and land and water use near the site.

3.2.2.1 Population Information

This section describes the population characteristics of the two-county areas around the NEF site.

3.2.2.1.1 Permanent Population and Distribution

The combined population of the two counties in the NEF vicinity, based on the 2000 U.S. Census is 68,515, which represents a 2.3% decrease over the 1990 population of 70,130 (Table 3.2-1, Population and Population Projections, 1970-2040). This rate of decrease is counter to the trends for the states of New Mexico and Texas, which had population increases of 20.1% and 22.8%, respectively during the same decade. Over that 10 year period, Lea County, New Mexico, where the site is located, had a growth decrease of 0.5% and the Andrews County, Texas decrease was 9.3%. Lea County experienced a sharp but short population increase in the mid-1980’s due to petroleum industry jobs. The change in the job market caused the population in Lea County to increase to over 65,000 during that period.

Based on projections made using historic data (Table 3.2-1), Lea County, New Mexico and Andrews County, Texas are likely to grow more slowly than their respective states over the next 30 years (the expected licensed period for the NEF).

Lea County covers 11,378 km^2 (4,393 mi^2) or approximately 1,142,238 ha (2,822,522 acres) which is three times the size of Rhode Island and only slightly smaller than Connecticut. The

county population density is 16% lower than the New Mexico state average (4.8 versus 5.8 people per square kilometer (12.6 versus 15.0 people per square mile)). The county housing density is 20% lower than the New Mexico state average (2.0 versus 2.5 housing units per square kilometer (5.3 versus 6.4 housing units per square mile)).

Andrews County covers 3,895 km^2 (1,504 mi^2). The county population density is 11% of the Texas state average (3.3 versus 30.6 per square kilometer (8.7 versus 79.6 population density per square mile)). The county housing density is low, at just over 11% of the Texas state average (1.4 versus 12.0 housing units per square kilometer (3.6 versus 31.2 housing units per square mile)).

3.2.2.1.2 Industrial Population

More than 98% of the area within an 8 km (5 mi) radius of the NEF is an extensive area of open land on which livestock wander and graze. Gas and oil field operations are widespread in the area, but significant petroleum potential is absent within at least 5 to 8 km (3 to 5 mi) of the site. Industrial operations near the site include:

- A quarry, operated by Wallach Concrete, Inc., and several oil recovery sludge ponds owned by the Sundance Services are located north of the site. The quarry owner leases land space to a “produced water” reclamation company that maintains three small “produced water” lagoons. Eight people are employed at the Wallach Concrete Quarry and nine people are employed by Sundance Services.
- Lea County operates a landfill on the south side of New Mexico State Highway 234, approximately 1 km (0.6 mi) from the center of Section 32. Four people are employed at the Lea County landfill.
- A vacant parcel of land is immediately east of the site. Land further east approximately 1.6 km (1 mi), in Texas, is occupied by Waste Control Specialists (WCS), LLC. WCS possesses a radioactive materials license from Texas, an NRC Agreement state. WCS is licensed to treat and temporarily store low-level and mixed low-level radioactive waste. WCS is also permitted to treat and dispose of hazardous toxic waste in a landfill. WCS employs 72 people.
- Dynegy’s Midstream Services Plant is located 6 km (4 mi) from the site. This facility is engaged in the gathering and processing of natural gas. The Dynegy Midstream Services Plant employs 40 people.

3.2.2.2 Population Centers

The proposed NEF site is in Lea County, New Mexico, approximately 1 km (0.6 mi) from the border of Andrews County, Texas, as shown on Figure 3.2-1. The figure also shows the city of Eunice, New Mexico, the closest population center to the site, at a distance of about 8 km (5 mi). Other population centers are at distances from the site as follows:

- Hobbs, Lea County, New Mexico: 32 km (20 mi) north
- Jal, Lea County, New Mexico: 37 km (23 mi) south
- Lovington, Lea County New Mexico: 64 km (39 mi) north-northwest

- Andrews, Andrews County Teas: 51 km (32 mi) east
- Seminole, Gaines County Texas, 51 km (32 mi) east-northeast
- Denver City, Gaines County, Texas 65 km (40 mi) north-northeast.

Aside from these communities, the population density in the site region is extremely low. Table 3.2-1, lists by year/decade, the estimated population in the site vicinity.

3.2.2.3 Public Service Facilities

3.2.2.3.1 Fire Department and Local Law Enforcement

Fire support service for the Eunice area is provided by Eunice Fire and Rescue, located approximately 8 km (5 mi) from the site. It is staffed by one full-time fire chief and 34 volunteer firefighters. Fire fighting equipment includes three pumpers, one tanker and three grass trucks. If additional fire equipment is needed, or if Eunice Fire and Rescue is unavailable, mutual aid agreements exist with all of the county fire departments.

The Eunice Police Department, with five full-time officers, provides local law enforcement. The Lea County Sheriff's Department also maintains a substation in Eunice. If additional resources are needed, officers from mutual aid communities within Lea County and Andrews County, Texas, can provide an additional level of response. The New Mexico State Police provide a third level of response.

3.2.2.3.2 School Population

There are four educational institutions within a radius of about 8 km (5 mi) of the NEF site, all in Lea County, New Mexico. These include an elementary school, a middle school, a high school and a private K-12 school. Table 3.2-2, Educational Facilities Near the Site, details the location of the educational facilities, population (including faculty/staff members), and student-teacher ratio. Apart from these schools, the next closest educational institutions are in Hobbs, New Mexico, 32 km (20 mi) north of the site.

The closest schools in Andrews County, Texas are in the community of Andrews about 51 km (32 mi) east of the NEF site.

3.2.2.3.3 Health Care Populations

There are two hospitals in Lea County, New Mexico. The Lea Regional Medical Center is located in Hobbs, New Mexico, about 32 km (20 mi) north of the proposed NEF site. This 250-bed hospital can handle acute and stable chronic care patients. In Lovington, New Mexico, 64 km (39 mi) north-northwest of the site, Covenant Medical Systems manages Nor-Lea Hospital, a full-service, 27-bed facility.

There are no nursing homes or retirement facilities in the site area. The closest such facilities are in Hobbs, New Mexico, about 32 km (20 mi) north of the site.

3.2.2.3.4 Recreational Population

There are no recreational facilities near the site. The Eunice Golf Course is located approximately 15 km (9.2 mi) from the site. A historical marker and picnic area is located about 3.2 km (2 mi) from the site at the intersection of New Mexico Highways 234 and 18.

3.2.2.4 Industrial Areas

More than 98% of the area within an 8 km (5 mi) radius of the NEF is an extensive area of open land on which livestock wander and graze. Gas and oil field operations are widespread in the area, but significant petroleum potential is absent within at least 5 to 8 km (3 to 5 mi) of the site. Industrial operations near the site include:

- A quarry, operated by Wallach Concrete, Inc., and several oil recovery sludge ponds owned by the Sundance Services are located north of the site. The quarry owner leases land space to a "produced water" reclamation company that maintains three small "produced water" lagoons. The operations at these facilities do not pose a safety concern for the NEF.
- Lea County operates a landfill on the south side of New Mexico State Highway 234, approximately 1 km (0.6 mi) from the center of Section 32. This facility does not pose a safety concern for the NEF.
- A vacant parcel of land is immediately east of the site. Land further east approximately 1.6 km (1 mi), in Texas, is occupied by WCS. WCS possesses a radioactive materials license from Texas, an NRC Agreement state. WCS is licensed to treat and temporarily store low-level and mixed low-level radioactive waste. WCS is also permitted to treat and dispose of hazardous toxic waste in a landfill. WCS does not pose a safety concern for the NEF.
- Dynegy's Midstream Services Plant is located 6 km (4 mi) from the site. This facility is engaged in the gathering and processing of natural gas.
- An underground CO2 pipeline currently traverses the property in a southeast-northwest direction. The 254 mm (10 in) diameter pipe operates at 134.4 bar (1,950 psi). The pipeline will be relocated along the western and southern boundary of Section 32 so that it will be at least 396.2 m (1,300 ft) from the facility Restricted Area. At this distance from the facility, the pipeline does not pose a safety concern.
- An underground natural gas pipeline is located along the south property line, paralleling New Mexico Highway 234. A risk assessment of the hazards posed by the pipeline has been performed. The assessment used a hazard model to estimate the likelihood of a gas line leak and subsequent explosion that could impact NEF operations. The model incorporated historical data on pipeline accidents obtained from the Department of Transportation (DOT, 2002) and accounted for the conditional probability that if an explosion were to occur, it would have to be substantial to have an impact on facility buildings. The model also accounted for the safe separation distance, i.e., if an explosion occurs beyond the safe separation distance for a critical structure, then the structure will be unaffected. The calculated probability of the hazard due to the natural gas pipeline in the vicinity of the proposed NEF is 4.2 E-6 per year.

3.2.2.5 Land Use

Surrounding property consists of vacant land and industrial developments. A railroad spur borders the site to the north. Beyond is a sand/aggregate quarry. A vacant parcel of land is situated immediately to the east. Cattle grazing are not allowed on this vacant parcel. Further east, at the state line and within Andrews County, Texas, is a hazardous waste treatment and disposal facility. A landfill is south-southeast of the site, across New Mexico Highway 234 and a petroleum contaminated soil treatment facility is adjacent to the west. Land further north, south and west has been mostly developed by the oil and gas industry. Land further east is ranchland. The nearest residences are situated approximately 4.3 km (2.63 mi) west of the site. Beyond is the city of Eunice, which is approximately 8 km (5 mi) to the west. There are no known public recreational areas with 8 km (5 mi) of the site. There is a historical marker and picnic area approximately 3.2 km (2 mi) from the site at the intersection of New Mexico Highways 234 and 18. Refer to Section 3.2.5.2 for further discussion on mineral resources in the site vicinity.

Rangeland comprises 98.5% of the area within an 8 km (5 mi) radius of the NEF site, encompassing 12,714 ha (31,415 acres) within Lea County, New Mexico, and 7,213 ha (17,823 acres) in Andrews County, Texas. Rangeland is an extensive area of open land on which livestock wander and graze and includes herbaceous rangeland, shrub and brush rangeland and mixed rangeland. Built-up land and barren land constitute the other two land use classifications in the site vicinity, but at considerably smaller percentages. Land cover due to built-up areas, which includes residential and industrial developments, makes up 1.2 percent of the land use. This equates to a combined total of 243 ha (601 acres) for Lea and Andrews Counties. The remaining 0.3% of land area is considered barren land which consists of bare exposed rock, transitional areas and sandy areas. This information is summarized in Table 3.2-3, Land Use Within 8 km (5 mi) of the Site. The above indicated land use classifications are identical to those used by the United States Geological Survey (USGS). No special land use classifications (i.e., Native American reservations, national parks, prime farmland) are within the vicinity of the site.

Except for the proposed construction of the NEF and the potential citing of a low-level radioactive waste disposal site in Andrews County, Texas, there are not other know current, future or proposed land use plans, including staged plans, for the site or immediate vicinity.

3.2.2.6 Water Use

The climate in southeast New Mexico is semi-arid. Average precipitation at the site is calculated to be only 33 to 38 cm (13 to 15 in) per year. The NEF site itself contains no surface water bodies or surface drainage features. Essentially all the precipitation that occurs at the site is subject to infiltration and/or evapotranspiration.

3.2.2.6.1 Recreation

There are no significant bodies of water or navigable waterways in the vicinity of the site.

3.2.2.6.2 Agricultural Water Use

Although various crops are grown within Lea and Andrews Counties, local and county officials report that there is no agricultural activity in the site vicinity, except for domestic livestock ranching. The principal livestock for both Lea and Andrews Counties is cattle. Although milk cows comprise a significant number of cattle in Lea County, the nearest dairy farms are about 32 km (20 mi) north of the subject site, near the city of Hobbs, New Mexico. There are no milk cows in Andrews County. Table 3.2-4, Agriculture Census, Crop, and Livestock Information, provides data on agricultural and livestock activities in Lea County, New Mexico, and Andrews County, Texas.

Known sources of water in the site vicinity include the following: a manmade pond on the adjacent quarry property to the north which is stocked with fish for private use; Baker Spring, an intermittent surface water feature, situated a little over 1.6 km (1 mi) northeast of the site which only contains water seasonally; several cattle watering holes where groundwater is pumped by windmill and stored in above ground tanks.

3.2.2.6.3 Municipal Use of Local Surface Water

Surface water is not a source of water for municipal use.

3.2.2.6.4 Groundwater Use

The NEF water supply is from the municipal water systems in Hobbs and Eunice, New Mexico, and thus no water will be drawn from either surface water or groundwater sources at the NEF site. The Eunice system obtains water from a groundwater source in the city of Hobbs, approximately 32 km (20 mi) north of the site. Supply of nearby groundwater users will thus not be affected by operation of the NEF. No subsurface or surface water uses such as withdrawals or consumption are made at the site by the NEF.

3.2.3 Meteorology

In this section, data characterizing the meteorology (e.g., winds, precipitation, and severe weather) for the site are presented. The discussion identifies the design basis natural events for the facility, including the likelihood of occurrence.

The meteorological conditions at the NEF have been evaluated and summarized in order to characterize the site climatology and to provide a basis for predicting the dispersion of gaseous effluents. No on-site meteorological data were available, however, WCS have a meteorological monitoring station within approximately 1.6 km (1 mi) from the proposed NEF site.

Climate information from Hobbs, New Mexico (32 km (20 mi) north of the site), obtained from the Western Regional Climate Center, were used. In addition, National Oceanic and Atmospheric Administration (NOAA) Local Climatological Data (LCD) recorded at Midland-Odessa Regional Airport, Texas (103 km (64 mi) southeast of the site) and at Roswell, New Mexico (161 km (100 mi) northwest of the site) were used. In the following summaries of meteorological data, the averages are based on:

- Hobbs station (WRCC, 2003) averages are based on a 30 year record (1971 to 2000) unless otherwise stated

- Midland-Odessa station (NOAA, 2002a) averages are based on a 30 year record (1961 to 1990) unless otherwise stated
- Roswell station (NOAA, 2002b) averages are based on a 30 year record (1961 to 1990) unless otherwise stated.

The WCS data was not used since it had not been fully verified by WCS. An analysis of the WCS data was performed and it was determined that the prevailing wind direction at the WCS facility agrees with the prevailing wind directions at Midland-Odessa and Roswell. Use of the Hobbs, Midland-Odessa, and Roswell observations for a general description of the meteorological conditions at the NEF was deemed appropriate as they are all located within the same region and have similar climates. Use of the Midland-Odessa data for predicting the dispersion of gaseous effluents was deemed appropriate. It is the closest first-order National Weather Service (NWS) station to the NEF site, and both Midland-Odessa and the NEF site have similar climates. In addition, wind direction frequency comparisons between Midland-Odessa and the closest source of meteorological measurements (WCS) to the NEF site show good agreement. Midland-Odessa and Roswell data were compiled and certified by the National Climatic Data Center. Hobbs data were compiled and certified by the Western Regional Climate Center.

3.2.3.1 Local Wind Patterns and Average and Maximum Wind Speeds

Monthly mean wind speeds and prevailing wind directions at Midland-Odessa are presented in Table 3.2-5, Midland-Odessa, Texas, Wind Data. The annual mean wind speed was 4.9 m/s (11.0 mi/hr) and the prevailing wind direction was 180 degrees with respect to true north. The maximum five-second wind speed was 31.3 m/s (70 mi/hr).

Monthly mean wind speeds and prevailing wind directions at Roswell are presented in Table 3.2-6, Roswell, New Mexico, Wind Data. The annual mean wind speed was 3.7 m/s (8.2 mi/hr) and the prevailing wind direction was wind from 160 degrees with respect to true north. The maximum five-second wind speed was 27.7 m/s (62 mi/hr).

Five years of data (1987-1991) from the Midland-Odessa NWS were used to generate joint frequency distributions of wind speed and direction. This data summary, for all Pasquill stability classes (A-F) combined, is provided in Table 3.2-7, Midland-Odessa Five Year (1987-1991) Annual Joint Frequency Distribution For All Stability Classes Combined.

Five years of data (1987-1991) from the Midland-Odessa NWS were used to generate joint frequency distributions of wind speed and direction as a function of Pasquill stability class (A-F). Stability class was determined using the solar radiation/cloud cover method. These data are given in Tables 3.2-8 through 3.2-13. The most stable classes, E and F, occur 18.3% and 13.6% of the time, respectively. The least stable class, A, occurs 0.4% of the time. Important conditions for atmospheric dispersion, stable (Pasquill class F) and low wind speeds 0.4-1.3 m/s (1.0-3.0 mi/hr), occur 2.2% of the time. The highest occurrences of Pasquill class F and low wind speeds, 0.4-1.3 m/s (1.0-3.0 mi/hr), with respect to wind direction are 0.28% and 0.23% with south and south-southeast winds.

3.2.3.2 Annual Amounts and Forms of Precipitation

The normal annual total rainfall as measured in Hobbs is 46.1 cm (18.15 in). Precipitation amounts range from an average of 1.2 cm (0.45 in) in March to 8 cm (3.1 in) in September. The record maximum and minimum monthly totals are 35.13 cm (13.83 in) and zero, respectively (WRCC, 2003). Table 3.2-14, Hobbs New Mexico Temperature and Precipitation Data, lists the monthly averages and extremes of precipitation for the Hobbs data. These precipitation summaries are based on 30 year records.

The normal annual total rainfall as measured in Midland-Odessa is 37.6 cm (14.8 in). Precipitation amounts range from an average of 1.1 cm (0.42 in) in March to 5.9 cm (2.31 in) in September. The record maximum and minimum monthly totals are 24.6 cm (9.70 in) and zero, respectively. The highest 24-hour precipitation total was 15.2 cm (6 in) in July 1968 (NOAA, 2002a). Table 3.2-15, Midland-Odessa, Texas, Precipitation Data, lists the monthly averages and extremes of precipitation for the Midland-Odessa data. These precipitation summaries are based on 30 year records.

The normal annual rainfall total as measured in Roswell, New Mexico, is 33.9 cm (13.34 in). The record maximum and minimum monthly totals are 17.5 cm (6.9 in) and zero, respectively (NOAA, 2002b, 2002a). The highest 24-hour precipitation total was 12.5 cm (4.91 in) in July 1981 (NOAA, 2002b). Table 3.2-16, Roswell, New Mexico, Precipitation Data, lists the monthly averages and extremes of precipitation for the Roswell data. These precipitation summaries are based on 30 year records.

3.2.3.3 Design Basis Values for Snow or Ice Load

Snowfall in Midland-Odessa, Texas, averages 13.0 cm (5.1 in) per year. Maximum monthly snowfall/ice pellets of 24.9 cm (9.8 in) fell in December 1998. The maximum amount of snowfall/ice pellets to fall in 24 hours was 24.9 cm (9.8 in) in December 1998 (NOAA, 2002a). Table 3.2-17, Midland-Odessa, Texas, Snowfall Data, lists the monthly averages and maximums of snowfall/ice pellets at Midland-Odessa, Texas. These snowfall summaries are based on 30 year records.

Snowfall in Roswell, New Mexico, averages 30.2 cm (11.9 in) per year. Maximum monthly snowfall/ice pellets of 53.3 cm (21.0 in) fell in December 1997. The maximum amount of snowfall/ice pellets to fall in 24 hours was 41.9 cm (16.5 in) in February 1988 (NOAA, 2002b). Table 3.2-18, Roswell, New Mexico, Snowfall Data, lists the monthly averages and maximums of snowfall/ice pellets at Roswell, New Mexico. These snowfall summaries are based on 30 year records.

The design basis snow load for the NEF was determined by combining the 100-year snowpack loading and 48 hour Probable Maximum Winter Precipitation (PMWP) loading for the area. Using the published 50 year snowpack loading of 48.8 kg/m^2 (10 lb/ft^2) (ASCE, 1998) and adjusting this value using the method described by ASCE, the 100 year snowpack loading is determined to be 58.6 kg/m^2 (12 lb/ft^2).

The 48-hour PMWP as determined by the methodology outlined in Hydrometeorlogical Report No. 33 (WB, 1956) is determined to be 483 mm (19 in), which corresponds to a loading of 96.6 kg/m^2 (19.8 lb/ft^2). These two values were used to develop a design basis snow loading of 156 kg/m^2 (32 lb/ft^2).

The design basis snow load does not explicitly account for loads due to frozen rain, ice, or hail. This type of loading is bounded by the conservative design basis snow load discussed above.

3.2.3.4 Type, Frequency, and Magnitude of Severe Weather

This section identifies the design basis severe weather events for the facility and describes the basis for their selection.

3.2.3.4.1 Tornados and Tornado Missiles

Tornadoes occur infrequently in the vicinity of the NEF. Only two tornadoes were reported in Lea County, New Mexico, (Grazulis, 1993) from 1880-1989. Across the state line, only one tornado was reported in Andrews County, Texas, (Grazulis, 1993) from 1880-1989.

Tornadoes are commonly classified by their intensities. The F-Scale classification of tornados is based on the appearance of the damage that the tornado causes. There are six classifications, F0 to F5, with an F0 tornado having winds of 64-116 km/hr (40-72 mi/hr) and an F5 tornado having winds of 420–512 km/hr (261-318 mi/hr) (AMS, 1996). The two tornadoes reported in Lea County were estimated to be F2 tornadoes (Grazulis, 1993).

The following steps were taken in performing the tornado hazard assessment for the site:

- Define a local region of latitude and longitude that surrounds the site of interest and obtain historical records of tornadoes that have touched down in the local region
- Determine occurrence rate and associated confidence limits
- Determine number of tornadoes per F-Scale category
- Estimate the damage path area for each F-Scale category and calculate damage areas associated with confidence limits
- Calculate tornado hazard probabilities for each F-Scale wind speed category.

An annual tornado hazard probability of 1E-05 was chosen for the design basis tornado. The tornado and tornado missile parameters from the site-specific study are provided below.

Annual Tornado Hazard Probability	1E-05
Tornado Wind Speed	302 km/hr (188 mi/hr)
Radius of Damaging Winds	130 m (425 ft)
Atmospheric Pressure Change (APC)	390 kg/m^2(80 lb/ft^2)
Rate of APC	146 kg/m^2/s (30 lb/ ft^2)

Missile: 2x4 Timber Plank, 6.80 kg (15 lb)

Horizontal Speed	136 km/hr (85 mi/hr)
Vertical Speed	88 km/hr (55 mi/hr)

Maximum Height above Ground	61 m (200 ft)

Missile: 76.2 mm (3-in.) Diameter Steel Pipe, 34 kg (75 lb)

Horizontal Speed	80 km/hr (50 mi/hr)
Vertical Speed	48 km/hr (30 mi/hr)
Maximum height above Ground	9.1 m (30 ft)

Missile: Automobile 1361 kg (3,000 lb)

Horizontal Speed	32 km/hr (20 mi/hr)

3.2.3.4.2 Extreme Winds

Annual extreme winds recorded at the Midland-Odessa, Texas, airport are used to model the straight wind hazard at the NEF site. The airport is located 103 km (64 mi) east-southeast of the site. The airport location features flat, open terrain. Due to proximity, common weather systems affect Eunice, New Mexico, and Midland-Odessa, Texas. The wind speeds used in the model are 3 second gust speeds at a 10 m height above ground. The set of annual extreme winds include the years 1973 to 1999.

A Fischer-Tippett Type I extreme value distribution is fit to the annual extreme wind speed data. Upper and lower bound values at 95% confidence level are also calculated. The results of the straight wind hazard assessment are provided in Table 3.2-19, Straight Wind Hazard Assessment.

An annual wind hazard probability of 1E-05 was chosen for the design basis wind speed. This wind speed is 252 km/hr (157 mi/hr), and is a 3 second gust, 10 m (33 ft) above ground.

3.2.3.4.3 Hurricanes

Hurricanes, or tropical cyclones, are low-pressure weather systems that develop over the tropical oceans. These storms are classified during their life cycle according to their intensity:

- Tropical depression – wind speeds less than 63 km/hr (39 mi/hr)
- Tropical storm – wind speed between 63 and 118 km/hr (39 and 73 mi/hr)
- Hurricane – wind speeds greater than 118 km/hr (73 mi/hr)

Hurricanes are fueled by the relatively warm tropical ocean water and lose their intensity quickly once they make landfall. Since the NEF is sited about 805 km (500 mi) from the coast, it is most likely that any hurricane that is tracked towards it would have dissipated to the tropical depression stage, that is, wind speeds less than 63 km/hr (39 mi/hr), before it reached the NEF. Therefore hurricanes are not a design basis event for the site.

3.2.3.4.4 Extreme Precipitation

The short duration – small area local intense probable maximum precipitation (PMP) was obtained from NOAA Hydrometeorological Report No. 52 (NOAA, 1982). The local intense PMP is 43.9 cm (17.3 in) in 1 hr over 2.6 km^2 (1 mi^2).

Roofs will be designed so as not to pond water to a depth during the local intense PMP that could exceed the design load for the roof. This will be accomplished by designing the parapets to a height which will preclude significant ponding on the roof. As an alternative, the parapets can be provided with scuppers that are designed to preclude significant roof ponding during the local intense PMP.

Local site runoff will be determined for the local plant site drainage area. Maximum ponding depths around the main plant structures will be determined using final site topography. The potential for water intrusion into critical plant areas will be precluded by final site grading.

3.2.3.4.5 Lightning

Thunderstorms occur during every month but are most common in the spring and summer months. Thunderstorms occur an average of 36.4 days/year in Midland-Odessa, Texas, based on a 54 year period of record. The seasonal averages are: 11 days in spring (March through May); 17.4 days in summer (June through August); 6.7 days in fall (September through November); and 1.3 days in winter (December through February).

J. L. Marshall (Marshall, 1973) presented a methodology for estimating lightning strike frequencies which includes consideration of the attractive area of structures. His method consists of determining the number of lightning flashes to earth per year per square kilometer and then defining an area over which the structure can be expected to attract a lightning strike. Assuming that there are 4 flashes to earth per year per square kilometer (2.1 flashes to earth per year per square mile) in the vicinity of the NEF (conservatively estimated using Figure 3.2-4, Average Lightning Flash Density, which is taken from the NWS (NWS, 2003). Marshall defines the total attractive area, A, of a structure with length L, width W, and height H, for lightning flashes with a current magnitude of 50% of all lightning flashes as:

$$A = LW + 4H (L + W) + 12.57 H^2$$

The following building complex dimensions were used to estimate conservatively the attractive area of the NEF:

L = 534 m (1,752 ft), W = 534 m (1,752 ft), H = 13 m (43 ft)

The total attractive area is therefore equal to 0.34 km^2 (0.13 mi^2). Consequently, the lightning strike frequency computed using Marshall's methodology is given as 1.36 flashes per year.

Lightning protection for the NEF is provided as described in Section 7.3.7, Lightning Protection of the SAR.

3.2.4 Hydrology

This section describes the NEF site's surface water and groundwater resources. Data is provided for the NEF site and the surrounding area, and the regional associations of those natural water systems are described. This information provides the basis for evaluation of any

potential facility impacts on surface water, aquifers, and the related social and economic structures of the area around the facility.

The information included in this section was largely obtained from prior site studies including extensive subsurface investigations for a nearby facility, WCS, located about 1.6 km (1 mi) to the east of the NEF site. In addition, literature searches were conducted to obtain additional reference material. Some of the WCS data has been collected on Section 33 located immediately east of the NEF site. These data are being supplemented by a groundwater exploration and sampling program on Section 32 initiated by LES in September 2003.

The NEF facility will make no use of either surface water or groundwater from the site. The collection and storage of runoff from specific site areas will be controlled. No significant adverse changes are expected in site hydrology as a result of construction or operation of the NEF.

3.2.4.1 Surface Hydrology

The NEF site itself contains no surface water bodies or surface drainage features. Essentially all the precipitation that occurs at the site is subject to infiltration and/or evapotranspiration. More information on the movement and fate of surface water and groundwater at the site is provided in the following sections.

3.2.4.2 Major Surface and Subsurface Hydrological Systems

The climate in southeast New Mexico is semi-arid. Average precipitation at the site is calculated to be 33 to 38 cm per year (13 to 15 in per year). Evaporation and transpiration rates are high. This results in minimal, if any, surface water occurrence or groundwater recharge.

The NEF site is relatively flat and contains no surface drainage features.. Some localized depressions exist, due to eolian processes, but the size of these features is too small to be of significance with respect to surface water collection.

Most precipitation is contained onsite due to infiltration and/or evapotranspiration. The vegetation on the site is primarily mesquite bush (Prosopis juliflora) and native grasses (e.g., Sporobolus giganteus). The surface soils are predominantly of an alluvial or eolian origin. The texture of the surface soils is generally silt to silty sands. Therefore, the surface soils are relatively low in permeability and tend to hold moisture in storage rather than allow rapid infiltration to depth. Water held in storage in the soil is subsequently subject to evapotranspiration. Nine subsurface borings were drilled at the site during September 2003. Only one of the borings produced cuttings that were slightly moist at 1.8 to 4.2 m (6 to 14 ft) below ground surface; other cuttings were very dry. Evapotranspiration processes are significant enough to short-circuit any potential groundwater recharge. This process is further discussed below.

There is some evidence for shallow, near-surface groundwater occurrence in areas to the north and east of the site. These conditions are intermittent and limited. A quarry operated by Wallach Concrete, Inc. is located just north of the NEF site. Wallach Concrete has extensively mined sand and gravel from the quarry. The typical geologic cross section at that site consists of a layer of caliche at the surface, referred to as the "caprock," underlain by a sand and gravel deposit, which in turn overlies a thick clay unit of the Dockum Group, referred to as red beds, and part of the Chinle Formation. Figure 3.2-5, Site Boring Plan and Profile, depicts this

stratigraphy. In some locations, the caprock (caliche) overlies sand and gravel, with the red bed clay Chinle Formation at the base of the pit. In some areas the caprock is missing and the sand and gravel is exposed at the surface. The caprock is generally fractured and following precipitation events may allow infiltration that quickly bypasses any roots from surface vegetation. In addition, gravel outcrops may allow rapid infiltration of precipitation. These conditions have led to instances of minor amounts of perched groundwater at the base of the sand and gravel unit, atop the red bed Chinle Formation. The Chinle red bed clay has a very low permeability, about 1×10^{-8} cm/s (4×10^{-9} in/s) (Rainwater, 1996), and serves as a confining unit arresting downward percolation of localized recharge flux. This shallow perched zone is not pervasive throughout the area.

Conditions at the NEF site are different than at the Wallach Concrete site. Two differences are of particular importance. First, the caprock is not present at the NEF site. Therefore, rapid infiltration through fractured caliche does not contribute to localized recharge at the NEF site. Second, the surface soils at the NEF site are finer-grained than the sand and gravel at the Wallach Concrete site. There is a thin layer of sand and gravel just above the red bed Chinle clay unit on the NEF site, but based on recent investigations, it is not saturated.

Another instance of possible saturation above the Chinle clay may be seen at Baker Spring, just to the northeast of the NEF site. Baker Spring is located at the edge of an escarpment, where the caprock ends. Baker Spring is intermittent, and water typically flows from it only after precipitation events. There may be some water seeping from the sand and gravel unit beneath the caprock and into Baker Spring. The area where Baker Spring is located is underlain by the Chinle clay. Deep infiltration of water is impeded by the low permeability of the clay. Therefore, seepage and/or precipitation/runoff into the Baker Spring area appear to be responsible for the intermittent localized flow and ponding of water in this area. Flows from this feature are intermittent, unlike those supplying the Wallach Concrete pits. This condition does not exist at the NEF site due to the absence of the caprock and the low permeability surface soils.

A recent investigation of the Baker Spring area supports the conclusion that the feature is man-made and results from the historical excavation of gravel and caprock materials that are present above the redbed clay. As a result of the excavation, Baker Spring is topographically lower than the surrounding area. Following rainfall events, ponding on the excavation floor occurs. Because the excavation floor consists of very low permeability clay of the redbed, limited vertical migration of the ponded water occurs. Shading from the high wall and trees that have flourished in the excavated area retard the natural evaporation rates and water stands in the pond for sometime. It is also suspected that during periods of ponding, surface water infiltrates into the sands at the base of the excavated wall and is retained as bank storage. As the surface water level declines, the bank storage is discharged back to the excavation floor.

A third instance of localized shallow groundwater occurrence exists to the east of the NEF site where several windmills on the WCS property were used to supply water for stock tanks. These windmills tapped small saturated lenses above the Chinle Formation red beds. The amount of groundwater in these zones is limited. The source of recharge for these localized perched zones is likely to be "buffalo wallows," (playas) depressions located near the windmills. The buffalo wallows are substantial surface depressions that collect surface water runoff. Water collecting in these depressions is inferred to infiltrate below the root zone due to the ponding conditions. WCS has drilled monitoring wells in these areas to characterize the nature and extent of the saturated conditions. Some of these wells are dry, owing to the localized nature of the perched conditions. When water is encountered in the sand and gravel above the Chinle

Formation red beds, its level is slow to recover following sampling events due to the low permeability of the perched saturated zones. The discontinuity of this saturated zone and its low permeability argue against its definition as an aquifer. No buffalo wallows or related groundwater conditions occur on or near the NEF site.

The hydrologic conditions that occur in the shallow surface regime at the NEF site are substantiated by field investigations including geochemical and soil-physics based techniques, as well as computer modeling, and show that there is no recharge occurring in thick, desert vadose zones with desert vegetation (Walvoord, 2002). Precipitation that infiltrates into the subsurface is efficiently transpired by the native vegetation. Vapor-phase movement of soil-moisture may occur, but it is also intercepted by the vegetation. In a thick vadose zone, such as at the NEF site, the deeper part of that zone has a natural thermal gradient that induces upward vapor diffusion. As a result, a small flux of water vapor rises from depth to the base of the root zone, and any infiltration coming from the land surface is captured by the roots of the plants within the top several meters of the profile. Effectively, there is a maximum negative pressure potential at the base of the root zone that acts like a sink, where water is taken up by the plants and transpired. These deep desert soil systems have functioned in this manner for thousands of years, essentially since the time of the last glacial period when precipitation rates fell dramatically. It is expected that these conditions will remain for several thousand more years (until the next glacial period), unless the hydrology and vegetation is altered dramatically.

3.2.4.3 Floods

The NEF site is located above the 100 or 500-year flood elevation (WBG, 1998 and FEMA, 1978).

The NEF site is contained within the Landreth-Monument Draw Watershed. The closest water conveyance is Monument Draw, a typically dry, intermittent stream located about 4 km (2.5 mi) west of the site. The maximum historical flow for Monument Draw is 36.2 m^3/s (1,280 ft^3/s) measured June 10, 1972. All other historical maximum measurements are below 2.0 m^3/s (70 ft^3/s) (USGS, 2003a). Therefore, a flood is not considered to be a design basis event for the NEF site.

3.2.4.4 Groundwater Hydrology

A subsurface investigation was performed for the NEF site during September 2003 to delineate specific hydrologic conditions. Figure 3.2-5 shows the locations of subsurface borings and observation wells.

The WCS facility, located east of the site in Texas, has had numerous subsurface investigations performed for the purpose of delineating and monitoring site subsurface hydrogeologic conditions. Much of this information is directly pertinent to the NEF site. The WCS hydrogeologic data was used in planning the recent NEF site investigations. A recent evaluation of potential groundwater impacts in the area provides a good overview of the investigations performed for the WCS facility. (Rainwater, 1996)

The NEF site investigation initiated in September 2003 had two main objectives: 1) to delineate the depth to the top of the Chinle Formation red beds to assess the potential for saturated conditions above the red beds, and 2) to complete three monitoring wells in the siltstone layer

beneath the red beds to monitor water level and water quality within this thin horizon of perched intermittent saturation.

Nine boreholes oriented on a three-by-three grid were drilled to the top of the Chinle Formation red beds (Figure 3.2-5). Only one of the borings produced cuttings that were slightly moist at 1.8 to 4.2 m (6 to 14 ft) below ground surface; other cuttings were very dry. Left open for at least a day, no groundwater was observed to enter any of these holes. No samples could be collected for water quality analysis at the time of well construction. One groundwater sample has since been collected due to the limited groundwater occurrence.

The land surface elevation was surveyed at each of the nine borehole locations and the elevation of the top of the Chinle Formation red beds was computed. This information was combined with similar information from the WCS facility to produce an elevation map of the top of the red beds (See Figure 3.2-5). The dry nature of the soils from each of these borings supports a conclusion that there is no recharge from the ground surface at the site (Walvoord, 2002).

The three monitoring wells were installed at the end of September 2003. (Figure 3.2-5). Through the first month of monitoring only one well, MW-2, located at the northeast corner of the site, produced water. Several samples have been taken from that well.

Another factor to consider relative to hydrologic conditions at the NEF site is the presence of the Triassic Chinle Formation red bed clay. This clay unit is approximately 323 to 333 m (1,060 to 1,092 ft) thick beneath the site. With an estimated hydraulic conductivity on the order of 2.0 E-8 cm/s (7.9 E-9 in/s), the unit is very tight. This permeability is of the same order prescribed for engineered landfill liner materials. The expected vertical travel times through this clay unit would be on the order of thousands of years, based on this permeability and the thickness of the unit.

The first presence of saturated porous media beneath the site appears to be at the base of the Chinle red bed clay where there exists a low-permeability silty sandstone or siltstone. Borings and monitor wells at the WCS facility directly to the east of the NEF site have encountered this zone approximately 61 to 91 m (200 to 300 ft) below land surface. Wells completed in this unit are very slow to produce water. This makes sampling quite difficult. It is arguable whether this zone constitutes an aquifer, given the low permeability of the unit. As discussed above, three monitoring wells were installed on the NEF site in September 2003 with screened intervals within this siltstone unit. These wells are approximately 73 m (240 ft) deep. There is also a 30.5-m (100-foot) water-bearing sandstone layer at about 183 m (600 ft) below ground surface.

The first occurrence of a well-defined aquifer is approximately 340 m (1,115 ft) below land surface, within the Santa Rosa formation. Because of the depth below land surface to this unit, and the fact that the thick Chinle clay unit would limit any potential migration to depth, this aquifer has not been investigated. No impacts are expected to the Santa Rosa aquifer.

Based on groundwater levels in MW-2 and data from the adjacent WCS site, a groundwater gradient of 0.011 m/m (ft/ft) was determined, generally sloping towards the south. Hydraulic conductivity of the saturated layer, based on slug tests is estimated to be approximately 3.7 E-6 cm/s (1.5 E-6 in/yr). Based on the data collected at the NEF and WCS, the groundwater gradient in the siltstone unit at NEF is estimated to range from approximately 0.011 to 0.017 m/m (0.011 to 0.017 ft/ft).

Figure 3.2-6, Water and Oil Wells in the Vicinity of the NEF Site, is a map of wells and surface water features in the vicinity of the NEF site. The figure also includes oil wells. No water wells are located within 1.6 km (1 mi) of the site boundary.

3.2.4.5 Groundwater Chemistry

As discussed in Section 3.2.4.4, water resources in the area of the NEF site are minimal. Precipitation runoff at the site is effectively collected and contained by detention/retention basins and through evapotranspiration. It is highly unlikely that any groundwater recharge will occur at the site.

The first occurrence of groundwater beneath the NEF site is in a silty sandstone or siltstone horizon in the Chinle Formation, approximately 65 to 68 m (214 to 222 ft) below the surface. This unit is low in permeability and does not yield water readily. Groundwater quality in monitoring wells in the Chinle Formation, the shallowest saturated zone, is poor due to natural conditions. Samples from monitoring wells within this horizon on the WCS facility have routinely been analyzed with Total Dissolved Solids (TDS) concentrations between about 2,880 and 6,650 mg/l. Metal analyses from four background monitoring wells at the WCS site sampled during the period 1997-2000 show that essentially all results are below maximum contaminate limits (MCL) for EPA drinking water standards. The tightness of the formation, the limited thickness of saturation, and the poor water quality, support the argument that this zone does not constitute an aquifer.

Three monitor wells MW-1, MW-2, and MW-3, have been drilled and installed on the NEF site as shown on (Figure 3.2-5), and several water quality samples have been obtained. Water quality characteristics are similar to those for WCS site samples. A detailed discussion of the groundwater sample analysis is presented in Section 3.4.2, Water Quality Characteristics, of the Environmental Report.

3.2.5 Geology

This section identifies the geological, seismological, and geotechnical characteristics of the NEF site and its vicinity. Some areas immediately adjacent to the site have been thoroughly studied in recent years in preparation for construction of other facilities including the Waste Control Specialists (WCS) site and the former proposed Atomic Vapor Laser Isotope Separation (AVLIS) site. Data remain available from these investigations in the form of reports (WBG, 1998; TTUWRC, 2000). These documents and related materials provide a significant description of geological conditions for the NEF site. In addition, LES performed field investigations, where necessary, to confirm site-specific conditions.

3.2.5.1 Regional Geology

The site is located near the boundary between the Southern High Plains Section (Llano Estacado) of the Great Plains Province to the east and the Pecos Plains Section to the west. The boundary between the two sections is the Mescalero Escarpment, locally referred to as Mescalero Ridge. That ridge abruptly terminates at the far eastern edge of the Pecos Plains. The ridge is an irregular erosional topographic feature in southern Lea County where it exhibits relief of about 9 to 15 m (30 to 50 ft) compared with a nearly vertical cliff and relief of approximately 45 m (150 ft) in northwestern Lea County. The lower relief of the ridge in

southeastern Lea County is due to partial cover by wind deposited sand (WBG, 1998). The dominant geologic feature of this region is the Permian Basin. The NEF site is located within the Central Basin Platform area. This platform occurs between the Midland and Delaware Basins, which comprises the Permian Basin. The basin, a 250 million-year-old feature, is the source of the region's prolific oil and gas reserves. The late Cretaceous to the early Tertiary (65 to 70 million years ago) marked the beginning of the Laramide Orogeny, which formed the Cordilleran Range to the west of the Permian Basin. That orogeny uplifted the region to its present elevation.

The primary difference between the Pecos Plains and the Southern High Plains physiographic sections is a change in topography. The High Plains is a large flat mesa which uniformly slopes to the southeast. In contrast, the Pecos Plains Section is characterized by its more irregular erosional topographic expression (WBG, 1998).

The Permian Basin, a massive subsurface bedrock structure, is a downward flexure of a large thickness of originally flat-lying, bedded, sedimentary rock. It dominates the geologic structure of the region. It extends to 4,880 m (16,000 ft) below msl. The NEF site is located above the Central Basin Platform that divides the Permian Basin into the Midland and Delaware sub-basins. The base of the Permian basin sediments extend about 1,525 m (5,000 ft) deep beneath the NEF site.

The top of the Permian deposits is approximately 434 m (1,425 ft) below ground surface. Overlying the Permian are the sedimentary rocks of the Triassic Age Dockum Group. The upper formation of the Dockum Group is the Chinle. Locally, the Chinle Formation consists of red, purple and greenish micaceous claystone and siltstone with interbedded fine-grained sandstone. The Chinle is regionally extensive with outcrops as far away as the Grand Canyon region in Arizona (WBG, 1998). Locally overlying the Chinle Formation in the Permian Basin is either the Tertiary Ogallala, Gatuña or Antlers Formations, or Quaternary alluvium. The Tertiary Ogallala Formation underlies all of the High Plains (to the east) and mantles several ridges in Lea County. Unconsolidated sediments northeast of the NEF site are recognized as the Ogallala and deposits west of the NEF site are mapped as the Gatuna or Antlers Formations. This sediment is described as alluvium (WBG, 1998) and is mined as sand and gravel in the NEF site.

The Chinle Formation is predominately red to purple moderately indurated claystone, which is highly impermeable (WBG, 1998). Red Bed Ridge is a significant topographic feature in this regional plain that is just north and northeast of the NEF site, and is capped by relatively resistant caliche. Ground surface elevation increases about 15 m (50 ft) from +1,045 m (+3,430 ft) to +1,059 m (+3,475 ft) across the ridge.

Recent deposits at the site and in the site area are primarily dune sands derived from Permian and Triassic rocks of the Permian Basin. The so-called Mescalero Sands cover approximately 80% of Lea County, locally as active sand dunes.

Two types of faulting were associated with early Permian deformation. Most of the faults were long, high-angle reverse faults with well over a hundred meters (several hundred feet) of vertical displacement that often involved the Precambrian basement rocks. The second type of faulting is found along the western margin of the platform where long strike-slip faults, with large displacements, are found. The nearest recent faulting to the site is defined by the New Mexico Bureau of Geology and Mineral Resources (NMIMT, 2003) and is over 161 km (100 mi) to the west associated with the deeper portions of the Permian Basin (Machette, 1998).

The large structural features of the Permian Basin are reflected only indirectly in the Mesozoic and Cenozoic rocks, as there has been virtually no tectonic movement within the basin since the Permian period. Figure 3.2-7, Permian Basin Geologic Structures and Profile, shows the structure that causes the draping of the Permian sediments over the Central Basin Platform structure, located approximately 2,134 m (7,000 ft) beneath the present land surface. The faults that uplifted the platform do not appear to displace the younger Permian sediments.

The Southeast New Mexico-West Texas area presently is structurally stable. The Permian Basin has subsided slightly since the Laramide Orogeny. This is believed to be a result of dissolution of the Permian evaporite layers by groundwater infiltration and possible from oil and gas extraction (WBG, 1998).

3.2.5.2 Site Geology

Topographic relief on the site is generally subdued. NEF site elevations range between about +1,033 and +1,045 m (+3,390 and +3,430 ft), mean sea level (msl) (See Figure 3.2-8, Site Topography). Finished site grade will range about +1,041 m (+3,415 ft), msl. The NEF site itself encompasses 220 ha (543 acres), of which 73 ha (180 acres) will be developed. Small-scale topographic features within the boundary of the proposed NEF site include a closed depression evident at the northern center of the site, the result of eolian processes, and a topographic high at the southwest corner of the site is created by dune sand. In general the site slopes from northeast to southwest with a general overall slope of about 0.5%. Red Bed Ridge (TTUWRC, 2000) is an escarpment of about 15 m (50 ft) in height that occurs just north and northeast of the NEF site. Geologically the site is located in an area where surface exposures consist mainly of Quaternary-aged eolian and piedmont sediments along the far eastern margin of the Pecos River Valley (NMIMT, 2003). Figure 3.2-9, Surficial Geologic Map of the NEF Site Area, is a portion of the Surficial Geologic Map of Southeast New Mexico (NMIMT, 1977), which includes the area of the NEF site. The surficial unit shown on this map at the NEF site is described as a sandy alluvium with subordinate amounts of gravel, silt and clay. Figure 3.2-9 also shows other surficial units in the site vicinity including caliche, a partly indurated zone of calcium carbonate accumulation formed in the upper layers of surficial deposits including tough slabby surface layers and subsurface nodules, fibers and veinlets; loose sand deposits, some gypsiferous, and subject to wind erosion. Other surficial deposits in the site area include floodplain channel deposits along dry channels and playa sands.

Recent deposits of dune sands are derived from Permian and Triassic rocks. These so-called Mescalero Sands (also known as the Blackwater Draw Formation) occur over 80% of Lea County and are generally described as fine to medium-grained and reddish brown in color. The USDA Soil Survey of Lea County identifies the dune sands at the site as the Brownsfield-Springer Association of reddish brown fine to loamy fine sands (USDA, 1974).

Figure 3.2-5 includes the NEF site and adjacent site borings and a geologic profile from the immediately adjacent parcel to the east that provides a representation of site geology. The profile shows alluvial deposits about 9 to 15 m (30 to 60 ft) thick, cemented by soft caliche layer 1 to 4 m (3 to 12 ft) that occurs at the top of the alluvium. Locally on the site dune sand overlies both these deposits. The alluvium rests on the red beds of the Chinle Formation, a silty clay with lenses of sandy clay or claystone and siltstone. Information from recent borings done on the NEF site is consistent with the data shown on Figure 3.2-5. Borings on the NEF site depicted on Figure 3.2-5 include:

- Three borings/monitoring wells (MW-1, MW2, and MW-3)
- Nine site groundwater exploration borings (B-1 through B-9)
- Five geotechnical borings (B-1 through B-5).

Other borings depicted on Figure 3.2-5, not on the NEF site, were performed by others.

The NEF site boring test records are shown on Figures 3.2-10 through 3.2-14. A key to the symbols and descriptions shown on the test records is provided in Figure 3.2-15, Soil Test Boring Key to Symbols and Descriptions.

The NEF site lies within the Landreth-Monument Draws Watershed. Site drainage is to the southwest with runoff not able to reach any water body before it evaporates. The only major regional drainage feature is Monument Draw, which is located just over 4 km (2.5 mi) west of the site, between the proposed NEF site and the city of Eunice, New Mexico (USDA, 1974). The draw begins with a southeasterly course to a point north of Eunice where it turns south and becomes a well defined cut approximately 9 m (30 ft) in depth and 550 to 610 m (1,800 to 2,000 ft) in width. The draw does not have through-going drainage and is partially filled with dune sand and alluvium.

Along Red Bed Ridge (TTUWRC, 2000), approximately 1.6 km (1.0 mi) northeast of the NEF site, is Baker Spring. The depression formed by Baker Spring contains water only intermittently.

No significant non-petroleum mineral deposits are known to exist in the vicinity of the NEF site. The surface cover of silty sand and gravel overlies a claystone of no economic value. No mineral operations are noted in Lea County by the New Mexico Bureau of Mines Inspection (NMBMI, 2001). Mining and potential mining of potash, a commonly extracted mineral in New Mexico, is followed by the New Mexico Energy, Minerals and Natural Resources Department, which maintains a map of areas with potash mines and mining potential (NMEMNRD, 2003). Those data indicate neither mining nor potential for mining of potash in the NEF site area.

The topographic quadrangle map that contains the site (USGS, 1979) contains 10 locations where sand and gravel have been mined from surface deposits, spread across the quadrangle, over an area about 12 by 14 km (7.5 by 8.9 mi), suggesting that suitable surficial deposits for borrow material are widespread.

Exploratory drill holes for oil and gas are absent from the site area and its vicinity, but are common 8 km (5 mi) west in and around the city of Eunice, New Mexico. That distribution, and the time period of exploration since the inception of exploration for this area, suggests that the potential for productive oil drilling at the NEF site is not significant.

Soil development in the region is generally limited due to its semi-arid climate. The site has a minor thickness of silty soil (generally less than 0.4 m (1.4 ft)) developed from subaerial weathering. Caliche deposits are common in the near-surface soils. A small deposit of active dune sand is present at the southwest corner of the site.

The U. S. Department of Agriculture soil survey for Lea County, New Mexico (USDA, 1974) categorizes site soils as hummocky loamy (silty) fine sand with moderately rapid permeability and slow runoff, well-drained non-calcareous loose sand, active dune sand and dune-associated sands. Near-surface caliche deposits may locally limit (limiting soil porosity) or enhance (fractured caliche) surface drainage. Figure 3.2-16, Site Soils Map, shows the soil map for the NEF site (USDA, 1974). The legend for that map lists each of the soils present at

the NEF site describing them and along with their unified soil classification designations (ASTM, 1993).

3.2.5.3 Geotechnical Investigations

Previously completed geotechnical investigations on property near the site provide the following subsurface information. Based on the data from those investigations, subsurface conditions are described as follows. Topsoil occurs as 0.3 m (1 ft) or less of brown organic silty sand that overlies a formation of white or tan caliche. The caliche consists of very hard to friable cemented sand, conglomerate limestone rock, silty sand and gravel. A sand and gravel layer varying from 0 to 6 m (0 to 20 ft) in thickness occurs at the bottom of the caliche strata. Below the caliche is a reddish brown silt clay that extends to the termination of the borings, 30 to 91 m (100 to 300 ft) below grade. The red beds consist of a highly consolidated, impervious clay:

- mottled reddish brown-gray clay
- purple-gray silty clay and
- yellowish brown-gray silty clay
- siltstones and sandstone layers found at various depths with varying thicknesses.

The depth to the top of the red beds in borings done for engineering purposes ranged from about 3.6 to 9.1 m (12 to 30 ft).

The dry density of the clay ranges from 1.86 to 2.32 g/cm^3 (116 to 145 lb/ft^3), averaging 2.11 g/cm^3 (132 lb/ft^3). The red, reddish-brown or purple silty clays range in moisture content from 2.5% to 25%, averaging 8% 12% for most samples. Liquid limits for the clays range from 35% to 55% with plasticity indices ranging from 24 to 38. Percent passing the #200 sieve for the clays ranges from 87% to 99.8%.

The measured permeabilities for the reddish brown silty clays, sandstones and siltstones indicate the clay is highly impervious. The siltstones are slightly more permeable but still have relatively low permeability.

Unconfined compressive tests on the clay resulted in values of 136,000 kg/m^2 to 485,000 kg/m^2 (13.9 to 49.7 tons/ft^2) with an average value of 293,000 kg/m^2 (30 tons/ft^2).

A geotechnical investigation of the NEF site conducted in September 2003 consisted of 5 widely-spaced test borings that extended to depths of about 12 to 30.5 m (40 to 100 ft) using a hollow-stem auger and split-spoon sampling. Based on the boring results, up to 0.6 m (2 ft) of loose eolian sand underlain by dense to very dense, fine- to medium-grained sand and silty sand of the Gatuña/Antlers Formation was encountered. These sands are locally cemented with caliche deposits. Beneath the Gatuña/Antlers Formation is the Chinle claystone, a very hard highly plastic clay, which was encountered at depths of about 10.7 to 12.2 m (35 to 40 ft). One boring extended to 30.5 m (100 ft) deep and ended in the Chinle Formation. Blow-count N-values for about the top 7.6 m (25 ft) of sand and gravel ranged from about 20 to 76. Beneath that horizon the unit becomes denser or contains gravel to the extent that useful blow counts are not obtained. Where caliche cements the sand and gravel, N-values of over 60 are typical. Standard N-values were not available for samples in the underlying clay due to its hardness causing blow counts to range upwards of 100.

For samples from the shallow sand and gravel unit, California Bearing Ratio values of 10.5 and 34.4 were obtained along with a maximum dry density value of 1.97 g/cm^3 (123 lbs/ft^3). Fines in this material were generally non-plastic with 17% to 31% of samples finer than 200 sieve size. Clay samples had relatively high liquid limits of 50% to 60% and plastic limits of 18% to 23%, suggesting high silt content.

Footings bearing in the firm and dense sandy soils below the upper loose eolian soils are estimated to have an allowable bearing pressure of 34,177 kg/m^2 (7,000 lb/ft^3).

3.2.6 Seismology

The majority of earthquakes in the United States are located in the tectonically active western portion of the country. However, areas within New Mexico and the southwestern United States also experiences earthquakes, although at a lower rate and at lower intensities. Earthquakes in the region around the NEF site are isolated or occur in small clusters of low to moderate size events toward the Rio Grande Valley of New Mexico and in Texas, southeast of the NEF site.

3.2.6.1 Seismic History of the Region and Vicinity

The NEF site is located within the Permian Basin as shown on Figure 3.2-17, Tectonic Subdivisions of the Permian Basin (Talley, 1997). Specifically, the site is located near the northern end of the Central Basin Platform (CBP). The CBP became a distinct dividing feature within the Permian Basin as a result of Pennsylvanian and early Permian compressional stresses. This tectonism resulted in a deeper Delaware Basin to the west and shallower Midland Basin to the east of the ridge-like CBP.

The last episode of tectonic activity centered on the late Cretaceous and early Tertiary Laramide Orogeny that formed the Cordilleran Range to the west of the Permian Basin. The Permian Basin region was uplifted to its present position during this orogenic event. There has not been any further tectonic activity since the early Tertiary. Structurally, the Permian Basin has subsided slightly since the Larmaide tectonic event. Dissolution of Permian evaporate layers by groundwater infiltration or possibly from oil and gas extraction is suggested as a possible cause for this observed subsidence.

The 250 million year old Permian Basin is the source of abundant gas and oil reserves that continue to be extracted. These oil fields in southeast New Mexico are characterized as “in mature stage of secondary recovery effort” (Talley, 1997). Water flooding began in the late 1970’s followed by CO_2 flooding now being used to enhance recovery in some fields. Industry case studies describe hydraulic fracturing procedures used in the Queen and San Andres formations near the NEF site that produced fracture half-lengths from 170 to 259 m (560 to 850 ft) in these formations.

Locations of recent tectonic faulting within the 322 km (200 mi) radius of the NEF site located in Lea County, New Mexico, were determined through literature research (DOE, 2003; Machette, 1998; Machette, 2000; USGS, 2004). No Quaternary faults are mapped for the site locale. The nearest recent faulting is situated more than 161 km (100 mi) west of the site (Machette, 1998). Figure 3.2-33, Quaternary Faults in New Mexico, and Figure 3.2-34, Quaternary Faults in Texas, illustrate traces of Quaternary Faults for New Mexico and adjacent areas of west Texas. The Quaternary geologic time period extends from 1.6 million years ago to the present. Other time sub-divisions within the Quaternary include the Late Quaternary that extends from 130,000

years ago to the present, and the Holocene, which includes the most recent 10,000-year time period.

Shown on Figures 3.2-33 and 3.2-34 are 1° Latitude by 2° Longitude geographic blocks. The NEF site is located in the Hobbs geographic block. Geographic blocks containing Quaternary faults are color-coded (i.e., non-gray). Figure 3.2-35, Quaternary Faults Within 322 km (200 mi) of NEF Site, shows geographic blocks for which Quaternary faults are mapped. All of these geographic blocks are located west of the NEF site. Figure 3.2-36, Locations of Nearest Faults to the NEF Site, shows the Quaternary fault locations detailed in the "Map and data for Quaternary faults and folds in New Mexico, U.S. Geological Survey (USGS) Open-File Report 98-521" (Machette, 2000). The block containing the site, as well as others due north, south, and east of the NEF site has no documented Quaternary faults. Quaternary faults within 322 km (200 mi) of the site are shown on Figure 3.2-35 using colored and numbered traces, and are plotted over shaded relief topographic maps. The use of topographic relief maps is highly illustrative, because ground deformations resulting from recent fault movements are usually manifested as prominent linear topographic features.

Figure 3.2-36 provides a summary of Quaternary fault locations, including fault names obtained from the "Map and data for Quaternary faults and folds in New Mexico, USGS Open-File Report 98-521" (Machette, 2000) and the "Earthquake Hazards Program, Quaternary Fault and Fold Database of the United States" (USGS, 2004).

Quaternary-Aged Faults designated as capable within 322 km (200 mi) of the NEF site include the West Delaware Mountain Fault Zone, the Guadalupe Fault, the East Sierra Diablo Fault, the East Flat Top Mountain Fault and the Alamogordo Fault at 185 km (115 mi), 191 km (119 mi), 196 km (122 mi), 200 km (124 mi) and 262 km (163 mi) from the site, respectively. In addition, the East Baylor Mountain – Carrizo Mountain Fault is located 201 km (125 mi) from the NEF and is considered a possible, capable fault, but movement within the last 35,000 years has not been demonstrated.

None of the capable faults pose a ground deformation hazard to the NEF site due to the distances (> 161 km (100 mi)) from the site, the northerly strike of these faults and the associated topographic landforms shown in Figure 3.2-36, Location of Nearest Faults to the NEF Site. The strikes of the assessed capable faults do not project toward the NEF site. Topographic features, like those correlated to the Quaternary faults west of the site, are not present near the NEF site, thus making it an unlikely scenario that unmapped, capable faults are located nearer than 161 km (100 mi) to the NEF site.

The study of historical seismicity includes earthquakes in the region of interest known from felt or damage records and from more recent instrumental records (since early 1960's). Most earthquakes in the region have left no observable surface fault rupture.

Figure 3.2-18, Seismicity Map for 200-Mile Radius of the NEF Site, indicates the location of earthquakes which have occurred within a 322 km (200 mi) radius of the NEF site with magnitude > 0. The earthquakes are also listed in Table 3.2-20, Location of Recorded Earthquakes Within a 322 km (200 mi) Radius of the NEF Site. Figure 3.2-19, Seismicity in the Immediate Vicinity of the NEF Site, indicates the location of earthquakes within about 97 km (60 mi) of the NEF site. Earthquakes, which have occurred within a 322 km (200 mi) radius of the NEF site with a magnitude of 3.0 and greater, are listed in Table 3.2-21, Earthquakes of Magnitude 3.0 and Greater Within 322 km (200 mi) Radius of the NEF Site.

The data reflected in the above figures and tables are from earthquake catalogs from the University of Texas Institute for Geophysics (UTIG, 2002), New Mexico Tech Historical Catalog (NMIMT, 2002), Advanced National Seismic System (USGS, 2003b) and the New Mexico Technical Regional Catalog, exclusive of Socorro New Mexico events (NMIMT, 2002).

Earthquake data for a 322 km (200 mi) radius of the NEF site were acquired from public domain resources. Table 3.2-22, Earthquake Data Sources for New Mexico and West Texas, lists organizations and data sources that were identified and earthquake catalogs that were obtained.

Earthquake parameters (e.g., date, time, location coordinates, magnitudes, etc.) from the data repositories listed in Table 3.2-22 were combined into a uniformly formatted database to allow statistical analyses and map display of the four catalogs. Through a process of comparison of earthquake entries among the four catalogs, duplicate events were purged to achieve a composite catalog. In addition, aftershocks and aftershock sequences were purged from one version of the catalog for computation of earthquake recurrence statistical models, which describe recurrence rates of earthquake main shocks. The composite list of earthquakes, with aftershock and aftershock sequences purged, for the 322 km (200 mi) radius of the NEF site is provided in Table 3.2-20. The regional seismicity map is shown on Figure 3.2-18. Local seismicity is shown on Figure 3.2-19, Seismicity in the Immediate Vicinity of the NEF Site. The large majority of events (i.e., 82%) in the composite catalog originate from the Earthquake Catalogs for New Mexico (exclusive of the Socorro New Mexico immediate area) (NMIMT, 2002) as observed in the event counts in Table 3.2-22. Earthquake magnitudes in these catalogs (NMIMT, 2002) are tied to the New Mexico duration magnitude scale, M_d, that in turn approximate Local Magnitude, M_L. All events in the composite catalog are specified to have an undifferentiated local magnitude.

Table 3.2-21 shows all earthquake main shocks of magnitude 3.0 and larger within a 322 km (200 mi) radius of the NEF site. The largest earthquake within 322 km (200 mi) of the NEF is the August 16, 1931 earthquake located near Valentine, Texas. This earthquake has an estimated magnitude of 6.0 to 6.4 and produced a maximum epicentral intensity of VIII on the Modified Mercalli Intensity (MMI) Scale. The intensity observed at the NEF site is IV on the MMI scale (NMGS, 1976). A copy of the MMI scale is provided in Table 3.2-23, Modified Mercalli Intensity Scale.

The closest of these moderate earthquakes occurred about 16 km (10 mi) southwest of the site on January 2, 1992.

It is noted that the University of Texas Geophysics Institute Catalog of West Texas Earthquakes reports a smaller magnitude of 4.6 and a more easterly epicenter location in Texas. Table 3.2-24, Comparison of Parameters for the January 2, 1992 Eunice, New Mexico Earthquake, shows the location and size parameters for the Earthquake. Parameters given by New Mexico Tech Regional Catalog were adopted for the seismic hazard assessment of the NEF site.

3.2.6.2 Correlation of Seismicity with Tectonic Features

Earthquake epicenters scaled to magnitude for the site region are plotted over Permian Basin tectonic elements on Figure 3.2-20, Regional Seismicity and Tectonic Elements of the Permian Basin. Most epicenters lie within the Central Basin Platform, however, earthquake clusters also occur within the Delaware and Midland Basins. Although events local to the NEF site are likely

induced by gas/oil recovery methods, the resulting ground motions are transmitted similar to earthquakes on tectonic faults and impacts at the NEF site are analyzed using standard seismic hazard methods. Furthermore, given the published uncertainties on discrimination between natural and induced seismic events and that earthquake focal depths, critical for correlation with oil/gas reservoirs, are largely unavailable, the January 2, 1992 event is attributed to a tectonic origin. For this magnitude 5 earthquake, focal depths range from 5 km (3.1 mi) (USGS, 2004) to 12 km (7.5 mi) (DOE, 2003). Therefore, studies conclude that seismological data are insufficient for this moderate earthquake to constrain the depth sufficiently to permit a correlation with local oil/gas producing horizons.

Analysis of the spatial density of earthquakes in the composite catalog is shown on Figure 3.2-21, Earthquake Frequency Contours and Tectonic Elements of the Permian Basin. This form of spatial analysis has historically been used to define the geometry of seismic source zones for seismic hazard investigations (USGS, 1997; USGS, 1976a). Seismic source areas for the NEF site region are determined on the basis of the earthquake frequency pattern shown on Figure 3.2-22, Seismic Source Areas for Earthquake Frequency Statistical Analyses. The NEF site is located near the northern end of the region of highest observed earthquake frequency within the CBP of the Permian Basin.

The Waste Isolation Pilot Plant (WIPP) Safety Analysis Report (SAR) (DOE, 2003) suggests that the cluster of small events located along the CBP (Figure 3.2-20) are not tectonic in origin, but are instead related to water injection and withdrawal for secondary recovery operations in oil fields in the CBP area. Such a mechanism for the CBP seismic activity could provide a reason why the CBP is separable from the rest of the Permian Basin on the basis of seismicity data but not by using other common indicators of tectonic character. Both the spatial and temporal association of CBP seismicity with secondary recovery projects at oil fields in the area are suggestive of some cause and effect relationship of this type.

3.2.6.3 Earthquake Recurrence Models

Earthquake recurrence models describe the exponential frequency versus magnitude behavior observed for earthquake activity (Gutenberg, 1944). The exponential recurrence model is commonly shown as Equation [3.2-1].

$$\mathrm{Log}_{10}\, N_C = a + b(M) \qquad \text{[Eq. 3.2-1]}$$

Where: N_C = cumulative number per time duration (i.e., per year)
a = a-value, indicator of activity rate
$b(M)$ = b-value, with negative slope due to observation that smaller magnitude events occur more frequently than larger magnitude events. Typical range of b-values is -0.5 to -1.5, normally closer to -1.0.

Earthquake recurrence models were computed for the entire 322 km (200 mi) radius composite catalog and for two smaller regions. The smaller regions are defined by patterns of seismic activity as noted at closer distances to the site. Region 1 shown on Figure 3.2-22 includes clusters of earthquakes within an approximate 161 km (100 mi) radius of the site. The second sub-region includes the high-density earthquake pattern observed in the CBP. A tectonic origin for all events in the CBP was conservatively assumed.

Results of statistical analyses performed on the 322 km (200 mi) composite catalog and two sub-regions are illustrated on Figures 3.2-23 through 3.2-25. Best fit models and models for

which the b-value is constrained to a value of -0.9 were computed. These models are numerically compared in Table 3.2-25, Earthquake Recurrence Models for the NEF Site Region.

Earthquake recurrence models provided in the WIPP SAR (DOE, 2003) for more distant seismic zones including the two Rio Grande Rift source zone alternatives (see Figure 3.2-26, Alternate Seismic Source Geometries Used in the WIPP Seismic Hazard Study) were used in the hazard assessment of the NEF site. Recurrence models from the WIPP SAR (DOE, 2003) are shown in Table 3.2-32, Horizontal Response Spectrum for the 10,000-Year Design Earthquake. Preparers of the WIPP SAR (DOE, 2003) expressed an opinion that magnitudes in the available earthquake catalog (pre-1983) were underestimated. Therefore, two models were used to address this magnitude scaling issue. The model for corrected magnitude raised the a-value in the recurrence models by 0.5 units. Both the magnitude-corrected and uncorrected recurrence models are listed in Table 3.2-26, Earthquake Recurrence Models for the CBP in the WIPP SAR.

3.2.6.4 Probabilistic Seismic Hazard Analysis

3.2.6.4.1 Ground Motion Attenuation Models

A site-specific probabilistic seismic hazard analysis was performed for the NEF site using the seismic source zone geometries shown on Figures 3.2-22 and 3.2-26 and earthquake recurrence models listed in Tables 3.2-25 and 3.2-26. Seismic hazard computations were performed using the EQRISK computer program (Cornell, 1968; USGS, 1976b).

In addition to seismic source zones and earthquake recurrence models, computations of probabilistic seismic hazard require ground motion attenuation models suited for the regional and local seismic wave transmission characteristics. Two attenuation models were used in the analysis. The WIPP SAR (DOE, 2003) selected an attenuation model developed by O.W. Nuttli (US Army WES, 1973) for application in the central United States. This model was selected due to the precedence of its usage in the WIPP SAR seismic hazard assessment, and to its conservative predictions compared to other published models. This ground acceleration model is given in Equation 3.2-2.

$$Ln(a) = 2.833 + 0.92(M_L) - 1.0(Ln(R)) \qquad \text{[Eq. 3.2-2]}$$

Where: a = horizontal ground acceleration in cm/s^2 units
M_L = Local Magnitude
R = distance from the earthquake focus to the site

Sensitivity to the attenuation model was studied by calculating seismic hazard curves for an attenuation model that approximates the Toro peak ground acceleration model (Toro, 1997). This model is provided in Equation 3.2-3 and is illustrated on Figure 3.2-27, Comparison of PGA Attenuation for a Magnitude 5.0 Earthquake.

$$Ln(a) = 2.80 + 0.92(M_L) - 1.05(Ln(R)) - 0.003(R) \qquad \text{[Eq. 3.2-3]}$$

Where: a = horizontal ground acceleration in cm/s^2 units
M_L = Local Magnitude
R = distance from the earthquake focus to the site

It is noted that the Toro attenuation model provides coefficients for magnitudes scaled to the Lg-phase, m_{bLg}, and for Moment magnitude, M_O. Due to the magnitude scaling of events in the composite catalog, the moment magnitude scaling is preferred to Lg magnitude scaling for the

Toro model. In addition, the Toro model has a more sophisticated functional form that flattens the PGA predictions at distances less than 10 km (6.2 mi).

In addition, probabilistic response spectra (i.e. uniform hazard response spectra) are computed for the NEF site using the Nuttli spectral attenuation models (Nuttli, 1986) listed in Table 3.2-27, Attenuation Model Formulas and Coefficients. The Nuttli spectral velocity attenuation models are considered to predict ground motions at “firm rock” conditions, which is the rock condition attributed to the Triassic Age claystones underlying the NEF site. For comparative purposes, the Nuttli (Nuttli, 1986), Toro (Toro, 1997) and WIPP SAR Nuttli (US Army WES, 1973) attenuation models are plotted on Figure 3.2-21 along with the McGuire (EPRI, 1988) attenuation model and the approximation of the Toro attenuation models.

3.2.6.4.2 Probabilistic Seismic Hazard Results

Total seismic ground motion hazard to a site results from summation of ground motion effects from all distant and local seismically active areas. The contribution to total hazard at the NEF site from more distant seismic activity in the Rio Grande Rift zones is examined first. As noted above, seismic source zone geometries (Figure 3.2-26) and recurrence rates (Table 3.2-26) were taken directly from the WIPP SAR (DOE, 2003). Recurrence rates for the magnitude corrected, and magnitude uncorrected recurrence models were used in the hazard calculations. This recurrence model variation coupled with two seismic source zone geometries results in four seismic hazard curves. In addition, maximum magnitudes of 7.8 for the Rio Grande Rift (DOE, 2003) were used for this hazard calculation. Peak ground acceleration seismic hazard results at the NEF site from the Rio Grande Rift source zone alternatives are listed in Table 3.2-28, Seismic Hazard Results at NEF Site From Rio Grande Rift Seismic Source Zones. These hazard results are plotted on Figure 3.2-28, Seismic Hazard at the NEF Site From Rio Grande Rift Seismic Sources. Seismic hazard curves shown on Figure 3.2-28 are annotated to identify the 250-year, 475-year and 10,000-year earthquake levels. It is noted that the 475-year event in most cases is strictly defined as the event with a 10% probability of being exceeded in 50 years. Strict maintenance of this probability in 50-years equates to an annual probability of 0.0021 of exceeding a 0.10 g peak horizontal acceleration and a return period of 475-years.

Seismic hazard results for the NEF site due to seismic activity in local seismic zones (i.e. seismic zones that contain the site) are listed in Table 3.2-29, Seismic Hazard Results at NEF Site From Local Source Zones. Seismic hazard curves are plotted on Figure 3.2-29, Seismic Hazard at the NEF Site From Local Seismic Zone Sources. Local seismic zones include those geometries shown on Figure 3.2-22. The largest zone includes the 322 km (200 mi) radius of the NEF site for which earthquake data were assembled. The largest earthquake contained in this 322 km (200 mi) zone is the 1931 Valentine, Texas, event with an estimated magnitude of 6.0 to 6.4. Alternative maximum magnitudes, M_X, of 6.5 and 6.0 are assigned to this 322 km (200 mi) region for seismic hazard computations.

The alternative local seismic source zone geometry is defined within a more limited site radius of 161 km (100 mi). Embedded within this 161 km (100 mi) zone is the sub-region defined by the enhanced density of earthquake epicenters centered on the CBP (see Figure 3.2-21 and Figure 3.2-22). The maximum historical earthquake within these zones is the January 2, 1992, earthquake. A maximum magnitude of 6.0 is used for computation of seismic hazard curves. An identical maximum magnitude of 6.0 was specified in the WIPP SAR (DOE, 2003) for its CBP seismic source zone alternatives. In addition, the WIPP study used a smaller maximum magnitude of 5.0 in their hazard analysis due to the lack of recent geologic evidence of

tectonism and likely association of events with secondary oil/gas recovery efforts in this area. Sensitivity to the maximum magnitude parameter is examined by computing seismic hazard curves for M_X set to 6.0 as well as to 5.25 for the 161 km (100 mi) zone and the CBP embedded zone. Seismic hazard results shown in Table 3.2-29 and on Figure 3.2-29, illustrate the various sensitivities to choices of seismic source zones, attenuation models and maximum magnitudes, M_X.

Figure 3.2-30, Zoom of Seismic Hazard at the NEF Site From Local Seismic Zone Sources, provides a zoomed-in view of the calculated seismic hazard curves for the NEF site. Table 3.2-30, Peak Acceleration Seismic Hazard Summary for the NEF Site, provides an interpretation of these hazard curves for the 250-year and 475-year earthquake levels.

Total seismic ground motion hazard to a site results from summation of ground motion effects from all distant and local seismically active areas. A total of 12 seismic hazard curves were developed for a combination of various source zones, attenuation models, b-values and upper bound magnitudes. For the purpose of selecting the characteristic peak ground acceleration associated with specific return periods, a resultant seismic hazard curve was developed through a weighted average of the individual curves. The seismic hazard curves and weighted average hazard result are shown in Figure 3.2-29 and Figure 3.2-30.

The 250-year and 475-year return period peak horizontal ground accelerations are estimated at 0.024 g and 0.036 g, respectively. The 10,000-year return period peak horizontal ground acceleration is estimated at 0.15 g. This return period is equivalent to a mean annual probability of 1.0 E-4.

Since it is currently not possible to definitively differentiate natural tectonic from induced seismic events in the study region, the probabilistic seismic hazard estimates for the NEF site assumed a tectonic origin for all events in the CBP sub-region. However, for cases of uncertainty, sensitivity analyses provide valuable insights into the impacts of induced earthquakes on the seismic hazard analysis. The following sensitivity analysis results are provided to show trends in seismic hazard results for assumptions that increasing percentages of earthquakes in the CPB seismic source zone are induced by oil/gas recovery activities.

Two hypotheses are considered in the seismic hazard sensitivity analyses. First is the case that a fraction of earthquakes of all magnitudes are induced. Second is the case that only smaller magnitude earthquakes (e.g., less than M=3.5) are likely induced while larger events result from tectonic processes. For the first case, the hypothesis is that a large fraction of events in the CBP was induced by oil/gas recovery efforts, is modeled by scaling the CBP recurrence model by factors of 0.15, 0.5, and 0.85. These scaling factors are applied to the entire recurrence model such that the predicted frequencies of events for all magnitudes are scaled by these factors. The three scaling factors are used to model the general commentary that a “large fraction” of CPB events are induced. For the second case, the concept that many of the small events could be induced while larger events have tectonic origins is modeled by re-computation of the recurrence model for the CPB following removal of 50% of events with magnitudes less than 3.5. This second case results in a recurrence model that predicts relatively fewer small magnitude events, and recurrence rate of larger events of magnitude 5.0 and greater remains unchanged.

Seismic hazard sensitivity results only show a significant impact when a scaling factor of 0.15 is applied to the total recurrence model. For this case, peak horizontal acceleration is reduced from about 0.15 g to about 0.10 g at 1.0 E-4 annual exceedance probability. Application of a

scaling factor of 0.50 to the entire model resulted in a peak horizontal acceleration near 0.13 g at 1.0 E-4 annual exceedance probability. Two of the cases, scaling the entire recurrence model by 0.85, and determination of a new model based on removal of 50% of events smaller than M=3.5, showed little sensitivity. Given uncertainties related to the tectonic vs. induced nature of larger regional events, and high likelihood that many smaller events are induced by ongoing oil/gas recovery activities, results of the last sensitivity analysis (e.g. removal of smaller events only) are preferred. The negligible sensitivity to removal of smaller events emphasizes that seismic hazard in large part is determined by the assessed regional frequency of events with magnitudes larger than 5.0.

3.2.6.4.3 Uniform Hazard Response Spectra

Probabilistic ground motion response spectra are derived for the NEF site using a combination of the Nuttli spectral attenuation model (Nuttli, 1986) and appropriate soil amplification factors currently used in Seismic Building Code applications. The Nuttli spectral velocity attenuation models are considered to predict ground motions at “firm rock” conditions, which is the rock condition attributed to the Triassic Age claystones underlying the NEF site. Descriptive characterization of the site surficial material composition and thickness supports a site soil classification of C. This site class (Dobry, 2000) accommodates gravelly soils underlain by soft rocks, which appear to be present at the site. Soil amplification factors for Site Class C include:

For $S_s < 0.25$; short period site amplification factor, $F_a = 1.2$
For $S_l < 0.10$; long period site amplification factor, $F_v = 1.7$
Where S_s and S_l are short and long period
rock acceleration levels, respectively.

Horizontal component bedrock and ground surface response spectra (five percent damping ratio) for soil profile type C for the 10,000-year earthquake are plotted on Figure 3.2-31, Horizontal Response Spectra for the 10,000-Year Earthquake, Bedrock and Soil Class C for the NEF Site. By definition of their calculation, these response spectra have an equal probability of 0.005% of being exceeded in 50 years at each period in the range of 0.02 to 2.0 s.

Horizontal and vertical component uniform hazard response spectra (five percent damping) for the 10,000-year earthquake at ground surface for Soil Class C are plotted on Figure 3.2-32. Vertical component earthquake response spectra are recommended in NRC Regulatory Guide 1.60 (NRC, 1973) to be determined as a function of frequency. Table 3.2-31, Regulatory Guide 1.60 Ratio of Vertical to Horizontal Component Design Response Spectra, summarizes the ratio of vertical and horizontal component earthquake response spectra.

The vertical component 10,000-year response spectrum was determined using the formulation shown in Table 3.2-31.

Numerical values for the 10,000-year horizontal and vertical design response spectra for five percent damping are listed in Table 3.2-32, Horizontal Response Spectrum for the 10,000-Year Design Earthquake, and Table 3.2-33, Vertical Response Spectrum for the 10,000-Year Design Earthquake, respectively.

3.2.6.5 Selection of the Design Basis Earthquake

While conducting the Integrated Safety Analysis (ISA), an unmitigated accident due to a seismic event was assumed to result in high public consequences. Therefore, the likelihood of the

event (seismically-induced high public consequences) needs to be “highly unlikely.” In accordance with NUREG-1520 (NRC, 2002), for the NEF this equates to a probability of occurrence of less than 1.0 E-5 per year.

To define the design basis earthquake (DBE), information from DOE Standard DOE-STD-1020-2002 (DOE, 2002) and ASCE Standard Seismic Design Criteria (ASCE, 2003) was considered along with the results of the seismic portion of the ISA and the site-specific probabilistic seismic hazard analysis performed for the NEF site.

The DOE and ASCE standards outline a methodology to demonstrate compliance to a target performance goal of 1.0 E-5 annual probability by designing to a seismic hazard of 1.0 E-4 annual probability. The difference between the design level and the performance target is accounted for in the detailed design process by confirmatory calculations.

Based on these approaches, the DBE for the NEF has been selected as the 10,000-year (1.0 E-4 mean annual probability) earthquake. For the NEF, following the DOE or ASCE approach provides a risk reduction ratio of design to target performance of 10 (1.0 E-4/1.0 E-5). This DBE will be used in the detailed design process to demonstrate compliance with the overall ISA performance requirements. This will be accomplished by confirmatory seismic performance calculations for the seismic Items Relied on for Safety (IROFS) during detailed design. The DOE and ASCE standards address design and evaluation of structures, systems, and components (SSCs). The equivalents of SSCs for the NEF are considered to be the IROFS and the items that may affect the function of IROFS. The objective of the NEF seismic design approach is to demonstrate that use of this DBE achieves a likelihood of unacceptable performance of less than approximately 1.0 E-5 per year, by introducing sufficient design safety margins, i.e., conservatism, during the design process to allow for demonstration of compliance to the target performance goal. The DOE and ASCE standards implement this objective using slightly different methodologies with the same end result, i.e., demonstration of compliance to the target performance goal.

In the DOE approach, the deterministic seismic evaluation and acceptance criteria are structured to achieve less than a 10% probability of unacceptable performance for a SSC subjected to the scaled design/evaluation basis earthquake (SDBE). The SDBE is defined in the DOE approach as the product of the DBE times a factor of 1.5 and a scale factor, which is a function of the slope of the seismic hazard curve.

The ASCE approach is based on achieving the target performance goal annual frequencies by incorporating sufficient conservatism in the seismic demand and structural capacity evaluations to achieve both of the following:

- Less than about a 1% probability of unacceptable performance for the DBE ground motion
- Less than a 10% probability of unacceptable performance for a ground motion equal to 150% of the DBE ground motion

The ASCE method is based on achieving both of the above probability goals, which represent two points on the underlying fragility curve. Meeting these two probability goals allows the target performance probabilities to be achieved with less possibility of non-conservatism. The resulting nominal factors of safety against conditional probability of failure are 1.0 and 1.5, respectively, for the above two goals.

The actual seismic design detailed approach for NEF will be based on the DOE or ASCE method and finalized prior to detailed design. The safety margins will be representative of those discussed above and described in more detail in the DOE and ASCE standards.

The difference between the mean annual probabilities for design (1.0 E-4) and performance (1.0 E-5) is achieved through conservatism in the design (factors of safety), elasticity in the structures, and conservatism in the evaluation of the design.

The design response spectra, horizontal and vertical, are based on the 10,000-year uniform hazard response spectra described in Section 3.2.6.4.3, Uniform Hazard Response Spectra. The soil amplification factors described in Section 3.2.6.4.3 will be verified during the detailed design phase of the NEF project.

3.2.7 Stability of Subsurface Materials

A geotechnical investigation of the site conducted in September 2003 consisted of 5 widely-spaced test borings that extended to depths of about 12 to 30.5 m (40 to 100 ft) using a hollow-stem auger and split-spoon sampling. Based on the boring results, up to 0.6 m (2 ft) of loose eolian sand underlain by dense to very dense, fine- to medium-grained sand and silty sand of the Gatuña/Antlers Formation was encountered. These sands are locally cemented with caliche deposits. Beneath the Gatuña/Antlers Formation is the Chinle claystone, a very hard highly plastic clay, which was encountered at depths of about 10.7 to 12.2 m (35 to 40 ft). One boring extended to 30.5 m (100 ft) deep and ended in the Chinle Formation. Blow-count N-values for about the top 7.6 m (25 ft) of sand and gravel ranged from about 20 to 76. Beneath that horizon the unit becomes denser or contains gravel to the extent that useful blow counts are not obtained. Where caliche cements the sand and gravel, N-values of over 60 are typical. Standard N-values were not available for samples in the underlying clay due to its hardness causing blow counts to range upwards of 100.

For samples from the shallow sand and gravel unit, California Bearing Ratio values of 10.5 and 34.4 were obtained along with a maximum dry density value of 1.97 g/cm^3 (123 lbs/ft^3). Fines in this material were generally non-plastic with 17% to 31% of samples finer than 200 sieve size. Clay samples had relatively high liquid limits of 50% to 60% and plastic limits of 18% to 23%, suggesting high silt content.

Footings bearing in the firm and dense sandy soils below the upper loose eolian soils are estimated to have an allowable bearing pressure of 34,177 kg/m^2 (7,000 lbs/ft^3).

The five borings are not sufficient to adequately define subsurface conditions for final design purposes, but they are acceptable for judging the feasibility of developing the site. Assuming that the borings are generally representative of subsurface conditions, the site is considered acceptable for the facility features supported on a system of shallow foundations.

The surface deposits silty sands will be removed to expose the more firm soil structures. In this case, footings bearing in the firm and dense sandy soils below the upper, loose eolian soils can be designed for an allowable bearing pressure of 34,000 kg/m^2 (7,000 lb/ft^2). Due consideration will be given to settlement and differential settlement during final design. Final design details will be based on a more comprehensive geotechnical investigation to be undertaken when additional project details are available.

3.2.7.1 Liquefaction Susceptibility

Liquefaction potential is greatest where the groundwater level is shallow; and submerged, loose fine sands occur within a depth of about 15 m (50 ft). Liquefaction potential decreases as grain size and clay and gravel content increase.

The soils at the site are dense to very dense. Groundwater was encountered in the site soil borings drilled to a depth of more than 30 m (100 ft) below the ground surface. The nature of the soils and the absence of groundwater near the surface would make the potential for liquefaction remote.

3.2.8 References

AMS, 1996. Glossary of Weather and Climate, With Related Oceanic and Hydrologic Terms, American Meteorological Society, 1996.

ASCE, 1998. Minimum Design Loads for Buildings and Other Structures, ASCE 7-98, American Society of Civil Engineers, 1998.

ASCE, 2003. Seismic Design Criteria for Structures, Systems, and Components in Nuclear Facilities and Commentary (Draft Standard), American Society of Civil Engineers, Nuclear Standards Committee, Dynamic Analysis of Nuclear Structures Subcommittee, July 2003

ASTM, 1993. Classification of Soils for Engineering Purposes, ASTM Standard D2487-93, American Society Testing Materials, 1993.

Cornell, 1968. Engineering seismic risk analysis, C.A. Cornell, Bulletin of the Seismological Society of America, Vol. 58, p. 1583-1606, 1968.

Dobry, 2000. New Site Coefficients and Site Classification System Used in Recent Building Seismic Code Provisions, Earthquake Spectra, Vol. 16, No. 1, pp. 41-67, R. Dobry, R.D. Borcherdt, C.B. Crouse, I.M. Idriss, W.B. Joyner, G.R. Martin, M.S. Power, E.E. Rinne, R.B. Seed, 2000.

DOE, 2002. Natural Phenomena Hazards Design and Evaluation Criteria for Department of Energy Facilities, DOE-STD-1020-2002, Department of Energy, January 2002.

DOE, 2003. WIPP Contact-Handled (CH) Waste Safety Analysis Report, DOE/WIPP-95-2065 Rev. 7, Department of Energy, June 2003.

DOT, 2002. Pipeline Statistics 1998-2001, Office of Pipeline Safety, Department of Transportation, 2002.

DOT, 2003. Airport Master Record, Federal Aviation Administration NR: 14606.1 *A, Department of Transportation, July 2003.

EPRI, 1988. Engineering Estimates of Earthquake Ground Motion for Eastern North America, NP-6074, Electrical Power Research Institute, 1988.

FEMA, 1978. Flood Hazard Boundary Map, City of Eunice, NM, Community No. 350028B, Federal Emergency Management Agency, August 1978.

Gutenberg, 1944. Frequency of earthquakes in California, B. Gutenberg and C.F. Richter, Bulletin of the Seismological Society of America, vol. 34, pp. 185-188, 1944.

Grazulis, 1993. Significant Tornadoes, 1680-1991, Environmental Films, July 1993.

LES, 2003. National Enrichment Facility Environmental Report, Louisiana Energy Services, December 2003.

Machette, 1998. Map of Quaternary Faults and Folds in New Mexico and Adjacent Areas, M.N. Machette, S.F. Personius, K.I. Kelson, K.M. Haller and R.L. Dart, 1998.

Machette, 2000. Map and Data for Quaternary Faults and Folds in New Mexico, Open-File Report 98-521, M.N. Machette, S.F. Personius, K.I. Kelson, K.M. Haller, and R.L. Dart, 2000.

Marshall, 1973. Lightning Protection, J. L. Marshall, 1973.

NMBMI, 2001. Mines, Mills and Quarries in New Mexico, 2001, New Mexico Bureau of Mine Inspection, 2001.

NMEMNRD, 2003. Potash Map, New Mexico Energy, Minerals and Natural Resources Department, 2003.

NMGS, 1976. New Mexico's Earthquake History, 1849-1975, in Tectonics and Mineral Resources of Southwestern North America, S.S. Northrup, New Mexico Geological Society, Special Publication No. 6, pp. 77-87, 1976.

NMIMT, 1977. Surficial Geology of Southeast New Mexico, Geologic Map 41, New Mexico Bureau of Mines and Mineral Resources, New Mexico Institute of Mining and Technology, 1977.

NMIMT, 2002. Earthquake Catalogs for New Mexico and Bordering Areas: 1869-1998, New Mexico Bureau of Geology and Mineral Resources, New Mexico Institute of Mining and Technology, Circular 210, 2002.

NMIMT, 2003. Geologic Map of New Mexico, New Mexico Bureau of Geology and Mineral Resources, a Division of New Mexico Institute of Mining and Technology, 2003.

NOAA, 1982. Application of Probable Maximum Precipitation Estimates – United States East of the 105th Meridian, Hydrometeorological Report No. 52, National Oceanic and Atmospheric Administration, August 1982.

NOAA, 2002a. Local Climatological Data Annual Summary with Comparative Data for Midland-Odessa, Texas, National Oceanic and Atmospheric Administration, ISSN 0198-5124, 2002.

NOAA, 2002b. Local Climatological Data Annual Summary with Comparative Data for Roswell, New Mexico, National Oceanic and Atmospheric Administration, ISSN 0198-3512, 2002.

NRC, 1973. Design Response Spectra for Seismic Design of Nuclear Power Plants, Regulatory Guide 1.60, Rev. 1, U.S. Nuclear Regulatory Commission, December 1973.

NRC, 1981. Standard Review Plan for Review of Safety Analysis Reports for Nuclear Power Plants, Section 3.5.1.6, Aircraft Hazards, NUREG-0800 Rev. 2, U.S. Nuclear Regulatory Commission, July 1981.

NRC, 2002. Standard Review Plan for the Review of License Application for a Fuel Cycle Facility, NUREG-1520, U.S. Nuclear Regulatory Commission, March 2002.

Nuttli, 1986. Nuttli-Newmark attenuation model, Letter to Dr. Jean Savy of Lawrence Livermore National Laboratory dated September 19, 1986.

NWS, 2003. Colorado Lightning Resource Center, National Weather Service, 2003.

Rainwater, 1996. Evaluation of Potential Groundwater Impacts by the WCS Facility in Andrews County, Texas, K. Rainwater, Submitted to the Andrews Industrial Foundation, December 1996.

TTUWRC, 2000. Geology of the WCS-Flying W Ranch, Andrews County, Texas, Texas Tech University Water Resources Center, April 2000.

Talley, 1997. Characterization of a San Andres Carbonate Reservoir Using Four Dimensional, Multicomponent Attribute Analysis, D.J. Talley, 2003.

Toro, 1997. Model of Strong Ground Motions from Earthquakes in Central and Eastern North America: Best Estimates and Uncertainties, Seismological Research Letters, Vol. 68, No. 1, pp. 41-57, G.R. Toro, N.A. Abrahamson, J.F. Schneider, 1997.

UTIG, 2002. Compendium of Texas Earthquakes, University of Texas Institute for Geophysics, 2002.

US Army WES, 1973. Design Earthquake for the Central United States, Miscellaneous Paper, S-73-1, U. S. Army Waterways Experiment Station, 1973.

USDA, 1974. Soil Survey of Lea County, New Mexico, United States Department of Agriculture, Soil Conservation Service, January 1974.

USGS, 1976a. A probabilistic estimate of maximum ground acceleration in rock in the contiguous United States, S.T. Algermissen, D.M. Perkins, U.S. Geological Survey Open File Report 76-416, 44 p, U.S. Geologial Survey, 1976.

USGS, 1976b. EQRISK, Evaluation of earthquake risk to a site, R.K. McGuire, Open-File Report 76-67, U.S. Geological Survey, 1976.

USGS, 1979. Topographic Quadrangle Map for Eunice NE, Tex-NM, 1:24,000 scale, U. S. Geological Survey, Photorevised, 1979.

USGS, 1997. Seismic Hazard Maps for the Conterminous United States: U. S. Geological Survey Open-File Report 97-130, Frankel, A.C., C.S. Mueller, T.P. Barnhard, D.M. Perkins, E.V. Leyendecker, N,C. Dickman, S.L. Hanson, and M.G. Hopper, U.S. Geological Survey, 1997.

USGS, 2003a. Peak Streamflow for New Mexico, United States Geological Survey 08437620 Monument Draw Tributary Near Monument, NM, U.S. Geological Survey, 2003.

USGS, 2003b. Advanced National Seismic System, U.S. Geological Survey, 2003.

USGS, 2004. Earthquake Hazards Program, Quaternary Fault and Fold Database of the United States, U.S. Geological Survey, 2004.

Walvoord, 2002. Deep Arid System Hydrodynamics – 1. Equilibrium States and Response Times in Thick Desert Vadose Zones, Water Resources Research, Vol. 38, No. 12, pp.44-1 to 44-15, M.A. Walvoord, M.A. Plummer, and F.M. Phillips, 2002.

WB, 1956. Hydrometeorological Report No. 33, Seasonal Variations of the Probable Maximum Precipitation East of the 105th Meridian for Areas from 10 to 1,000 Square Miles and Durations of 6, 12, 24 and 48 Hours, Weather Bureau, 1956.

WBG, 1998. Atomic Vapor Laser Isotope Separation Enrichment Facility, Lea County, New Mexico, Weaver, Boos & Gordon, Inc., 1998.

WRCC, 2003. Hobbs, New Mexico, NCDC 1971-2000 Monthly Normals, Desert Research Institute, Western Regional Climate Center, 2003.

TABLES

Table 3.2-1 Population and Population Projections, 1970-2040

Topic	Area				
	Lea County, NM	Andrews County, TX	Lea-Andrews Combined	New Mexico	Texas
Population/Projected Growth					
1970	49,554	10,372	59,926	1,017,055	11,198,567
1980	55,993	13,323	69,316	1,303,303	14,225,512
1990	55,765	14,338	70,103	1,515,069	16,986,510
2000	55,511	13,004	68,515	1,819,046	20,851,820
2010	60,702	15,572	76,274	2,091,675	23,812,815
2020	62,679	16,497	79,176	2,358,278	26,991,548
2030	64,655	17,423	82,078	2,624,881	30,170,281
2040	66,631	18,348	84,979	2,891,483	33,349,013
Percent Change					
1970-1980	13.0	28.5	15.7	28.1	27.0
1980-1990	-0.4	7.6	1.1	16.2	19.4
1990-2000	-0.5	-9.3	-2.3	20.1	22.8
2000-2010	9.4	19.7	11.3	15.0	14.2
2010-2020	3.3	5.9	3.8	12.7	13.3
2020-2030	3.2	5.6	3.7	11.3	11.8
2030-2040	3.1	5.3	3.5	10.2	10.5

Source: U. S. Census Bureau

Table 3.2-2 Educational Facilities Near the Site

School	Grades	Distance km (mi)	Direction	Population	Student-Teacher Ratio
Lea County, New Mexico					
Eunice High School	9-12	8.6 (5.3)	W	207	16:1
Caton Middle School	6-8	8.6 (5.3)	W	128	15:1
Mettie Jordan Elementary School	DD, K-5	8.6 (5.3)	W	269	21:1
Eunice Holiness Academy	1-12	8.2 (5.1)	W	14	6:1

Note: DD = Development Delayed Class

Source: Eunice School District
National Center for Educational Statistics
U.S. Census Bureau

Table 3.2-3 Land Use Within 8 km (5 mi) of the Site

Classification	Area						Percent	Description
	(Hectares)			(Acres)				
	New Mexico	Texas	Total	New Mexico	Texas	Total		
Built Up	243	0	243	601	0	601	1.2	Residential; industrial; commercial services
Rangeland	12,714	7,213	19,927	31,415	17,823	49,238	98.5	Herbaceous rangeland; shrub and brush rangeland; mixed rangeland
Barren	69	0	69	170	0	170	0.3	Bare exposed rock; transitional areas; beaches; sandy areas other than beaches
Total	13,026	7,213	20,239	32,186	17,823	50,009	100.0	

Table 3.2-4 Agriculture Census, Crop, and Livestock Information
Page 1 of 2

Information	County			
	Lea (New Mexico)		Andrews (Texas)	
Census Data (1992 & 1997)	1997	1992	1997	1992
Number of Farms	528	544	142	134
Total Land in Farms ha (acres)	810,161 (2,001,931)	869,861 (2,149,450)	335,431 (828,859)	389,545 (962,576)
Avg. Farm Size ha (acres)[1]	1,535 (3,792)	1,599 (3,951)	2,362 (5,837)	2,907 (7,183)
Crop Annual Average Yields (Most Current)	Area Harvested Hectares (Acres) in 2001	Yield per Hectare (Acre) in 2001	Area Harvested Hectares (Acres) in 2002	Yield per Unit Area in 2001
Chili Peppers	324 (800)	4.49 MT/ha (2.0 tons/acre)	0	0
Wheat	3,035 (7,500)	3.91 m^3/ha (45.0 bu/acre)	81 (200)	2.61 m^3/ha (30 bu/acre)
Grain Sorghum	688 (1,700)	3.66 m^3/ha (42.1 bu/acre)	688 (1,700)	1,384 kg/ha (1,235 lb/acre)
Peanuts	5,828 (14,400)	3,182 kg/ha (2,840 lb/acre)	2,266 (5,600)	4,521 kg/ha (4,035 lb/acre)
All Hay	4,047 (10,000)	10.9 MT/ha (4.72 tons/acre)	0	0
Alfalfa Hay	2,428 (6,000)	13.6 MT/ha (6.0 tons/acre)	0	0
Pecans[2]	213 (526)	0	0	0
Upland Cotton	8,984 (22,200)	703 kg/ha (627 lb/acre)	7,811 (19,300)	435 kg/ha (388 lb/acre)

Table 3.2-4 Agriculture Census, Crop, and Livestock Information
Page 2 of 2

Information	County	
	Lea (New Mexico)	**Andrews (Texas)**
Livestock (Most Current)	Number in 2001	Number in 2002
All Cattle	82,000	13,000
Beef Cows	27,000	6,000
Milk Cows	25,000	0
Other Cattle (includes cattle on feed)	30,000	0
Sheep and Lambs	4,000	0

1 Average Value per ha (acre) [1998]: New Mexico $536 ($217)/Texas $1,465 ($593) (USDA, National Agricultural Statistical Service)

2 1997 Census Data

Table 3.2-5 Midland-Odessa, Texas, Wind Data
1961-1990
Page 1 of 1

	Jan	Feb	Mar	Apr	May	Jun	Jul	Aug	Sept	Oct	Nov	Dec	Year
Mean Speed m/sec (mi/hr)	4.6 (10.4)	5.0 (11.2)	5.5 (12.4)	5.6 (12.6)	5.5 (12.4)	5.5 (12.2)	4.8 (10.7)	4.4 (9.9)	4.4 (9.9)	4.4 (9.9)	4.6 (10.3)	4.5 (10.1)	4.9 (11.0)
Prevailing Direction degrees from True North	180	180	180	180	180	160	160	160	160	180	180	180	180
Max 5-second speed m/sec (mi/hr)	22.8 (51.0)	23.2 (52.0)	24.1 (54.0)	26.4 (59.0)	24.6 (55.0)	21.9 (49.0)	26.4 (59.0)	28.6 (64.0)	31.3 (70.0)	20.6 (46.0)	20.1 (45.0)	21.9 (49.0)	31.3 (70.0)

Local Climatological Data Annual Summary with Comparative Data for Midland-Odessa, Texas, National Oceanic and Atmospheric Administration, 2002.

Table 3.2-6 Roswell, New Mexico, Wind Data
1961-1990
Page 1 of 1

	Jan	Feb	Mar	Apr	May	Jun	Jul	Aug	Sept	Oct	Nov	Dec	Year
Mean Speed m/sec (mi/hr)	3.1 (6.9)	3.6 (8.1)	4.2 (9.5)	4.4 (9.8)	4.3 (9.6)	4.3 (9.6)	3.8 (8.5)	3.4 (7.7)	3.4 (7.6)	3.3 (7.3)	3.2 (7.2)	3.1 (6.9)	3.7 (8.2)
Prevailing Direction degrees from True North	360	160	160	160	160	160	140	140	160	160	160	360	160
Max 5-second speed m/sec (mi/hr)	24.1 (54.0)	24.1 (54.0)	24.1 (54.0)	26.4 (59.0)	24.6 (55.0)	27.7 (62.0)	26.4 (59.0)	20.1 (45.0)	22.8 (51.0)	21.5 (48.0)	23.7 (53.0)	22.8 (51.0)	27.7 (62.0)

Local Climatological Data Annual Summary with Comparative Data for Roswell, New Mexico, National Oceanic and Atmospheric Administration, 2002.

Table 3.2-7 Midland-Odessa Five Year (1987-1991) Annual Joint Frequency Distribution For All Stability Classes Combined

Jan. 1, 1987-Dec. 31, 1991

Wind Speed (mi/hr)

Calm = 2.53 percent

Page 1 of 1

Direction	1-3	4-7	8-12	13-18	19-24	≥ 24.5	Total
N	119	702	722	563	225	57	2388
NNE	71	291	509	556	207	58	1692
NE	64	285	645	776	272	61	2103
ENE	51	382	738	726	170	27	2094
E	69	623	1176	713	95	15	2691
ESE	72	589	1061	557	75	12	2366
SE	70	931	1266	818	134	18	3237
SSE	127	1156	1555	1391	371	48	4648
S	168	1755	2763	3178	820	100	8784
SSW	100	813	1276	807	133	7	3136
SW	61	446	943	757	115	23	2345
WSW	68	356	667	637	191	78	1997
W	84	331	577	517	207	171	1887
WNW	77	244	281	269	75	51	997
NW	91	332	350	224	69	38	1104
NNW	79	500	365	228	80	20	1272
SubTotal	1371	9736	14894	12717	3239	784	42741

Table 3.2-8 Midland-Odessa Five Year (1987-1991) Annual Joint Frequency Distribution Stability Class A
Jan. 1, 1987-Dec. 31, 1991
Wind Speed (mi/hr)
Calm = 0.06 percent
Page 1 of 1

Direction	1-3	4-7	8-12	13-18	19-24	≥ 24.5	Total
N	3	16	0	0	0	0	19
NNE	3	7	0	0	0	0	10
NE	0	8	0	0	0	0	8
ENE	2	12	0	0	0	0	14
E	3	15	0	0	0	0	18
ESE	3	8	0	0	0	0	11
SE	2	10	0	0	0	0	12
SSE	0	10	0	0	0	0	10
S	3	16	0	0	0	0	19
SSW	2	9	0	0	0	0	11
SW	0	12	0	0	0	0	12
WSW	1	6	0	0	0	0	7
W	0	5	0	0	0	0	5
WNW	0	2	0	0	0	0	2
NW	1	7	0	0	0	0	8
NNW	0	5	0	0	0	0	5
SubTotal	21	145	0	0	0	0	171

Table 3.2-9 Midland-Odessa Five Year (1987-1991) Annual Joint Frequency Distribution Stability Class B
Jan. 1, 1987-Dec. 31, 1991
Wind Speed (mi/hr)
Calm = 0.11 percent
Page 1 of 1

Direction	1-3	4-7	8-12	13-18	19-24	≥ 24.5	Total
N	20	43	22	0	0	0	85
NNE	17	25	19	0	0	0	61
NE	16	32	22	0	0	0	70
ENE	14	46	36	0	0	0	96
E	6	69	62	0	0	0	137
ESE	17	50	44	0	0	0	111
SE	9	48	45	0	0	0	102
SSE	15	54	64	0	0	0	133
S	25	96	138	0	0	0	259
SSW	12	53	59	0	0	0	124
SW	14	42	49	0	0	0	105
WSW	12	43	43	0	0	0	98
W	16	51	17	0	0	0	84
WNW	11	25	13	0	0	0	49
NW	18	21	14	0	0	0	53
NNW	15	27	9	0	0	0	51
SubTotal	235	722	652	-5	-5	24.5	1618

Table 3.2-10 Midland-Odessa Five Year (1987-1991) Annual Joint Frequency Distribution Stability Class C
Jan. 1, 1987-Dec. 31, 1991
Wind Speed (mi/hr)
Calm = 0.12 percent
Page 1 of 1

Direction	1-3	4-7	8-12	13-18	19-24	≥ 24.5	Total
N	9	54	124	20	8	3	218
NNE	3	36	87	37	5	1	169
NE	5	37	95	46	11	3	197
ENE	0	52	93	43	4	1	193
E	2	54	164	50	7	0	277
ESE	4	41	147	60	7	0	259
SE	3	36	179	109	10	1	338
SSE	1	65	264	199	52	5	586
S	6	103	527	408	95	19	1158
SSW	5	82	266	124	13	1	491
SW	1	59	238	115	11	2	426
WSW	3	43	180	61	22	7	316
W	5	39	100	76	21	10	251
WNW	4	36	57	25	7	1	130
NW	7	21	51	21	4	0	104
NNW	4	32	48	8	8	3	103
SubTotal	60	787	2616	1397	280	81.5	5216

Table 3.2-11 Midland-Odessa Five Year (1987-1991) Annual Joint Frequency Distribution Stability Class D
Jan. 1, 1987-Dec. 31, 1991
Wind Speed (mi/hr)
Calm = 0.18 percent
Page 1 of 1

Direction	1-3	4-7	8-12	13-18	19-24	≥ 24.5	Total
N	8	112	308	543	217	54	1242
NNE	14	65	302	519	202	57	1159
NE	7	79	389	730	261	58	1524
ENE	6	104	426	683	166	26	1411
E	7	108	550	663	88	15	1431
ESE	13	95	458	497	68	12	1143
SE	5	92	514	709	124	17	1461
SSE	11	98	618	1192	319	43	2281
S	13	151	949	2770	725	81	4689
SSW	3	74	369	683	120	6	1255
SW	1	46	259	642	104	21	1073
WSW	2	42	182	576	169	71	1042
W	4	49	177	441	186	161	1018
WNW	5	29	81	244	68	50	477
NW	3	30	95	203	65	38	434
NNW	7	47	121	220	72	17	484
SubTotal	107	1218	5794	11310	2949	751.5	22124

Table 3.2-12 Midland-Odessa Five Year (1987-1991) Annual Joint Frequency Distribution Stability Class E
Jan. 1, 1987-Dec. 31, 1991
Wind Speed (mi/hr)
Calm = 0.00 percent
Page 1 of 1

Direction	1-3	4-7	8-12	13-18	19-24	≥ 24.5	Total
N	0	133	268	0	0	0	401
NNE	0	64	101	0	0	0	165
NE	0	66	139	0	0	0	205
ENE	0	81	183	0	0	0	264
E	0	143	400	0	0	0	543
ESE	0	131	412	0	0	0	543
SE	0	236	528	0	0	0	764
SSE	0	259	609	0	0	0	868
S	0	380	1149	0	0	0	1529
SSW	0	145	582	0	0	0	727
SW	0	65	397	0	0	0	462
WSW	0	60	262	0	0	0	322
W	0	42	283	0	0	0	325
WNW	0	36	130	0	0	0	166
NW	0	50	190	0	0	0	240
NNW	0	98	187	0	0	0	285
SubTotal	-2	1986	5816	-5	-5	24.5	7809

Table 3.2-13 Midland-Odessa Five Year (1987-1991) Annual Joint Frequency Distribution Stability Class F
Jan. 1, 1987-Dec. 31, 1991
Wind Speed (mi/hr)
Calm = 2.07 percent
Page 1 of 1

Direction	1-3	4-7	8-12	13-18	19-24	≥ 24.5	Total
N	79	344	0	0	0	0	423
NNE	34	94	0	0	0	0	128
NE	36	63	0	0	0	0	99
ENE	29	87	0	0	0	0	116
E	51	234	0	0	0	0	285
ESE	35	264	0	0	0	0	299
SE	51	509	0	0	0	0	560
SSE	100	670	0	0	0	0	770
S	121	1009	0	0	0	0	1130
SSW	78	450	0	0	0	0	528
SW	45	222	0	0	0	0	267
WSW	50	162	0	0	0	0	212
W	59	145	0	0	0	0	204
WNW	57	116	0	0	0	0	173
NW	62	203	0	0	0	0	265
NNW	53	291	0	0	0	0	344
SubTotal	938	4860	-4	-5	-5	24.5	5803

Table 3.2-14 Hobbs, New Mexico, Precipitation Data

Precip cm (in)	Jan	Feb	Mar	Apr	May	Jun	Jul	Aug	Sept	Oct	Nov	Dec	Annual
Average	1.3 (0.51)	1.7 (0.66)	1.2 (0.48)	2 (0.78)	6.6 (2.58)	5.2 (2.03)	6.1 (2.42)	6.4 (2.52)	8 (3.13)	3.7 (1.45)	2.2 (0.87)	1.8 (0.72)	46.1 (18.15)
Max	5.2 (2.03)	5.6 (2.21)	7.6 (2.98)	7.3 (2.86)	35.1 (13.83)	13.6 (5.37)	23.9 (9.41)	23 (9.06)	33 (12.99)	20.7 (8.15)	11 (4.33)	12.9 (5.08)	35.1 (13.83)
Min	0.0 (0.0)	0.0 (0.0)	0.0 (0.0)	0.0 (0.0)	0.0 (0.0)	0.0 (0.0)	0.6 (0.22)	0.3 (0.11)	0.2 (0.08)	0.0 (0.0)	0.0 (0.0)	0.0 (0.0)	0.0 (0.0)

Table 3.2-15 Midland-Odessa, Texas, Precipitation Data
1961-1990
Page 1 of 1

Precip cm (in)	Jan	Feb	Mar	Apr	May	Jun	Jul	Aug	Sept	Oct	Nov	Dec	Annual
Average	1.3 (0.53)	1.5 (0.58)	1.1 (0.42)	1.9 (0.73)	4.5 (1.79)	4.3 (1.71)	4.8 (1.89)	4.5 (1.77)	5.9 (2.31)	4.5 (1.77)	1.7 (0.65)	1.7 (0.65)	37.6 (14.8)
Max	9.3 (3.66)	6.5 (2.55)	7.3 (2.86)	7.2 (2.85)	19.4 (7.63)	10.0 (3.93)	21.6 (8.5)	11.3 (4.43)	24.6 (9.7)	18.9 (7.45)	5.9 (2.32)	8.4 (3.3)	24.6 (9.7)
Min	0.0 (0.0)	0.0 (0.0)	T T	0.0 (0.0)	0.1 (0.02)	0.03 (0.01)	T T	0.1 (0.05)	0.0 (0.0)	0.0 (0.0)	0.0 (0.0)	T T	0.0 (0.0)
Max in 24 hours	2.9 (1.15)	3.4 (1.32)	5.6 (2.2)	4.1 (1.62)	12.1 (4.75)	7.8 (3.07)	15.2 (5.99)	6.1 (2.41)	11.1 (4.37)	9.1 (3.59)	5.5 (2.16)	2.3 (0.9)	15.2 (5.99)

T = trace amount

Local Climatological Data Annual Summary with Comparative Data for Midland-Odessa, Texas, National Oceanic and Atmospheric Administration, 2002.

Table 3.2-16 Roswell, New Mexico, Precipitation Data

Precip cm (in)	Jan	Feb	Mar	Apr	May	Jun	Jul	Aug	Sept	Oct	Nov	Dec	Annual
Average	1.0 (0.39)	1.0 (0.41)	0.9 (0.35)	1.5 (0.58)	3.3 (1.30)	4.1 (1.62)	5.1 (1.99)	5.9 (2.31)	5.0 (1.98)	3.3 (1.29)	1.3 (0.53)	1.5 (0.59)	33.9 (13.34)
Max	2.6 (1.03)	5.1 (2.02)	7.2 (2.84)	6.3 (2.48)	11.6 (4.57)	12.8 (5.02)	17.5 (6.88)	16.5 (6.48)	16.7 (6.58)	15.0 (5.91)	5.4 (2.11)	7.8 (3.07)	17.5 (6.88)
Min	0.1 (0.03)	0.0 (0.0)	0.0 (0.0)	0.03 (0.01)	T T	0.1 (0.02)	0.03 (0.01)	0.2 (0.07)	0.1 (0.05)	T T	0.0 (0.0)	0.0 (0.0)	0.0 (0.0)
Max in 24 hours	1.7 (0.67)	3.6 (1.41)	5.6 (2.22)	5.7 (2.24)	4.5 (1.77)	7.7 (3.05)	12.5 (4.91)	10.0 (3.94)	6.9 (2.71)	9.9 (3.89)	3.4 (1.33)	2.8 (1.1)	12.5 (4.91)

T = trace amount

Local Climatological Data Annual Summary with Comparative Data for Roswell, New Mexico, National Oceanic and Atmospheric Administration, 2002.

Table 3.2-17 Midland-Odessa, Texas, Snowfall Data
1961-1990
Page 1 of 1

Snowfall cm (in)	Jan	Feb	Mar	Apr	May	Jun	Jul	Aug	Sept	Oct	Nov	Dec	Annual
Average	5.6 (2.2)	1.8 (0.7)	0.5 (0.2)	0.3 (0.1)	0.0 (0.0)	0.0 (0.0)	0.0 (0.0)	0.0 (0.0)	0.0 (0.0)	0.* (0.*)	1.3 (0.5)	3.6 (1.4)	13.0 (5.1)
Max	22.9 (9.0)	9.9 (3.9)	15.0 (5.9)	5.1 (2.0)	T T	T T	T T	T T	T T	1.5 (0.6)	20.3 (8.0)	24.9 (9.8)	24.9 (9.8)
Max in 24 hours	17.3 (6.8)	9.9 (3.9)	12.7 (5.0)	5.1 (2.0)	T T	T T	T T	T T	T T	1.5 (0.6)	15.2 (6.0)	24.9 (9.8)	24.9 (9.8)

T = trace amount

0.* indicates the value is between 0.0 and 1.3 cm (0.0 and 0.05 in)

Local Climatological Data Annual Summary with Comparative Data for Midland-Odessa, Texas, National Oceanic and Atmospheric Administration, 2002.

Table 3.2-18 Roswell, New Mexico, Snowfall Data
1961-1990

Snowfall cm (in)	Jan	Feb	Mar	Apr	May	Jun	Jul	Aug	Sept	Oct	Nov	Dec	Annual
Average	7.9 (3.1)	6.6 (2.6)	2.3 (0.9)	1.0 (0.4)	0.* (0.*)	0.0 (0.0)	0.0 (0.0)	0.0 (0.0)	0.0 (0.0)	0.8 (0.3)	3.3 (1.3)	8.4 (3.3)	30.2 (11.9)
Max	26.4 (10.4)	42.9 (16.9)	12.2 (4.8)	13.5 (5.3)	2.0 (0.8)	2.5 (1.0)	0.0 (0.0)	0.0 (0.0)	2.5 (1.0)	10.7 (4.2)	31.2 (12.3)	53.3 (21.0)	53.3 (21.0)
Max in 24 hours	18.5 (7.3)	41.9 (16.5)	12.2 (4.8)	10.2 (4.0)	5.1 (2.0)	2.5 (1.0)	0.0 (0.0)	0.0 (0.0)	2.5 (1.0)	7.9 (3.1)	16.0 (6.3)	24.6 (9.7)	41.9 (16.5)

0.* indicates the value is between 0.0 and 1.3 cm (0.0 and 0.05 in)

Local Climatological Data Annual Summary with Comparative Data for Roswell, New Mexico, National Oceanic and Atmospheric Administration, 2002.

Table 3.2-19 Straight Wind Hazard Assessment

Annual Probability	Expected Wind Speed km/hr (mi/hr)	Upper Bound Wind Speed km/hr (mi/hr)	Lower Bound Wind Speed km/hr (mi/hr)
1E-01	134 (83)	146 (91)	119 (74)
1E-02	162 (101)	188 (117)	138 (86)
1E-03	193 (120)	230 (143)	156 (97)
1E-04	222 (138)	271(169)	174 (108)
1E-05	252 (157)	312 (194)	191 (119)
1E-06	282 (175)	354 (220)	209 (130)

Table 3.2-20 Location of Recorded Earthquakes Within a 322 km (200 mi) Radius of the NEF Site

NEF Site Coordinates			Longitude -103.0820	Latitude 32.4360							
Year	Month	Day	Longitude (°W)	Latitude (°N)	Focal (km)	Depth[1] (mi)	MAG[2]	MAG Type[3]	Epicentral Distance (km)	Epicentral Distance (mi)	Data Sources[4]
1931	8	16	-104.60	30.70			6.00	M	240.3	149.3	UTIG
1949	5	23	-105.20	34.60			4.50	M	310.0	192.6	NMTH
1955	1	27	-104.50	30.60			3.30	M	244.0	151.6	UTIG
1962	3	6	-104.80	31.20			3.50	M	212.3	131.9	UTIG
1963	12	19	-104.27	34.82			3.40	M	287.0	178.3	NMTR
1964	2	11	-103.94	34.23			2.10	M	214.2	133.1	NMTR
1964	3	3	-103.60	34.84			2.90	M	271.0	168.4	NMTR
1964	6	19	-105.77	32.95			1.90	M	257.4	159.9	NMTR
1964	8	14	-102.94	31.97			1.90	M	53.1	33.0	NMTR
1964	9	7	-102.92	31.94			1.60	M	56.9	35.3	NMTR
1964	11	8	-103.10	31.90			3.00	M	59.5	37.0	UTIG
1964	11	21	-103.10	31.90			3.10	M	59.5	37.0	UTIG
1964	11	27	-102.97	31.89			1.90	M	61.1	38.0	NMTR
1965	1	21	-102.85	32.02			1.30	M	50.9	31.6	NMTR
1965	2	3	-103.10	31.90			3.30	M	59.5	37.0	UTIG
1965	8	30	-103.00	31.90			3.50	M	60.0	37.3	UTIG
1966	8	14	-103.00	31.90			3.40	M	60.0	37.3	UTIG
1966	9	17	-103.98	34.89			2.70	M	284.6	176.9	NMTR
1966	10	6	-104.12	35.13			2.90	M	314.4	195.4	NMTR
1966	11	26	-105.44	30.95			3.50	M	277.5	172.4	NMTR
1968	3	23	-105.91	32.67			2.60	M	265.7	165.1	NMTR
1968	5	2	-105.24	33.10			2.60	M	214.3	133.1	NMTR
1969	6	1	-105.21	34.20			1.90	M	277.7	172.5	NMTR
1969	6	8	-105.19	34.15			2.60	M	272.8	169.5	NMTR
1971	7	30	-103.00	31.72	10.0	6.2	3.00	mb	79.9	49.6	ANSS
1971	7	31	-103.06	31.70	10.0	6.2	3.40	mb	81.4	50.6	ANSS
1971	9	24	-103.20	31.60			3.20	M	93.5	58.1	UTIG
1972	7	26	-104.01	32.57			3.10	M	88.3	54.9	NMTR
1973	3	17	-102.36	31.59			2.50	M	115.7	71.9	NMTR
1973	8	2	-105.56	31.04			3.60	M	280.7	174.5	NMTR
1973	8	4	-103.22	35.11			3.00	M	296.6	184.3	NMTR
1974	7	31	-104.19	33.11			0.00	M	128.0	79.5	NMTR
1974	10	2	-100.86	31.87			0.00	M	217.7	135.3	NMTR
1974	10	27	-104.83	30.63			0.00	M	259.6	161.3	NMTR
1974	11	12	-102.67	32.14			0.00	M	51.0	31.7	NMTR
1974	11	21	-102.75	32.07			0.00	M	51.0	31.7	NMTR

Year	Month	Day	Longitude (°W)	Latitude (°N)	Focal Depth[1] (km)	Focal Depth[1] (mi)	MAG[2]	MAG Type[3]	Epicentral Distance (km)	Epicentral Distance (mi)	Data Sources[4]
1974	11	22	-101.26	32.94			0.00	M	179.2	111.3	NMTR
1974	11	22	-105.21	33.78			0.00	M	247.7	153.9	NMTR
1974	11	28	-103.94	32.58			0.00	M	82.2	51.1	NMTR
1974	11	28	-104.14	32.31	5.0	3.1	3.90	mb	100.4	62.4	ANSS
1974	12	30	-103.10	30.90			3.70	M	170.5	106.0	UTIG
1975	1	30	-103.08	30.95			2.10	M	165.1	102.6	NMTR
1975	2	2	-103.19	35.05			3.00	M	290.7	180.6	NMTR
1975	4	8	-101.69	32.18			0.00	M	133.9	83.2	NMTR
1975	7	25	-102.62	29.82			0.00	M	293.4	182.3	NMTR
1975	8	1	-104.60	30.49			0.00	M	259.5	161.3	NMTR
1975	8	1	-104.00	31.40			3.00	M	143.9	89.4	UTIG
1975	8	3	-104.45	30.71			0.00	M	231.0	143.5	NMTR
1975	10	10	-105.02	33.36			0.00	M	207.4	128.9	NMTR
1975	12	12	-102.31	31.61			3.00	M	117.5	73.0	NMTR
1976	1	10	-102.76	31.79			0.00	M	78.4	48.7	NMTR
1976	1	15	-102.32	30.98			0.00	M	176.6	109.7	NMTR
1976	1	19	-103.09	31.90			3.50	M	59.5	37.0	UTIG
1976	1	21	-102.29	30.95			0.00	M	180.8	112.4	NMTR
1976	1	22	-103.07	31.90	1.0	0.6	2.80	un	59.5	37.0	ANSS
1976	1	25	-103.08	31.90	2.0	1.2	3.90	un	59.3	36.8	ANSS
1976	1	28	-100.89	31.99			0.00	M	211.8	131.6	NMTR
1976	2	4	-103.53	31.68			0.00	M	94.1	58.4	NMTR
1976	2	14	-102.47	31.63			0.00	M	106.2	66.0	NMTR
1976	3	5	-102.25	31.66			0.00	M	116.7	72.5	NMTR
1976	3	15	-102.58	32.50			0.00	M	47.3	29.4	NMTR
1976	3	18	-102.96	32.33			0.00	M	16.5	10.3	NMTR
1976	3	20	-104.94	31.27			0.00	M	217.4	135.1	NMTR
1976	3	20	-103.06	32.22			0.00	M	24.4	15.2	NMTR
1976	3	27	-103.07	32.22			0.00	M	23.7	14.7	NMTR
1976	4	3	-103.10	31.24			0.00	M	132.5	82.3	NMTR
1976	4	12	-103.00	32.27			0.00	M	20.2	12.5	NMTR
1976	4	21	-102.89	32.25			0.00	M	27.7	17.2	NMTR
1976	4	30	-103.09	31.98			0.00	M	50.7	31.5	NMTR
1976	4	30	-103.11	31.92			0.00	M	57.6	35.8	NMTR
1976	5	1	-103.06	32.37			0.00	M	8.0	5.0	NMTR
1976	5	3	-105.66	32.41			0.00	M	241.7	150.2	NMTR
1976	5	3	-103.20	32.03			0.00	M	47.0	29.2	NMTR
1976	5	3	-103.03	32.03			0.00	M	45.6	28.3	NMTR
1976	5	4	-103.23	31.86			0.00	M	65.3	40.6	NMTR
1976	5	6	-103.18	31.97			0.00	M	53.1	33.0	NMTR
1976	5	6	-103.16	31.87			0.00	M	63.3	39.3	NMTR
1976	5	11	-102.92	32.29			0.00	M	22.2	13.8	NMTR
1976	5	21	-105.59	32.49			0.00	M	234.9	146.0	NMTR
1976	6	14	-102.49	31.52			0.00	M	116.5	72.4	NMTR
1976	6	15	-102.34	31.56			0.00	M	120.0	74.6	NMTR

Year	Month	Day	Longitude (°W)	Latitude (°N)	Focal Depth[1] (km)	Focal Depth[1] (mi)	MAG[2]	MAG Type[3]	Epicentral Distance (km)	Epicentral Distance (mi)	Data Sources[4]
1976	6	15	-102.37	31.60			0.00	M	115.0	71.5	NMTR
1976	7	28	-102.29	33.02			0.00	M	98.7	61.4	NMTR
1976	8	5	-101.73	30.87			0.00	M	216.3	134.4	NMTR
1976	8	5	-103.00	31.60			3.00	M	93.1	57.9	UTIG
1976	8	6	-102.59	31.78			2.10	M	86.3	53.6	NMTR
1976	8	10	-102.03	31.77			0.00	M	123.8	76.9	NMTR
1976	8	10	-102.06	31.79			0.00	M	119.5	74.3	NMTR
1976	8	25	-101.94	31.55			0.00	M	146.1	90.8	NMTR
1976	8	26	-102.01	31.84			0.00	M	120.8	75.1	NMTR
1976	8	30	-101.98	31.57			0.00	M	141.7	88.0	NMTR
1976	8	31	-102.18	31.46			0.00	M	137.4	85.4	NMTR
1976	9	3	-103.48	31.55			2.00	M	105.2	65.4	NMTR
1976	9	5	-102.74	32.23			0.00	M	39.3	24.4	NMTR
1976	9	17	-103.06	32.24			0.00	M	22.4	13.9	NMTR
1976	9	17	-102.50	31.40			3.10	M	127.4	79.2	UTIG
1976	9	19	-104.57	30.47			0.00	M	259.7	161.4	NMTR
1976	10	22	-102.16	31.55			0.00	M	131.6	81.8	NMTR
1976	10	23	-102.38	31.62			0.00	M	112.2	69.7	NMTR
1976	10	25	-102.53	31.84			0.00	M	84.3	52.4	NMTR
1976	10	26	-103.28	31.33			2.40	M	124.2	77.2	NMTR
1976	11	3	-102.27	30.92			0.00	M	185.6	115.3	NMTR
1976	12	12	-102.46	31.57			2.80	M	112.5	69.9	NMTR
1976	12	12	-102.49	31.61			1.90	M	107.3	66.6	NMTR
1976	12	15	-102.22	31.59			1.40	M	124.2	77.2	NMTR
1976	12	18	-103.02	31.62			1.80	M	90.8	56.4	NMTR
1976	12	19	-102.45	31.87			2.20	M	86.0	53.5	NMTR
1976	12	19	-103.14	32.25			1.80	M	20.9	13.0	NMTR
1976	12	19	-103.08	32.27			2.70	M	18.7	11.6	NMTR
1977	1	29	-104.59	30.58			0.00	M	250.3	155.5	NMTR
1977	2	4	-104.70	30.59			0.00	M	256.1	159.2	NMTR
1977	2	18	-103.05	32.24			0.00	M	21.7	13.5	NMTR
1977	3	5	-102.66	31.16			0.00	M	146.9	91.3	NMTR
1977	3	14	-101.01	33.04			0.00	M	204.7	127.2	NMTR
1977	3	20	-103.10	32.21			0.00	M	25.5	15.8	NMTR
1977	3	29	-103.28	31.60			0.00	M	94.2	58.5	NMTR
1977	4	3	-103.17	31.49			1.90	M	105.3	65.5	NMTR
1977	4	3	-103.20	31.47			0.00	M	107.8	67.0	NMTR
1977	4	4	-103.36	31.00			0.00	M	161.4	100.3	NMTR
1977	4	7	-103.05	32.19			0.00	M	27.7	17.2	NMTR
1977	4	7	-102.70	31.32			0.00	M	129.3	80.3	NMTR
1977	4	7	-102.94	31.35			0.00	M	120.9	75.1	NMTR
1977	4	12	-102.55	31.28			0.00	M	137.4	85.4	NMTR
1977	4	17	-102.35	31.50			0.00	M	124.7	77.5	NMTR
1977	4	18	-103.25	31.60			0.00	M	93.7	58.2	NMTR
1977	4	22	-103.02	32.18			0.00	M	28.8	17.9	NMTR
1977	4	25	-102.81	32.07			0.00	M	47.9	29.8	NMTR

Year	Month	Day	Longitude (°W)	Latitude (°N)	Focal Depth[1] (km)	Focal Depth[1] (mi)	MAG[2]	MAG Type[3]	Epicentral Distance (km)	Epicentral Distance (mi)	Data Sources[4]
1977	4	26	-103.08	31.90	4.0	2.5	3.30	un	59.3	36.8	ANSS
1977	4	28	-102.52	31.83			0.00	M	86.1	53.5	NMTR
1977	4	28	-101.99	31.87			0.00	M	120.6	75.0	NMTR
1977	4	29	-102.65	31.77			0.00	M	84.0	52.2	NMTR
1977	6	7	-100.75	33.06	5.0	3.1	4.00	un	228.5	142.0	ANSS
1977	6	8	-100.83	32.83			0.00	M	215.4	133.9	NMTR
1977	6	8	-100.82	32.92			0.00	M	218.4	135.7	NMTR
1977	6	8	-101.04	32.87			0.00	M	196.4	122.1	NMTR
1977	6	17	-100.95	32.90			2.70	M	206.1	128.1	NMTR
1977	6	28	-103.30	31.54			2.30	M	101.6	63.1	NMTR
1977	7	1	-103.34	31.50			2.00	M	106.7	66.3	NMTR
1977	7	11	-102.62	31.80			0.00	M	83.1	51.6	NMTR
1977	7	11	-102.68	31.79			0.00	M	81.4	50.6	NMTR
1977	7	12	-102.64	31.77			0.00	M	84.6	52.6	NMTR
1977	7	18	-102.70	31.78			0.00	M	81.4	50.6	NMTR
1977	7	22	-102.72	31.80			0.00	M	78.2	48.6	NMTR
1977	7	22	-102.70	31.80			3.00	M	79.2	49.2	UTIG
1977	7	24	-102.70	31.79			0.00	M	79.7	49.5	NMTR
1977	8	20	-103.33	31.60			1.90	M	95.7	59.5	NMTR
1977	8	21	-104.91	30.54			0.00	M	272.4	169.3	NMTR
1977	10	13	-100.81	32.91			2.20	M	218.8	135.9	NMTR
1977	10	17	-102.46	31.57			1.80	M	112.6	69.9	NMTR
1977	11	14	-104.96	31.52			0.00	M	203.7	126.6	NMTR
1977	11	27	-101.14	33.02			0.00	M	192.7	119.8	NMTR
1977	11	28	-100.84	32.95	5.0	3.1	3.50	un	217.4	135.1	ANSS
1977	12	16	-102.40	31.52			0.00	M	120.2	74.7	NMTR
1977	12	21	-102.41	31.52			0.00	M	120.3	74.7	NMTR
1977	12	31	-102.46	31.60			2.10	M	109.7	68.2	NMTR
1978	1	2	-102.53	31.60			2.20	M	106.3	66.1	NMTR
1978	1	12	-102.30	31.49			0.00	M	128.1	79.6	NMTR
1978	1	15	-101.70	31.36			0.00	M	177.0	110.0	NMTR
1978	1	18	-103.23	31.61			0.00	M	92.9	57.7	NMTR
1978	1	19	-103.71	32.56			0.00	M	60.5	37.6	NMTR
1978	2	5	-102.60	31.89			0.00	M	76.2	47.4	NMTR
1978	2	5	-104.55	31.41			0.00	M	179.5	111.5	NMTR
1978	2	18	-104.69	31.21			2.30	M	203.8	126.6	NMTR
1978	3	2	-103.06	32.82			1.50	M	42.5	26.4	NMTR
1978	3	2	-102.38	31.58			3.30	M	115.4	71.7	NMTR
1978	3	2	-102.61	31.59			2.10	M	103.9	64.6	NMTR
1978	3	2	-102.56	31.55			3.50	M	109.9	68.3	UTIG
1978	3	19	-102.49	31.47			1.60	M	120.5	74.9	NMTR
1978	6	16	-100.80	33.00			3.40	M	222.1	138.0	UTIG
1978	6	16	-100.77	33.03	10.0	6.2	5.30	un	226.1	140.5	ANSS
1978	6	29	-102.42	31.08			3.20	M	163.1	101.4	NMTR
1978	7	5	-102.20	31.61			0.00	M	123.2	76.5	NMTR
1978	7	18	-104.36	30.36			0.00	M	260.4	161.8	NMTR

Year	Month	Day	Longitude (°W)	Latitude (°N)	Focal Depth[1] (km)	Focal Depth[1] (mi)	MAG[2]	MAG Type[3]	Epicentral Distance (km)	Epicentral Distance (mi)	Data Sources[4]
1978	7	21	-102.77	31.34			0.00	M	125.0	77.7	NMTR
1978	8	14	-102.18	31.58			2.20	M	127.4	79.2	NMTR
1978	9	29	-102.42	31.52			0.00	M	119.2	74.1	NMTR
1978	9	30	-102.17	31.36			0.00	M	146.7	91.1	NMTR
1978	10	2	-102.43	31.53			0.00	M	117.6	73.1	NMTR
1978	10	2	-102.19	31.51			0.00	M	132.5	82.3	NMTR
1978	10	2	-102.36	31.48			0.00	M	126.4	78.5	NMTR
1978	10	3	-102.99	31.90			0.00	M	59.7	37.1	NMTR
1978	10	6	-102.36	31.55			0.00	M	119.8	74.4	NMTR
1979	4	28	-104.72	30.47			0.00	M	267.7	166.3	NMTR
1979	7	17	-103.73	32.65			2.00	M	65.4	40.6	NMTR
1979	8	3	-100.81	32.87			2.40	M	217.5	135.1	NMTR
1980	1	21	-105.00	34.20			1.30	M	264.2	164.2	NMTR
1980	3	21	-102.34	31.57			1.60	M	118.5	73.6	NMTR
1981	8	13	-102.70	31.90			2.20	M	69.7	43.3	NMTR
1981	9	16	-105.23	33.72			1.80	M	245.2	152.4	NMTR
1982	1	4	-102.49	31.18	5.0	3.1	3.90	un	149.9	93.2	ANSS
1982	4	26	-100.84	33.02	5.0	3.1	2.80	un	218.8	136.0	ANSS
1982	5	1	-103.04	32.33			2.10	M	12.3	7.6	NMTR
1982	10	17	-102.71	30.90			2.00	M	174.0	108.1	NMTR
1982	10	26	-103.59	33.67			1.50	M	144.6	89.8	NMTR
1982	10	26	-103.61	33.63			1.50	M	141.3	87.8	NMTR
1982	11	25	-100.78	32.89			2.30	M	220.7	137.1	NMTR
1982	11	28	-100.84	33.00	5.0	3.1	3.30	un	218.4	135.7	ANSS
1983	1	9	-104.19	30.65			1.90	M	224.3	139.4	NMTR
1983	1	12	-105.19	34.32			1.50	M	286.7	178.2	NMTR
1983	1	29	-102.08	31.75			2.20	M	121.2	75.3	NMTR
1983	3	3	-104.35	29.96			2.80	M	299.6	186.2	NMTR
1983	6	5	-105.35	32.52			1.30	M	212.6	132.1	NMTR
1983	6	21	-103.58	33.63			1.60	M	140.9	87.5	NMTR
1983	7	21	-105.14	30.97			1.60	M	253.4	157.5	NMTR
1983	8	4	-105.14	32.57			1.30	M	193.4	120.2	NMTR
1983	8	19	-102.23	31.31			1.80	M	148.8	92.5	NMTR
1983	8	22	-105.08	34.06			1.30	M	258.6	160.7	NMTR
1983	8	23	-105.52	31.17			2.10	M	269.7	167.6	NMTR
1983	8	26	-102.53	33.62			1.60	M	140.9	87.5	NMTR
1983	8	29	-100.62	31.80			2.60	M	242.0	150.4	NMTR
1983	9	15	-104.43	34.92			3.10	M	302.6	188.1	NMTR
1983	9	29	-104.45	34.89			2.70	M	300.0	186.4	NMTR
1983	9	30	-103.97	30.57			1.70	M	224.0	139.2	NMTR
1983	12	1	-101.99	31.86			1.40	M	121.1	75.3	NMTR
1983	12	3	-103.32	30.97			2.10	M	164.1	102.0	NMTR
1983	12	26	-102.88	30.77			1.70	M	186.4	115.8	NMTR
1984	1	2	-102.12	31.81			1.80	M	114.4	71.1	NMTR
1984	1	3	-102.69	31.21			1.70	M	141.3	87.8	NMTR
1984	1	3	-103.04	30.76			2.00	M	186.3	115.8	NMTR

Year	Month	Day	Longitude (°W)	Latitude (°N)	Focal Depth[1] (km)	Focal Depth[1] (mi)	MAG[2]	MAG Type[3]	Epicentral Distance (km)	Epicentral Distance (mi)	Data Sources[4]
1984	1	16	-102.20	31.56			1.40	M	127.5	79.2	NMTR
1984	3	2	-104.84	30.81			1.90	M	245.5	152.5	NMTR
1984	3	23	-100.78	32.45			1.50	M	215.2	133.7	NMTR
1984	5	21	-102.59	31.14			1.30	M	151.3	94.0	NMTR
1984	5	21	-102.23	35.07	5.0	3.1	3.10	un	302.5	188.0	ANSS
1984	6	27	-102.48	31.22			2.00	M	146.5	91.0	NMTR
1984	7	17	-105.77	32.85			1.30	M	255.7	158.9	NMTR
1984	8	18	-103.56	30.78			1.80	M	189.8	118.0	NMTR
1984	8	24	-104.48	30.67			1.30	M	236.8	147.1	NMTR
1984	8	26	-104.27	30.38			2.10	M	254.4	158.1	NMTR
1984	9	11	-100.70	31.99	5.0	3.1	3.20	un	229.4	142.5	ANSS
1984	9	19	-100.69	32.03	5.0	3.1	3.00	un	229.3	142.5	ANSS
1984	9	27	-103.42	32.59			1.60	M	36.0	22.4	NMTR
1984	10	4	-102.70	33.58			1.30	M	132.3	82.2	NMTR
1984	10	4	-102.24	31.65			1.30	M	118.4	73.6	NMTR
1984	10	11	-100.56	31.95			2.40	M	243.2	151.1	NMTR
1984	10	27	-104.56	30.62			1.70	M	245.1	152.3	NMTR
1984	11	27	-105.41	33.57			1.60	M	250.6	155.7	NMTR
1984	12	4	-101.93	30.10			2.30	M	281.6	175.0	NMTR
1984	12	4	-103.21	32.64			2.10	M	25.4	15.8	NMTR
1984	12	4	-103.56	32.27	5.0	3.1	2.90	un	48.3	30.0	ANSS
1984	12	12	-105.61	33.36			1.50	M	256.9	159.6	NMTR
1985	2	21	-100.75	32.88			1.40	M	223.3	138.7	NMTR
1985	2	21	-100.81	32.72			1.50	M	214.6	133.4	NMTR
1985	3	9	-105.12	33.97			1.30	M	254.4	158.1	NMTR
1985	5	3	-104.95	31.04			1.90	M	234.5	145.7	NMTR
1985	6	1	-102.83	31.06			1.50	M	154.6	96.0	NMTR
1985	6	2	-102.28	31.18			1.60	M	158.7	98.6	NMTR
1985	6	12	-103.90	34.64			1.60	M	255.9	159.0	NMTR
1985	8	2	-104.34	32.48			1.40	M	118.0	73.3	NMTR
1985	9	5	-103.77	33.66			1.80	M	150.1	93.3	NMTR
1985	9	18	-103.42	30.90			2.00	M	173.1	107.6	NMTR
1985	10	21	-101.88	32.04			1.30	M	121.3	75.4	NMTR
1985	11	13	-103.08	32.10			1.80	M	37.8	23.5	NMTR
1985	11	28	-101.99	31.61			1.80	M	138.2	85.9	NMTR
1985	12	5	-102.94	32.42			1.60	M	13.9	8.6	NMTR
1986	1	25	-100.73	32.06	5.0	3.1	2.90	un	224.3	139.4	ANSS
1986	1	30	-104.01	33.54			1.90	M	150.1	93.3	NMTR
1986	1	30	-100.69	32.07	5.0	3.1	3.30	un	228.0	141.7	ANSS
1986	2	7	-105.44	32.54			1.40	M	221.0	137.3	NMTR
1986	2	14	-100.76	31.53			2.60	M	240.9	149.7	NMTR
1986	3	1	-102.57	31.16			1.70	M	149.6	92.9	NMTR
1986	3	11	-105.08	32.11			2.00	M	190.7	118.5	NMTR
1986	3	21	-105.64	33.43			1.60	M	262.8	163.3	NMTR
1986	5	28	-105.12	31.76			1.60	M	205.8	127.9	NMTR
1986	6	12	-102.22	31.77			1.80	M	109.6	68.1	NMTR

Year	Month	Day	Longitude (°W)	Latitude (°N)	Focal Depth[1] (km)	Focal Depth[1] (mi)	MAG[2]	MAG Type[3]	Epicentral Distance (km)	Epicentral Distance (mi)	Data Sources[4]
1986	6	27	-102.01	32.06			2.20	M	109.3	67.9	NMTR
1986	7	9	-102.48	31.55			1.60	M	113.3	70.4	NMTR
1986	7	20	-105.00	33.47			1.50	M	212.8	132.2	NMTR
1986	8	2	-103.79	33.68			1.70	M	153.4	95.3	NMTR
1986	8	6	-103.03	33.86			2.40	M	158.4	98.5	NMTR
1986	8	14	-104.66	32.53			1.30	M	148.0	92.0	NMTR
1986	8	15	-103.43	33.14			1.70	M	84.2	52.3	NMTR
1986	8	29	-102.41	31.31			1.40	M	140.1	87.1	NMTR
1986	9	18	-102.37	31.51			1.80	M	123.2	76.5	NMTR
1986	10	18	-102.69	30.07			1.60	M	265.4	164.9	NMTR
1986	10	25	-102.13	31.60			1.70	M	129.0	80.2	NMTR
1986	11	3	-104.64	31.09			2.00	M	209.5	130.2	NMTR
1986	11	6	-104.58	32.55			1.60	M	140.4	87.2	NMTR
1986	11	17	-100.73	33.08			2.00	M	230.6	143.3	NMTR
1986	11	24	-102.16	31.68			2.00	M	121.1	75.3	NMTR
1986	12	6	-102.16	31.59			2.40	M	127.6	79.3	NMTR
1986	12	6	-102.23	31.47			2.10	M	133.9	83.2	NMTR
1986	12	6	-102.17	31.65			1.70	M	122.0	75.8	NMTR
1986	12	6	-102.09	31.72			2.20	M	122.6	76.2	NMTR
1986	12	15	-103.19	35.07			1.50	M	292.9	182.0	NMTR
1986	12	15	-102.02	31.76			1.50	M	125.0	77.7	NMTR
1987	1	25	-104.86	31.74			1.70	M	184.3	114.5	NMTR
1987	2	9	-103.45	30.69			2.30	M	196.8	122.3	NMTR
1987	2	9	-101.96	31.86			1.60	M	123.6	76.8	NMTR
1987	2	12	-101.94	31.66			1.60	M	137.9	85.7	NMTR
1987	2	17	-104.52	30.60			2.10	M	244.8	152.1	NMTR
1987	3	2	-105.08	30.78			1.80	M	263.6	163.8	NMTR
1987	3	3	-105.44	31.17			1.50	M	263.4	163.7	NMTR
1987	3	10	-105.66	31.13			1.50	M	282.7	175.7	NMTR
1987	3	26	-103.28	30.96			2.60	M	165.2	102.6	NMTR
1987	3	31	-104.95	31.52			2.80	M	203.4	126.4	NMTR
1987	4	23	-105.02	32.03			1.60	M	187.7	116.7	NMTR
1987	4	25	-105.22	33.97			1.90	M	261.2	162.3	NMTR
1987	4	29	-105.92	32.67			2.30	M	267.0	165.9	NMTR
1987	7	5	-104.77	30.85			2.00	M	237.5	147.6	NMTR
1987	7	23	-103.03	35.29			1.90	M	316.9	196.9	NMTR
1987	7	30	-103.87	34.54			1.50	M	244.4	151.9	NMTR
1987	8	4	-102.12	31.87			1.70	M	110.1	68.4	NMTR
1987	9	11	-103.62	33.61			2.00	M	139.1	86.4	NMTR
1987	9	21	-103.74	33.68			1.80	M	150.6	93.6	NMTR
1987	10	1	-105.16	30.47			1.60	M	294.1	182.7	NMTR
1987	10	1	-103.76	33.66			1.50	M	150.0	93.2	NMTR
1987	10	9	-104.59	31.07			1.40	M	208.4	129.5	NMTR
1987	10	31	-105.31	32.86			1.30	M	213.8	132.9	NMTR
1987	11	3	-103.71	33.70			1.30	M	151.6	94.2	NMTR
1987	11	17	-101.97	32.06			1.60	M	112.9	70.1	NMTR

Year	Month	Day	Longitude (°W)	Latitude (°N)	Focal Depth[1] (km)	Focal Depth[1] (mi)	MAG[2]	MAG Type[3]	Epicentral Distance (km)	Epicentral Distance (mi)	Data Sources[4]
1987	12	6	-102.76	31.83			1.60	M	74.2	46.1	NMTR
1987	12	20	-103.07	32.29			2.20	M	15.8	9.8	NMTR
1987	12	28	-102.25	31.47			2.10	M	133.3	82.8	NMTR
1987	12	29	-102.11	31.58			1.50	M	132.1	82.1	NMTR
1988	1	26	-102.42	31.24			2.30	M	146.4	90.9	NMTR
1988	2	14	-102.06	31.78			1.40	M	121.0	75.2	NMTR
1988	2	21	-103.02	30.45			1.40	M	220.3	136.9	NMTR
1988	2	27	-103.75	33.67			1.80	M	150.3	93.4	NMTR
1988	3	9	-102.44	31.24			1.70	M	146.0	90.7	NMTR
1988	3	15	-105.52	31.72			1.30	M	242.7	150.8	NMTR
1988	3	17	-102.20	31.66			1.60	M	119.8	74.4	NMTR
1988	4	5	-102.33	31.44			2.10	M	131.6	81.8	NMTR
1988	4	6	-102.09	31.94			1.30	M	107.9	67.1	NMTR
1988	5	3	-104.39	30.52			1.30	M	246.2	153.0	NMTR
1988	5	10	-105.20	30.96			1.40	M	258.4	160.6	NMTR
1988	5	27	-102.12	31.78			1.30	M	116.1	72.1	NMTR
1988	5	27	-102.02	32.06			1.30	M	108.3	67.3	NMTR
1988	7	4	-100.74	33.74			2.00	M	261.5	162.5	NMTR
1988	7	11	-103.25	35.28			1.90	M	316.6	196.7	NMTR
1988	7	20	-102.43	29.77			2.20	M	301.9	187.6	NMTR
1988	7	25	-104.91	31.98			1.50	M	178.9	111.2	NMTR
1988	7	26	-105.14	30.94			1.50	M	255.5	158.8	NMTR
1988	8	23	-102.02	32.26			1.50	M	101.1	62.8	NMTR
1988	9	15	-103.32	31.68			1.50	M	86.7	53.9	NMTR
1988	9	19	-102.45	32.46			2.00	M	59.3	36.8	NMTR
1988	10	2	-103.79	33.63			1.30	M	147.8	91.8	NMTR
1988	11	10	-102.40	31.55			1.90	M	117.3	72.9	NMTR
1989	1	9	-102.59	31.44			1.80	M	119.6	74.3	NMTR
1989	1	9	-102.12	31.78			1.30	M	116.5	72.4	NMTR
1989	1	20	-101.97	32.08			1.90	M	112.1	69.6	NMTR
1989	2	21	-103.39	35.29			2.30	M	318.4	197.8	NMTR
1989	3	19	-103.55	31.19			1.50	M	145.2	90.2	NMTR
1989	3	21	-102.33	31.42			1.50	M	133.5	83.0	NMTR
1989	3	30	-102.86	33.24			1.40	M	91.5	56.9	NMTR
1989	6	5	-102.09	32.10			2.10	M	100.1	62.2	NMTR
1989	6	23	-102.23	31.59			1.60	M	123.2	76.6	NMTR
1989	6	28	-105.08	30.93			2.30	M	252.3	156.8	NMTR
1989	7	13	-105.27	33.53			1.50	M	237.1	147.3	NMTR
1989	7	24	-100.93	32.92			1.60	M	208.3	129.5	NMTR
1989	7	25	-101.76	30.90			2.10	M	211.2	131.3	NMTR
1989	8	8	-102.70	31.30			2.30	M	131.3	81.6	NMTR
1989	8	16	-101.96	31.70			1.60	M	133.3	82.8	NMTR
1989	9	5	-102.50	34.25			2.50	M	208.9	129.8	NMTR
1989	11	2	-100.94	33.02			2.00	M	210.4	130.7	NMTR
1989	11	16	-103.12	35.11			2.60	M	296.7	184.4	NMTR
1989	12	7	-103.67	34.58			1.40	M	244.1	151.7	NMTR

Year	Month	Day	Longitude (°W)	Latitude (°N)	Focal Depth[1] (km)	Focal Depth[1] (mi)	MAG[2]	MAG Type[3]	Epicentral Distance (km)	Epicentral Distance (mi)	Data Sources[4]
1989	12	28	-101.06	31.70			2.10	M	207.6	129.0	NMTR
1989	12	28	-100.96	32.04			1.70	M	203.9	126.7	NMTR
1990	1	16	-105.32	31.74			1.80	M	224.4	139.4	NMTR
1990	3	4	-103.92	30.53			1.70	M	226.3	140.6	NMTR
1990	3	30	-100.53	32.96			2.30	M	245.1	152.3	NMTR
1990	3	30	-100.56	32.99			2.20	M	243.5	151.3	NMTR
1990	4	6	-103.36	31.51			1.90	M	106.3	66.0	NMTR
1990	5	10	-102.37	31.14			2.20	M	159.2	98.9	NMTR
1990	5	10	-101.96	32.13			1.60	M	110.9	68.9	NMTR
1990	5	16	-102.04	31.86			2.40	M	117.2	72.8	NMTR
1990	5	22	-102.09	30.24			2.20	M	261.5	162.5	NMTR
1990	6	22	-100.76	32.58			2.20	M	218.3	135.7	NMTR
1990	7	3	-102.22	31.44			1.50	M	137.6	85.5	NMTR
1990	7	13	-101.81	34.86			2.70	M	293.9	182.6	NMTR
1990	8	3	-100.69	32.21			3.40	M	225.6	140.2	NMTR
1990	8	9	-102.67	31.21			1.90	M	141.8	88.1	NMTR
1990	8	14	-102.26	31.39			1.80	M	139.8	86.9	NMTR
1990	8	25	-102.01	31.91			1.80	M	116.0	72.1	NMTR
1990	10	8	-105.12	30.94			1.30	M	254.0	157.8	NMTR
1990	12	20	-103.14	35.27			2.50	M	315.1	195.8	NMTR
1991	1	1	-105.27	32.44			1.60	M	205.4	127.6	NMTR
1991	1	29	-103.04	32.89			1.40	M	50.8	31.6	NMTR
1991	2	3	-104.49	32.81			1.30	M	137.7	85.6	NMTR
1991	2	3	-103.96	35.00			2.10	M	296.2	184.0	NMTR
1991	3	10	-103.97	30.47			2.10	M	234.3	145.6	NMTR
1991	3	10	-103.33	33.58			2.00	M	128.8	80.0	NMTR
1991	4	8	-103.13	34.98			2.10	M	282.4	175.5	NMTR
1991	5	16	-103.75	33.67			2.00	M	150.4	93.5	NMTR
1991	6	4	-102.31	32.05			2.00	M	83.9	52.1	NMTR
1991	7	16	-101.12	33.09			2.10	M	197.3	122.6	NMTR
1991	8	1	-104.02	34.59			2.70	M	254.6	158.2	NMTR
1991	8	7	-104.81	31.62			1.80	M	186.1	115.6	NMTR
1991	8	17	-100.99	32.09			2.00	M	200.2	124.4	NMTR
1991	9	22	-101.30	31.32			2.10	M	209.2	130.0	NMTR
1991	9	28	-103.77	33.63			1.70	M	147.3	91.6	NMTR
1991	9	30	-100.73	31.85			2.20	M	230.5	143.2	NMTR
1991	10	5	-105.41	31.38			2.20	M	248.6	154.5	NMTR
1992	1	2	-103.19	32.30			5.00	M	17.8	11.0	NMTR
1992	1	2	-103.19	32.30			1.80	M	17.8	11.0	NMTR
1992	1	2	-103.19	32.30			1.50	M	17.8	11.0	NMTR
1992	1	2	-103.19	32.30			2.40	M	17.8	11.0	NMTR
1992	1	2	-103.19	32.30			1.80	M	17.8	11.0	NMTR
1992	1	3	-103.19	32.30			1.90	M	17.8	11.0	NMTR
1992	1	4	-103.19	32.30			1.50	M	17.8	11.0	NMTR
1992	1	7	-103.19	32.30			2.40	M	17.8	11.0	NMTR
1992	1	9	-103.19	32.30			2.80	M	17.8	11.0	NMTR

Year	Month	Day	Longitude (°W)	Latitude (°N)	Focal Depth[1] (km)	Focal Depth[1] (mi)	MAG[2]	MAG Type[3]	Epicentral Distance (km)	Epicentral Distance (mi)	Data Sources[4]
1992	1	11	-103.19	32.30			2.00	M	17.8	11.0	NMTR
1992	1	23	-102.29	31.84			1.90	M	99.2	61.7	NMTR
1992	2	2	-102.86	32.17			1.90	M	36.4	22.6	NMTR
1992	3	15	-104.12	34.92			1.70	M	292.1	181.5	NMTR
1992	3	28	-105.39	33.45			1.80	M	242.2	150.5	NMTR
1992	4	3	-103.03	32.26			2.10	M	19.9	12.4	NMTR
1992	4	6	-102.61	31.86			1.70	M	77.7	48.3	NMTR
1992	4	7	-102.29	31.56			1.60	M	122.6	76.2	NMTR
1992	4	7	-102.29	31.56			2.30	M	122.6	76.2	NMTR
1992	4	7	-102.29	31.56			1.70	M	122.6	76.2	NMTR
1992	4	8	-104.86	32.41			1.60	M	166.9	103.7	NMTR
1992	4	30	-104.31	30.66			1.70	M	229.0	142.3	NMTR
1992	5	9	-104.34	30.49			1.60	M	246.7	153.3	NMTR
1992	5	15	-103.08	32.28			1.60	M	17.5	10.9	NMTR
1992	5	16	-102.34	31.75			1.70	M	103.0	64.0	NMTR
1992	6	14	-103.10	32.30			2.30	M	15.1	9.4	NMTR
1992	6	20	-102.42	31.43			1.60	M	127.5	79.2	NMTR
1992	6	20	-102.42	31.43			1.50	M	127.5	79.2	NMTR
1992	6	29	-102.47	31.42			1.40	M	126.9	78.8	NMTR
1992	6	29	-102.47	31.42			1.40	M	126.9	78.8	NMTR
1992	6	29	-102.47	31.42			2.00	M	126.9	78.8	NMTR
1992	7	5	-102.39	31.88			1.50	M	89.4	55.6	NMTR
1992	7	5	-102.39	31.88			1.30	M	89.4	55.6	NMTR
1992	7	21	-103.13	32.28			1.90	M	17.8	11.1	NMTR
1992	8	12	-102.41	31.39			1.50	M	131.9	82.0	NMTR
1992	8	18	-102.45	31.46			1.90	M	123.5	76.7	NMTR
1992	8	19	-100.92	33.11			2.20	M	215.3	133.8	NMTR
1992	8	26	-102.71	32.17	5.0	3.1	3.00	un	45.6	28.4	ANSS
1992	8	28	-100.98	32.38			1.70	M	197.4	122.6	NMTR
1992	9	4	-102.26	31.42			1.90	M	136.8	85.0	NMTR
1992	9	15	-103.02	32.16			2.20	M	31.6	19.6	NMTR
1992	10	8	-102.81	32.25			1.60	M	33.1	20.6	NMTR
1992	10	10	-102.41	31.71			1.60	M	102.2	63.5	NMTR
1992	10	27	-101.93	34.12			1.30	M	215.1	133.7	NMTR
1992	11	22	-103.16	32.29			1.70	M	18.0	11.2	NMTR
1992	11	27	-102.49	31.44			1.30	M	124.0	77.1	NMTR
1992	12	2	-102.35	31.42			2.40	M	131.5	81.7	NMTR
1992	12	3	-103.74	33.66			1.90	M	149.6	93.0	NMTR
1992	12	5	-102.51	31.87			1.40	M	83.0	51.6	NMTR
1993	1	4	-105.27	31.06			1.30	M	256.5	159.4	NMTR
1993	1	28	-102.58	31.85			1.80	M	80.3	49.9	NMTR
1993	1	31	-104.64	30.60			1.50	M	250.8	155.9	NMTR
1993	2	11	-105.23	31.12			2.00	M	250.1	155.4	NMTR
1993	2	28	-102.43	31.21			1.30	M	149.4	92.8	NMTR
1993	2	28	-102.41	31.22			1.50	M	149.3	92.8	NMTR
1993	3	8	-103.33	30.87			1.60	M	175.9	109.3	NMTR

Year	Month	Day	Longitude (°W)	Latitude (°N)	Focal Depth[1] (km)	Focal Depth[1] (mi)	MAG[2]	MAG Type[3]	Epicentral Distance (km)	Epicentral Distance (mi)	Data Sources[4]
1993	3	21	-102.37	31.43			1.50	M	130.4	81.0	NMTR
1993	4	23	-102.47	31.21			1.70	M	147.8	91.9	NMTR
1993	5	5	-105.16	32.29			2.10	M	195.3	121.4	NMTR
1993	5	16	-105.06	30.44			2.20	M	290.1	180.2	NMTR
1993	5	17	-102.33	31.42			2.30	M	133.3	82.9	NMTR
1993	5	23	-102.42	31.42			1.60	M	128.7	80.0	NMTR
1993	5	28	-103.12	32.75			2.50	M	34.6	21.5	NMTR
1993	6	17	-102.56	31.80			1.70	M	86.5	53.8	NMTR
1993	6	23	-102.44	31.51			1.40	M	119.5	74.2	NMTR
1993	6	23	-102.54	31.43			2.50	M	123.2	76.6	NMTR
1993	6	23	-102.52	31.43			2.80	M	123.2	76.5	NMTR
1993	6	23	-102.52	31.43			2.10	M	123.2	76.5	NMTR
1993	6	23	-102.54	29.66			1.90	M	312.3	194.0	NMTR
1993	6	23	-102.51	31.35	5.0	3.1	2.80	un	132.5	82.3	ANSS
1993	6	24	-102.45	31.48			2.10	M	121.9	75.7	NMTR
1993	7	3	-102.43	31.44			1.50	M	126.7	78.7	NMTR
1993	7	3	-102.34	31.50			2.20	M	125.5	78.0	NMTR
1993	7	3	-102.38	31.54			1.60	M	119.3	74.1	NMTR
1993	8	13	-102.52	31.89			1.30	M	80.1	49.8	NMTR
1993	8	29	-102.91	32.35			2.50	M	19.0	11.8	NMTR
1993	9	5	-100.96	32.28			2.00	M	200.1	124.4	NMTR
1993	9	6	-100.91	32.48			1.80	M	203.6	126.5	NMTR
1993	9	11	-103.76	34.72			1.50	M	260.9	162.1	NMTR
1993	9	26	-103.52	35.08			1.50	M	296.6	184.3	NMTR
1993	9	30	-103.80	33.64			1.90	M	149.0	92.6	NMTR
1993	10	3	-103.84	33.61			1.70	M	148.5	92.3	NMTR
1993	11	6	-102.19	31.75			1.50	M	113.6	70.6	NMTR
1993	11	24	-104.74	32.34			1.30	M	156.2	97.1	NMTR
1993	11	25	-102.10	34.27			2.60	M	223.0	138.5	NMTR
1993	11	25	-104.38	30.49			1.30	M	248.6	154.5	NMTR
1993	12	2	-102.34	31.27			1.30	M	147.3	91.5	NMTR
1993	12	3	-102.23	31.68			1.60	M	115.6	71.8	NMTR
1993	12	10	-102.29	31.74			1.60	M	106.8	66.4	NMTR
1993	12	18	-103.41	30.21			1.80	M	249.5	155.0	NMTR
1993	12	22	-105.68	33.33	10.0	6.2	3.20	un	261.9	162.8	ANSS
1994	1	6	-105.09	31.95			2.40	M	196.3	122.0	NMTR
1994	1	7	-102.32	31.24			1.70	M	151.0	93.8	NMTR
1994	3	15	-103.56	30.11			2.00	M	261.9	162.8	NMTR
1994	4	21	-103.12	32.31			1.40	M	14.1	8.8	NMTR
1994	4	25	-104.62	30.60			1.90	M	250.5	155.7	NMTR
1994	5	23	-102.64	32.11			1.60	M	55.0	34.2	NMTR
1994	6	30	-102.33	31.36			1.30	M	138.6	86.2	NMTR
1994	8	22	-102.21	33.34			1.60	M	129.0	80.2	NMTR
1994	8	30	-102.32	31.38			1.40	M	137.3	85.3	NMTR
1994	8	30	-102.32	31.34			1.50	M	141.5	87.9	NMTR
1994	8	30	-102.30	31.42			1.30	M	135.1	84.0	NMTR

Year	Month	Day	Longitude (°W)	Latitude (°N)	Focal Depth[1] (km)	Focal Depth[1] (mi)	MAG[2]	MAG Type[3]	Epicentral Distance (km)	Epicentral Distance (mi)	Data Sources[4]
1994	9	24	-102.36	31.43			2.00	M	131.1	81.4	NMTR
1994	11	24	-100.80	32.39			2.70	M	214.3	133.2	NMTR
1995	1	1	-102.45	31.77			1.40	M	94.7	58.8	NMTR
1995	1	4	-102.38	31.48			1.30	M	125.0	77.6	NMTR
1995	2	1	-104.09	34.51			1.80	M	248.7	154.6	NMTR
1995	3	19	-104.21	35.00	5.0	3.1	3.30	un	303.1	188.4	ANSS
1995	4	14	-103.35	30.28			5.70	M	240.7	149.5	UTIG
1995	4	18	-102.27	31.44			1.90	M	134.5	83.6	NMTR
1995	4	18	-105.34	31.10			1.60	M	259.8	161.4	NMTR
1995	4	21	-103.35	30.30	10.0	6.2	2.90	un	238.5	148.2	ANSS
1995	5	11	-105.20	32.71			2.40	M	200.4	124.5	NMTR
1995	5	15	-102.42	31.40			1.80	M	131.1	81.5	NMTR
1995	5	27	-102.34	31.34			2.30	M	140.1	87.0	NMTR
1995	5	30	-105.21	32.71			2.10	M	200.9	124.8	NMTR
1995	7	11	-105.06	30.87			1.80	M	255.5	158.8	NMTR
1995	7	17	-104.94	31.15			1.40	M	226.0	140.4	NMTR
1995	8	1	-105.27	33.14			1.30	M	218.9	136.0	NMTR
1995	8	2	-103.36	30.31			1.80	M	237.2	147.4	NMTR
1995	8	12	-103.07	30.79			1.90	M	183.1	113.8	NMTR
1995	8	14	-102.96	30.41			1.50	M	225.3	140.0	NMTR
1995	10	19	-104.84	32.05			2.00	M	170.4	105.9	NMTR
1995	10	25	-103.42	30.35			2.20	M	233.6	145.2	NMTR
1995	11	12	-103.35	30.30	10.0	6.2	3.60	ML	238.5	148.2	ANSS
1995	12	3	-104.90	31.93			1.50	M	180.1	111.9	NMTR
1995	12	4	-104.90	31.93			1.40	M	180.1	111.9	NMTR
1995	12	4	-104.90	31.93			1.30	M	180.1	111.9	NMTR
1996	3	15	-105.69	33.59	10.0	6.2	2.90	ML	274.6	170.6	ANSS
1998	4	15	-103.30	30.19	10.0	6.2	3.60	ML	250.4	155.6	ANSS
1999	3	1	-104.66	32.57	1.0	0.6	2.90	ML	148.1	92.0	ANSS
1999	3	14	-104.63	32.59	1.0	0.6	4.00	ML	145.9	90.7	ANSS
1999	3	17	-104.67	32.58	1.0	0.6	3.50	Mc	149.7	93.0	ANSS
1999	5	30	-104.66	32.58	10.0	6.2	3.90	ML	148.9	92.5	ANSS
1999	8	9	-104.59	32.57	5.0	3.1	2.90	Mc	142.0	88.3	ANSS
2000	2	2	-104.63	32.58	5.0	3.1	2.70	ML	145.7	90.5	ANSS
2000	2	26	-103.61	30.24	5.0	3.1	2.80	ML	248.6	154.5	ANSS
2001	6	2	-103.14	32.33	5.0	3.1	3.30	ML	12.6	7.8	ANSS
2001	11	22	-102.63	31.79	5.0	3.1	3.10	ML	83.7	52.0	ANSS
2002	9	17	-104.63	32.58	10.0	6.2	3.50	ML	145.8	90.6	ANSS
2002	9	17	-104.63	32.58	10.0	6.2	3.30	ML	145.8	90.6	ANSS
2003	6	21	-104.51	32.67	5.0	3.1	3.60	ML	135.5	84.2	ANSS

Notes:

[1] Focal depth information only available for events reported in ANSS Catalog
[2] MAG - Magnitude
[3] MAG Type
- M – Moment Magnitude
- mb – Body – wave Magnitude
- un – Unspecified Magnitude
- ML – Local Magnitude
- Mc – Coda – wave Magnitude

[4] Data Sources
- UTIG – University of Texas Institute for Geophysics
- NMTH – New Mexico Tech Historical Catalog
- NMTR – New Mexico Tech Regional Catalog, Exclusive of Socorro NM Events
- ANSS – Advanced National Seismic System

Table 3.2-21 Earthquakes of Magnitude 3.0 and Greater Within 322 km (200 mi) Radius of the NEF Site

NEF Site Coordinates			Longitude 103.0820	Latitude 32.4360							
Year	Month	Day	Longitude (°W)	Latitude (°N)	Focal (km)	Depth[1] (mi)	MAG[2]	MAG Type[3]	Epicentral Distance (km)	Epicentral Distance (mi)	Data Sources[4]
1931	8	16	-104.60	30.70			6.00	M	240.3	149.3	UTIG
1949	5	23	-105.20	34.60			4.50	M	310.0	192.6	NMTH
1955	1	27	-104.50	30.60			3.30	M	244.0	151.6	UTIG
1962	3	6	-104.80	31.20			3.50	M	212.3	131.9	UTIG
1963	12	19	-104.27	34.82			3.40	M	287.0	178.3	NMTR
1964	11	8	-103.10	31.90			3.00	M	59.5	37.0	UTIG
1964	11	21	-103.10	31.90			3.10	M	59.5	37.0	UTIG
1965	2	3	-103.10	31.90			3.30	M	59.5	37.0	UTIG
1965	8	30	-103.00	31.90			3.50	M	60.0	37.3	UTIG
1966	8	14	-103.00	31.90			3.40	M	60.0	37.3	UTIG
1966	11	26	-105.44	30.95			3.50	M	277.5	172.4	NMTR
1971	7	30	-103.00	31.72	10.0	6.2	3.00	mb	79.9	49.6	ANSS
1971	7	31	-103.06	31.70	10.0	6.2	3.40	mb	81.4	50.6	ANSS
1971	9	24	-103.20	31.60			3.20	M	93.5	58.1	UTIG
1972	7	26	-104.01	32.57			3.10	M	88.3	54.9	NMTR
1973	8	2	-105.56	31.04			3.60	M	280.7	174.5	NMTR
1973	8	4	-103.22	35.11			3.00	M	296.6	184.3	NMTR
1974	11	28	-104.14	32.31	5.0	3.1	3.90	mb	100.4	62.4	ANSS
1974	12	30	-103.10	30.90			3.70	M	170.5	106.0	UTIG
1975	2	2	-103.19	35.05			3.00	M	290.7	180.6	NMTR
1975	8	1	-104.00	31.40			3.00	M	143.9	89.4	UTIG
1975	12	12	-102.31	31.61			3.00	M	117.5	73.0	NMTR
1976	1	19	-103.09	31.90			3.50	M	59.5	37.0	UTIG
1976	1	25	-103.08	31.90	2.0	1.2	3.90	un	59.3	36.8	ANSS
1976	8	5	-103.00	31.60			3.00	M	93.1	57.9	UTIG
1976	9	17	-102.50	31.40			3.10	M	127.4	79.2	UTIG
1977	4	26	-103.08	31.90	4.0	2.5	3.30	un	59.3	36.8	ANSS
1977	6	7	-100.75	33.06	5.0	3.1	4.00	un	228.5	142.0	ANSS
1977	7	22	-102.70	31.80			3.00	M	79.2	49.2	UTIG
1977	11	28	-100.84	32.95	5.0	3.1	3.50	un	217.4	135.1	ANSS
1978	3	2	-102.38	31.58			3.30	M	115.4	71.7	NMTR
1978	3	2	-102.56	31.55			3.50	M	109.9	68.3	UTIG
1978	6	16	-100.80	33.00			3.40	M	222.1	138.0	UTIG
1978	6	16	-100.77	33.03	10.0	6.2	5.30	un	226.1	140.5	ANSS
1978	6	29	-102.42	31.08			3.20	M	163.1	101.4	NMTR
1982	1	4	-102.49	31.18	5.0	3.1	3.90	un	149.9	93.2	ANSS
1982	11	28	-100.84	33.00	5.0	3.1	3.30	un	218.4	135.7	ANSS
1983	9	15	-104.43	34.92			3.10	M	302.6	188.1	NMTR
1984	5	21	-102.23	35.07	5.0	3.1	3.10	un	302.5	188.0	ANSS
1984	9	11	-100.70	31.99	5.0	3.1	3.20	un	229.4	142.5	ANSS

Table 3.2-21 Earthquakes of Magnitude 3.0 and Greater Within 322 km (200 mi) Radius of the NEF Site

Year	Month	Day	Longitude (°W)	Latitude (°N)	Focal (km)	Depth[1] (mi)	MAG[2]	MAG Type[3]	Epicentral Distance (km)	Epicentral Distance (mi)	Data Sources[4]
1984	9	19	-100.69	32.03	5.0	3.1	3.00	un	229.3	142.5	ANSS
1986	1	30	-100.69	32.07	5.0	3.1	3.30	un	228.0	141.7	ANSS
1990	8	3	-100.69	32.21			3.40	M	225.6	140.2	NMTR
1992	1	2	-103.19	32.30			5.00	M	17.8	11.0	NMTR
1992	8	26	-102.71	32.17	5.0	3.1	3.00	un	45.6	28.4	ANSS
1993	12	22	-105.68	33.33	10.0	6.2	3.20	un	261.9	162.8	ANSS
1995	3	19	-104.21	35.00	5.0	3.1	3.30	un	303.1	188.4	ANSS
1995	4	14	-103.35	30.28			5.70	M	240.7	149.5	UTIG
1995	11	12	-103.35	30.30	10.0	6.2	3.60	ML	238.5	148.2	ANSS
1998	4	15	-103.30	30.19	10.0	6.2	3.60	ML	250.4	155.6	ANSS
1999	3	14	-104.63	32.59	1.0	0.6	4.00	ML	145.9	90.7	ANSS
1999	3	17	-104.67	32.58	1.0	0.6	3.50	Mc	149.7	93.0	ANSS
1999	5	30	-104.66	32.58	10.0	6.2	3.90	ML	148.9	92.5	ANSS
2001	6	2	-103.14	32.33	5.0	3.1	3.30	ML	12.6	7.8	ANSS
2001	11	22	-102.63	31.79	5.0	3.1	3.10	ML	83.7	52.0	ANSS
2002	9	17	-104.63	32.58	10.0	6.2	3.50	ML	145.8	90.6	ANSS
2002	9	17	-104.63	32.58	10.0	6.2	3.30	ML	145.8	90.6	ANSS
2003	6	21	-104.51	32.67	5.0	3.1	3.60	ML	135.5	84.2	ANSS

Notes:

1 Focal depth information only available for events reported in ANSS Catalog
2 MAG - Magnitude
3 MAG Type
- M – Moment Magnitude
- mb – Body – wave Magnitude
- un – Unspecified Magnitude
- ML – Local Magnitude
- Mc – Coda – wave Magnitude

4 Data Sources
- UTIG – University of Texas Institute for Geophysics
- NMTH – New Mexico Tech Historical Catalog
- NMTR – New Mexico Tech Regional Catalog, Exclusive of Socorro NM Events
- ANSS – Advanced National Seismic System

Table 3.2-22 Earthquake Data Sources for New Mexico and West Texas
Page 1 of 1

Data Source	Time Span	Number of events in 322 km (200 mi) Radius
New Mexico Tech, Regional Catalog	1962 - 1995	504
New Mexico Tech, Historical Catalog	1869 - 1992	2
University of Texas Institute of Geophysics	1931 - 1998	42
Advanced National Seismic System	1962 - 2003	64

Table 3.2-23 Modified Mercalli Intensity Scale

Intensity Value	Description
I	Not felt except by a very few under especially favorable circumstances.
II	Felt only by a few persons at rest, especially on upper floors of buildings. Delicately suspended objects may swing.
III	Felt quite noticeably indoors, especially on upper floors of buildings, but many people do not recognize it as an earthquake. Standing automobiles may rock slightly. Vibration like passing of truck.
IV	During the day felt indoors by many, outdoors by few. At night some awakened. Dishes, windows, doors disturbed; walls make creaking sound. Sensation like heavy truck striking building. Standing automobiles rocked noticeably.
V	Felt by nearly everyone, many awakened. Some dishes, windows, and so on broken; cracked plaster in a few places; unstable objects overturned. Disturbances of trees, poles, and other tall objects sometimes noticed. Pendulum clocks may stop.
VI	Felt by all, many frightened and run outdoors. Some heavy furniture moved; a few instances of fallen plaster and damaged chimneys. Damage slight.
VII	Everybody runs outdoors. Damage negligible in buildings of good design and construction; slight to moderate in well-built ordinary structures; considerable in poorly built or badly designed structures; some chimneys broken. Noticed by persons driving cars.
VIII	Damage slight in specially designed structures; considerable in ordinary substantial buildings, with partial collapse; great in poorly built structures. Panel walls thrown out of frame structures. Fall of chimneys, factory stacks, columns, monuments, walls. Heavy furniture overturned. Sand and mud ejected in small amounts. Changes in well water. Persons driving cars disturbed.
IX	Damage considerable in specially designed structures; well-designed frame structures thrown out of plumb; great in substantial buildings, with partial collapse. Buildings shifted off foundations. Ground cracked conspicuously. Underground pipes broken.
X	Some well-built wooden structures destroyed; most masonry and frame structures destroyed with foundations; ground badly cracked. Rails bent. Landslides considerable from river banks and steep slopes. Shifted sand and mud. Water splashed, slopped over banks.
XI	Few, if any (masonry) structures remain standing. Bridges destroyed. Broad fissures in ground. Underground pipelines completely out of service. Earth slumps and land slips in soft ground. Rails bent greatly.
XII	Damage total. Waves seen on ground surface. Lines of sight and level distorted. Objects thrown in the air.

Table 3.2-24 Comparison of Parameters for the January 2, 1992 Eunice, New Mexico Earthquake

Year	Month	Day	Longitude	Latitude	Magnitude	Data Source[1]
1992	1	2	-103.1863	32.3025	5.0	NMTR
1992	1	2	-102.97	32.36	4.6	UTIG
1992	1	2	-103.2	32.3	5.0	NMTH
1992	1	2	-103.101	32.336	5.0	ANSS

[1]Data Sources:

UTIG University of Texas Institute for Geophysics

NMTH New Mexico Tech Historical Catalog

ANSS Advanced National Seismic System

NMTR New Mexico Tech Regional Catalog, exclusive of Socorro New Mexico events

Table 3.2-25 Earthquake Recurrence Models for the NEF Site Region

Earthquake Recurrence Models							
Zone	**Area (km^2)**		**a-value**	**b-value**	**Beta**	**Rate/yr M > = 5.0**	**Return Period M > = 5.0**
200 Mile Radius	253,502	best fit	2.15	-0.74	-1.704	0.0282	35
		fixed b, -0.9	2.80	-0.90	-2.072	0.0200	50
Region 1 – 100 Mile Radius	78,758	best fit	2.25	-0.89	-2.049	0.0063	158
		fixed b, -0.9	2.40	-0.90	-2.072	0.0079	126
Central Basin Earthquake Cluster	15,065	best fit	1.98	-0.86	-1.980	0.0048	209
		fixed b, -0.9	2.20	-0.90	-2.072	0.0050	200

Table 3.2-26 Earthquake Recurrence Models for the Central Basin Platform (CBP)in the Waste Isolation Pilot Project (WIPP) Safety Analysis Report (SAR)

WIPP SAR Earthquake Recurrence Models

Zone	Area (km^2)	a-value	b-value	Beta	Rate/yr M > = 5.0	Return Period M > = 5.0
WIPP SAR						
Background	10,000 M uncorrected	1.439	-1.000	2.303	0.0003	3639
Background	10,000 M corrected	1.939	-1.000	2.303	0.0009	1151
Rio Grande Rift	110,000 M uncorrected	2.560	-1.000	2.303	0.0036	275
Rio Grande Rift	110,000 M corrected	3.060	-1.000	2.303	0.0115	87
Basin & Range Subregion	640,000 M uncorrected	2.750	-1.000	2.303	0.0056	178
Basin & Range Subregion	640,000 M corrected	3.250	-1.000	2.303	0.0178	56
WIPP Central Basin Platform	7,500 M uncorrected	2.740	-0.900	2.072	0.0174	58
WIPP Central Basin Platform	7,500 M corrected	3.190	-0.900	2.072	0.0490	20

Table 3.2-27 Attenuation Model Formulas and Coefficients

Model	Ground Motion Parameter (y)	c_1	c_2	c_3	c_4
EPRI, 1988	psrv (1 Hz)	-7.95	2.14	-1.00	-0.0018
Hard Rock Site Condition	psrv (2.5 Hz)	-3.82	1.49	-1.00	-0.0024
$\sigma_{ln(y)} = 0.5$	psrv (5 Hz)	-2.11	1.20	-1.00	-0.0031
	psrv (10 Hz)	-1.55	1.05	-1.00	-0.0039
	psrv (25 Hz)	-1.63	0.98	-1.00	-0.0053
	PGA	2.55	1.00	-1.00	-0.0046
Equation:	$\ln(y) = c_1 + c_2 m_{Lg} + c_3 \ln(R) + c_4 R$				
Nuttli, 1986	psrv (1 Hz)†	0.29	1.15	-0.83	-0.0028
Firm Rock Site Condition	psrv (2.5 Hz)†	-0.62	1.15	-0.83	-0.0028
$\sigma_{ln(y)} = 0.5$	psrv (5 Hz)†	-1.32	1.15	-0.83	-0.0028
	psrv (10 Hz)†	-2.13	1.15	-0.83	-0.0028
	psrv (25 Hz)†	-3.53	1.15	-0.83	-0.0028
	PGA	1.38	1.15	-0.83	-0.0028
Equations:	**† For a given m_{Lg} and R, ln(y) is the smaller of:** $c_1 + c_2 m_{Lg} + c_3 \ln R + c_4 R$ **and,** $-8.3 + 2.3 m_{Lg} - 0.83 \ln(R) - 0.0012R$				

		c_1	c_2	c_3	c_4	c_5	c_6	c_7
Toro, 1997	Sa (0.5 Hz)	-0.74	1.86	-0.31	0.92	0.46	0.0017	6.9
Midcontinent,	Sa (1 Hz)	0.09	1.42	-0.20	0.90	0.49	0.0023	6.8
Moment magnitude scaling	Sa (2.5 Hz)	1.07	1.05	-0.10	0.93	0.56	0.0033	7.1
	Sa (5 Hz)	1.73	0.84	0	0.98	0.66	0.0042	7.5
	Sa (10 Hz)	2.37	0.81	0	1.10	1.02	0.0040	8.3
	Sa (25 Hz)	3.68	0.80	0	1.46	1.77	0.0013	10.5
	Sa (35 Hz)	4.00	0.79	0	1.57	1.83	0.0008	11.1
	PGA	2.20	0.81	0	1.27	1.16	0.0021	9.3
Equations:	$\ln(y) = c_1 + c_2(M-6) + c_3(M-6)^2 - c_4 \ln(R_M) - (c_5-c_4)\max[\ln(R_M/100),0] - c_6 R_M + \varepsilon_U + \varepsilon_r$ $R_M = (R^2 + c_7^2)^{1/2}$							

Note: psrv = pseudo relative velocity at given frequency
PGA = peak ground acceleration
Sa = Spectral acceleration at given frequency

Table 3.2-28 Seismic Hazard Results at NEF Site From Rio Grande Rift Seismic Source Zones

cm/s^2	(g)	WIPP Basin and Range	WIPP Rio Grande Rift	WIPP M corr Basin and Range	WIPP M corr Rio Grande Rift
peak ground accel.		**Annual probability of PGA being exceeded**			
4.94	0.005	4.45E-03	2.78E-03		
9.81	0.010	2.29E-03	1.35E-03	7.26E-03	4.31E-03
49.01	0.050	4.84E-05	2.42E-05	1.54E-04	7.74E-05
73.55	0.075	1.08E-05	5.09E-06	3.44E-05	1.63E-05
98.10	0.100	3.13E-06	1.39E-06	9.95E-06	4.46E-06
122.61	0.125	1.06E-06	4.52E-07	3.38E-06	1.45E-06
147.08	0.150	4.05E-07	1.65E-07	1.29E-06	5.28E-07
196.17	0.200	7.41E-08	2.81E-08	2.36E-07	8.98E-08
245.18	0.250	1.70E-08	6.08E-09	5.40E-08	1.94E-08
294.12	0.300	4.59E-09	1.56E-09	1.46E-08	4.98E-09
392.29	0.400	4.68E-10	1.46E-10	1.49E-09	4.67E-10
490.29	0.500	6.61E-11	1.92E-11	2.10E-10	6.14E-11

Table 3.2-29 Seismic Hazard Results at NEF Site From Local Source Zones

PGA (g)	B100B9W Mx=6.0	B100BFW Mx=6.0	B200B9W Mx=6.5	B200BFW Mx=6.5	Bk53B9W Mx=5.25	Bk53BFW Mx=5.25	B260B9W Mx=6.0	B260BFW Mx=6.0	Bk53B9T Mx=5.25	Bk53BFT Mx=5.25	B260B9T Mx-=6.0	B260BFT Mx=6.0	Weighted Average
Annual Probability of PGA Being Exceeded													
0.010	8.09E-03	7.21E-03	1.32E-02	1.91E-02	7.66E-03	6.83E-03	1.26E-02	1.81E-02	4.97E-03	4.45E-03	4.72E-03	6.87E-03	8.88E-03
0.050	1.69E-03	1.54E-03	1.27E-03	1.99E-03	1.09E-03	9.93E-04	9.74E-04	1.45E-03	5.65E-04	5.15E-04	4.18E-04	6.17E-04	1.01E-03
0.075	8.30E-04	7.60E-04	5.61E-04	8.88E-04	4.99E-04	4.55E-04	4.20E-04	6.26E-04	2.67E-04	2.43E-04	2.00E-04	2.97E-04	4.62E-04
0.100	4.75E-04	4.36E-04	3.07E-04	4.87E-04	2.69E-04	2.46E-04	2.26E-04	3.38E-04	1.43E-04	1.31E-04	1.13E-04	1.68E-04	2.53E-04
0.125	2.97E-04	2.74E-04	1.88E-04	3.01E-04	1.58E-04	1.45E-04	1.37E-04	2.05E-04	8.21E-05	7.50E-05	6.97E-05	1.04E-04	1.52E-04
0.150	1.97E-04	1.82E-04	1.25E-04	2.00E-04	9.81E-05	8.97E-05	8.89E-05	1.34E-04	4.91E-05	4.49E-05	4.55E-05	6.85E-05	9.76E-05
0.200	9.59E-05	8.88E-05	6.25E-05	1.02E-04	4.12E-05	3.77E-05	4.25E-05	6.45E-05	1.90E-05	1.73E-05	2.15E-05	3.26E-05	4.44E-05
0.250	5.12E-05	4.75E-05	3.51E-05	5.77E-05	1.87E-05	1.71E-05	2.26E-05	3.45E-05	7.89E-06	7.21E-06	1.11E-05	1.70E-05	2.21E-05
0.300	2.91E-05	2.70E-05	2.12E-05	3.53E-05	8.93E-06	8.17E-06	1.28E-05	1.98E-05	3.44E-06	3.15E-06	6.04E-06	9.38E-06	1.17E-05
0.400	1.06E-05	9.84E-06	8.85E-06	1.51E-05	2.23E-06	2.04E-06	4.66E-06	7.29E-06	7.00E-07	6.39E-07	2.02E-06	3.20E-06	3.64E-06
0.500	4.32E-06	4.03E-06	4.20E-06	7.32E-06	5.87E-07	5.35E-07	1.89E-06	3.00E-06	1.40E-07	1.27E-07	7.53E-07	1.21E-06	1.23E-06

Notes:

PGA = Peak horizontal ground acceleration in firm rock
W = WIPP attenuation model; T = Toro et al. (1997) approx. model
Mx = Maximum magnitude

Table 3.2-30 Peak Acceleration Seismic Hazard Summary for the NEF Site

Page 1 of 1

Seismic Source	250 – year earthquake PGA as % g	475 – year earthquake PGA as % g
Local seismic zones	2.4%	3.6%
Max. for Rio Grande Rift	1.0%	1.8%

Table 3.2-31 Regulatory Guide 1.60 Ratio of Vertical to Horizontal Component Design Response Spectra

Period range	**Ratio Vertical/Horizontal**
> 4.0 s (< 0.25 Hz)	2/3
< 0.29 s (> 3.5 Hz)	1.0
Between 0.29 and 4.0 s	Varies between 2/3 and 1.0

Table 3.2-32 Horizontal Response Spectrum for the 10,000-Year Design Earthquake

Soil Class C			
Period s	**psrv cm/s**	**Sa (g)**	**SD mm**
0.020	0.472	0.151	0.015
0.030	0.715	0.151	0.034
0.040	1.420	0.227	0.090
0.100	5.473	0.351	0.871
0.200	10.809	0.346	3.440
0.400	10.809	0.173	6.881
1.000	10.809	0.069	17.202
2.000	5.404	0.017	17.202

psrv = pseudo relative velocity
Sa = spectral acceleration
SD = spectral displacement

Table 3.2-33 Vertical Response Spectrum for the 10,000-Year Design Earthquake

Soil Class C			
Period s	**psrv cm/s**	**Sa (g)**	**SD mm**
0.020	0.472	0.151	0.015
0.030	0.715	0.151	0.034
0.040	1.420	0.227	0.090
0.100	5.473	0.351	0.871
0.200	7.242	0.232	2.305
0.400	7.242	0.116	4.610
1.000	7.242	0.046	11.526
2.000	3.621	0.012	11.526

psrv = pseudo relative velocity
Sa = spectral acceleration
SD = spectral displacement

FIGURES

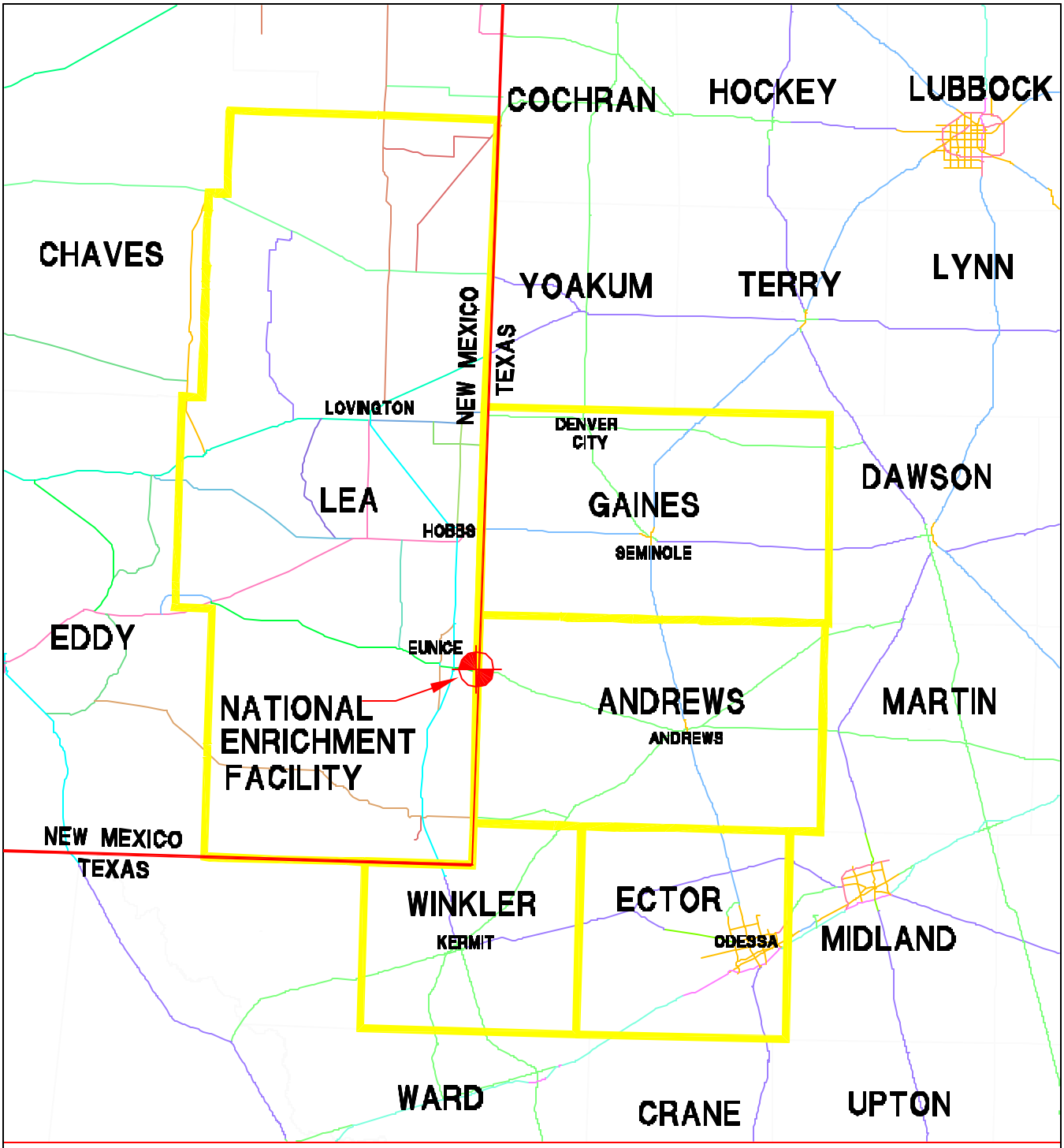

14 0 14 28 42 56 70 KM

14 0 14 28 42 MILES

NORTH

REFERENCE NUMBER
Fig_1.1-2.dwg

MAP SOURCE:
U.S.CENSUS BUREAU
2000 INCORPORATED PLACES

FIGURE 3.2-1
COUNTY MAP

REVISION DATE: DECEMBER 2003

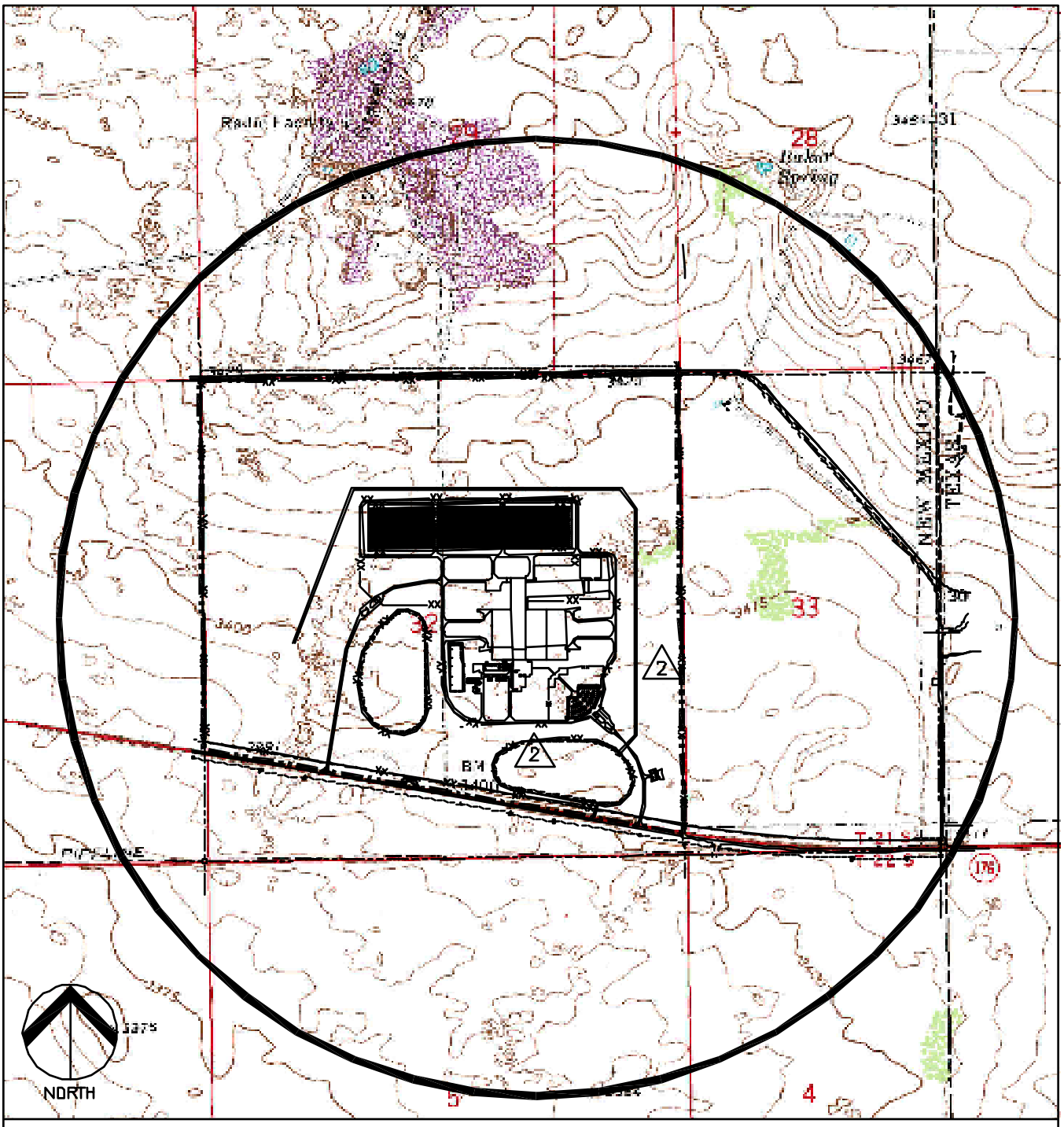

MAP SOURCE:
USGS 7.5 MINUTE
EUNICE NE QUADRANGLE
TEX.–N. MEX. 1:24000

CONTOUR INTERVAL:
5 FEET

LOCKWOOD GREENE
ENGINEERING & CONSTRUCTION

REFERENCE NUMBER
Figure_3.2–2.dwg

FIGURE 3.2-2

PLOT PLAN
(1 MILE RADIUS)

REVISION 2 DATE: JULY 2004

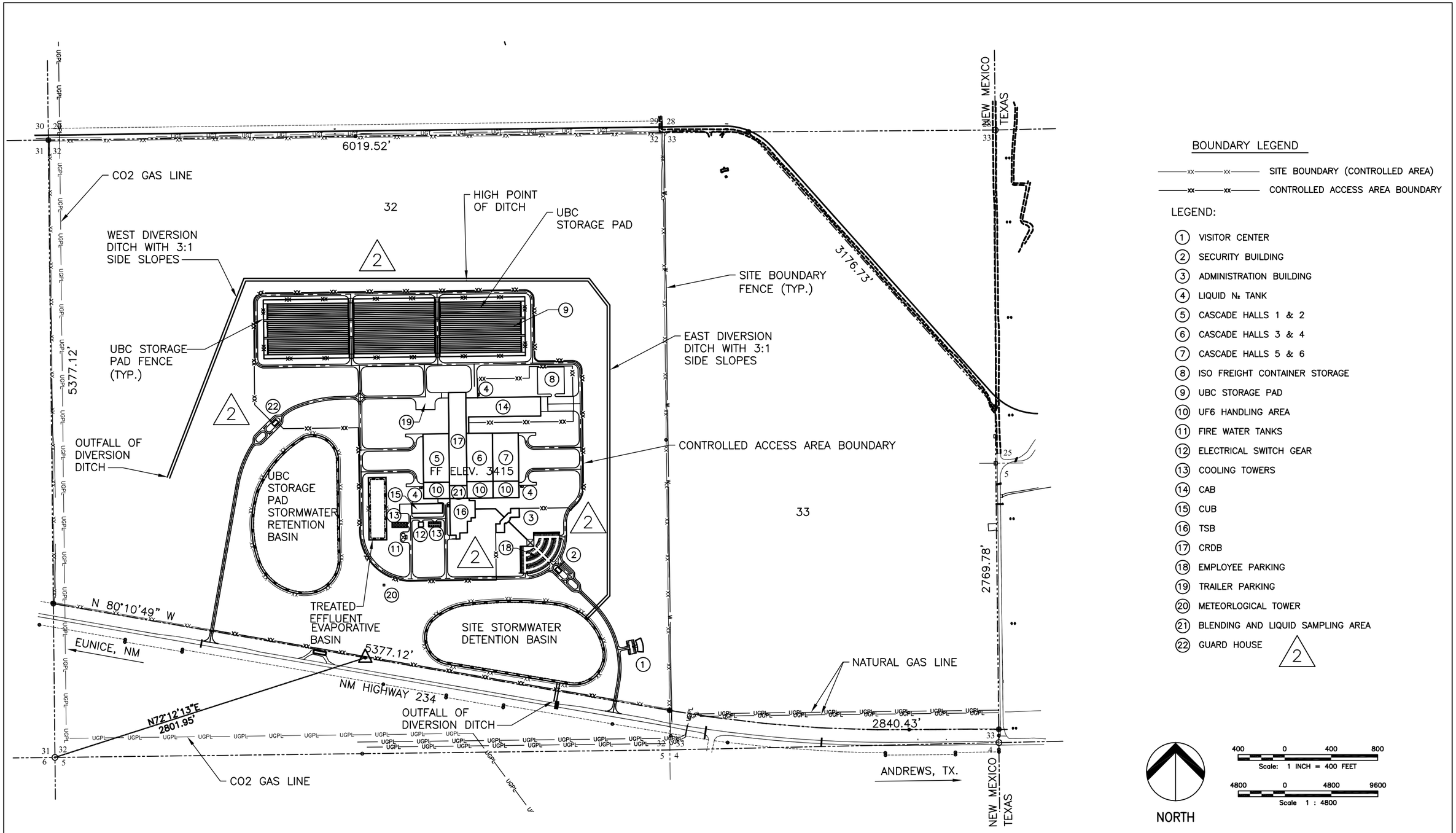

BOUNDARY LEGEND

SITE BOUNDARY (CONTROLLED AREA)

CONTROLLED ACCESS AREA BOUNDARY

LEGEND:

1. VISITOR CENTER
2. SECURITY BUILDING
3. ADMINISTRATION BUILDING
4. LIQUID N_2 TANK
5. CASCADE HALLS 1 & 2
6. CASCADE HALLS 3 & 4
7. CASCADE HALLS 5 & 6
8. ISO FREIGHT CONTAINER STORAGE
9. UBC STORAGE PAD
10. UF6 HANDLING AREA
11. FIRE WATER TANKS
12. ELECTRICAL SWITCH GEAR
13. COOLING TOWERS
14. CAB
15. CUB
16. TSB
17. CRDB
18. EMPLOYEE PARKING
19. TRAILER PARKING
20. METEORLOGICAL TOWER
21. BLENDING AND LIQUID SAMPLING AREA
22. GUARD HOUSE

LOCKWOOD GREENE
ENGINEERING & CONSTRUCTION
Spartanburg, South Carolina

REFERENCE NUMBER
c0000001.dwg

FIGURE 3.2-3
SITE PLAN

REVISION 2 DATE: JULY 2004

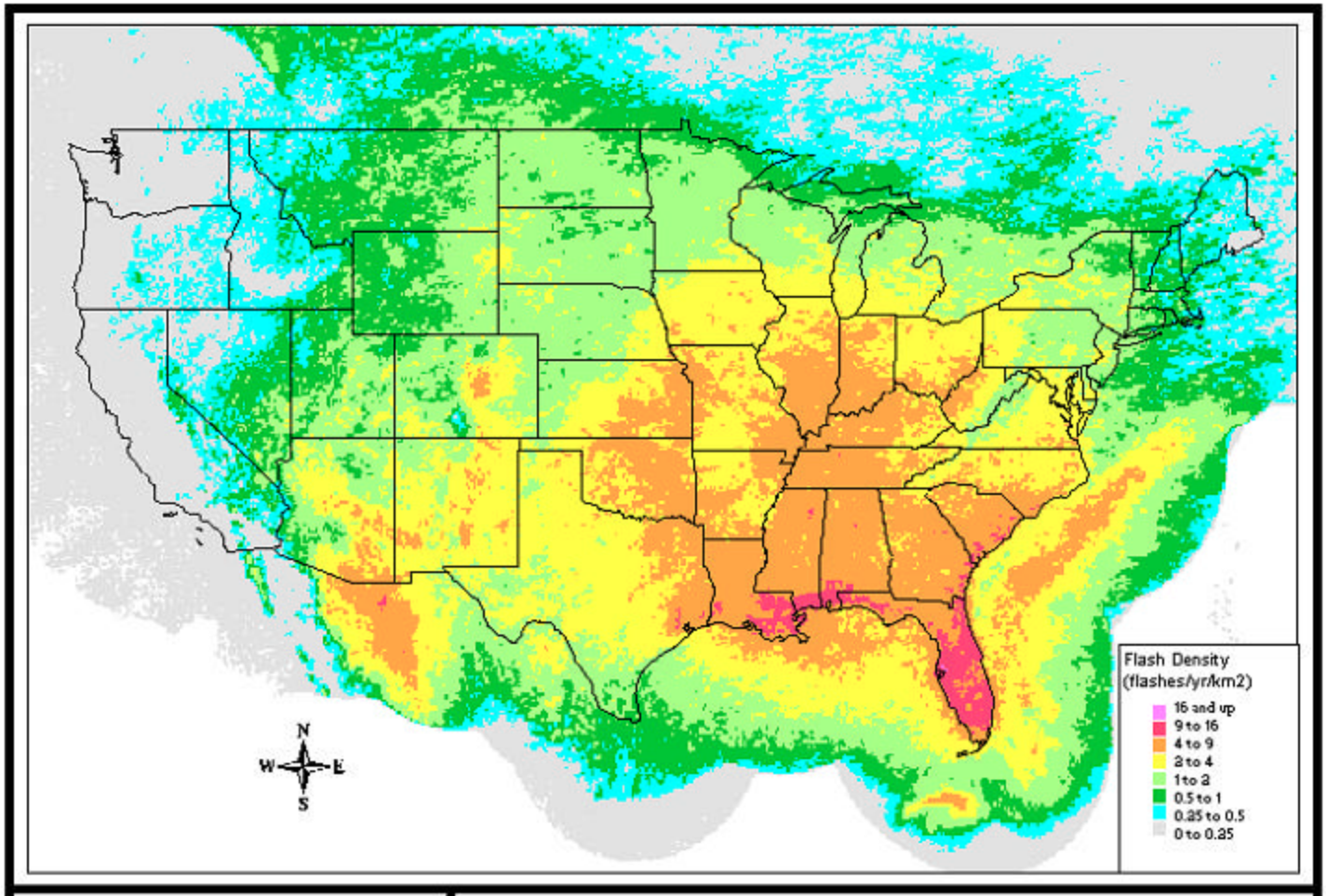

1996-2000 FLASH DENSITY MAP

(NWS, 2003)

REFERENCE NUMBER
Figure 3.2-4.dwg

FIGURE 3.2-4
AVERAGE LIGHTNING FLASH DENSITY

REVISION DATE: DECEMBER 2003

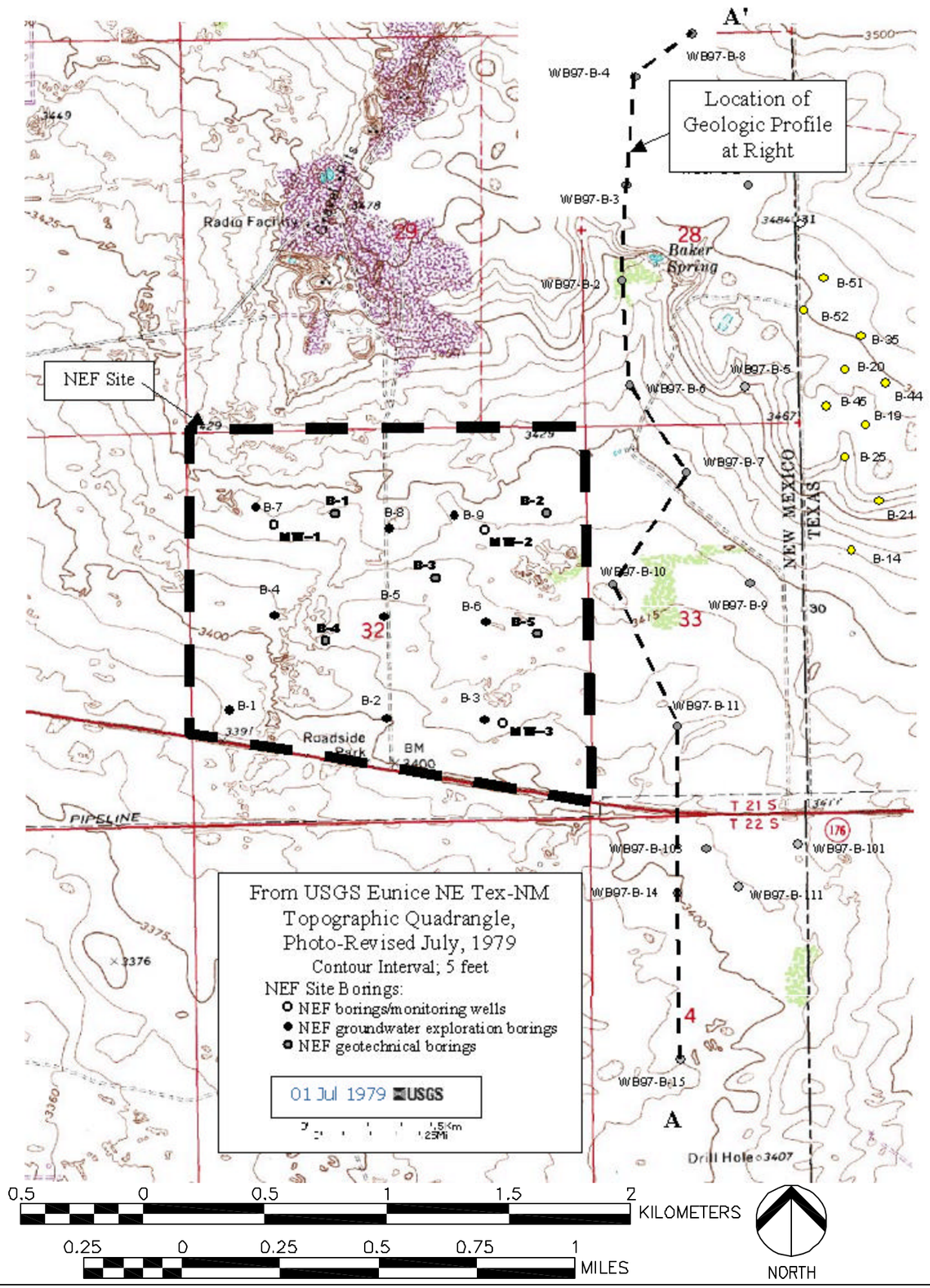

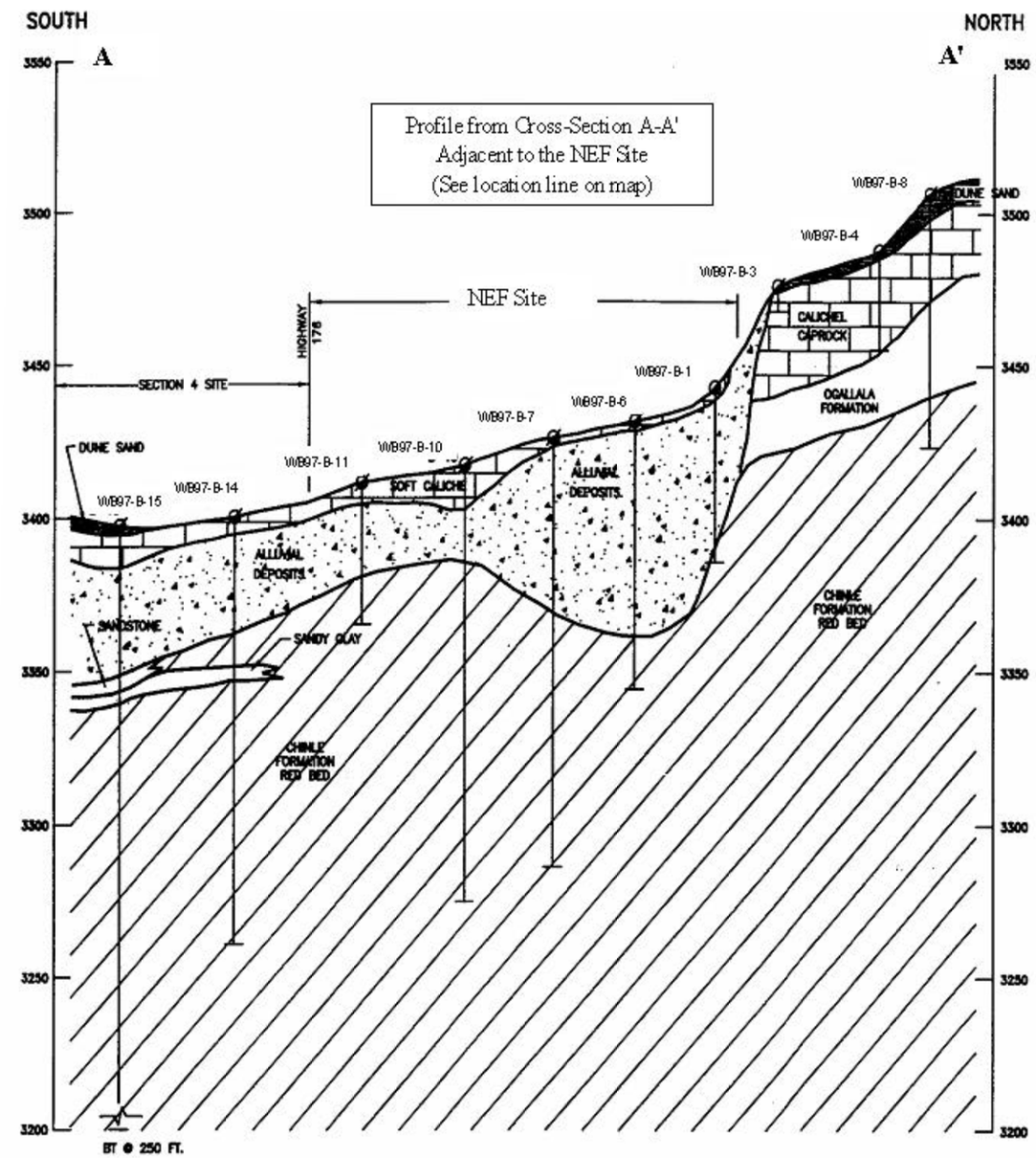

FIGURE 3.2-5

SITE BORING PLAN AND PROFILE

REFERENCE NUMBER
Figure 3.2-5.dwg

REVISION DATE: DECEMBER 2003

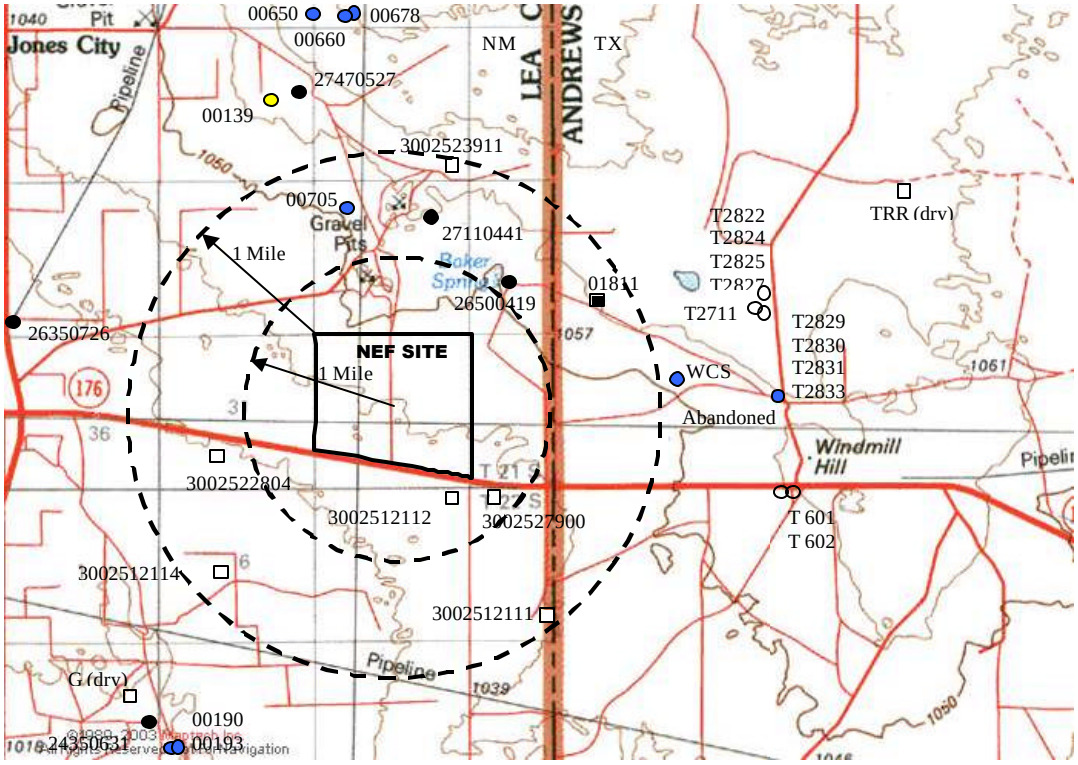

Water Wells

- ○ **Undetermined**
- ● **Observation wells: USGS**
- ● **Livestock well**
- ● **Domestic Well**

Oil Wells

- ■ □ **Open symbol represents dry, plugged and/or abandoned hole**

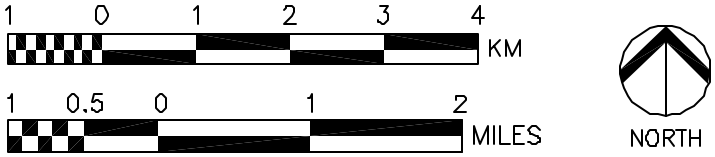

REFERENCE NUMBER
Figure 3.2-6.dwg

FIGURE 3.2-6

WATER AND OIL WELLS
IN THE VICINITY OF THE NEF SITE

REVISION DATE: DECEMBER 2003

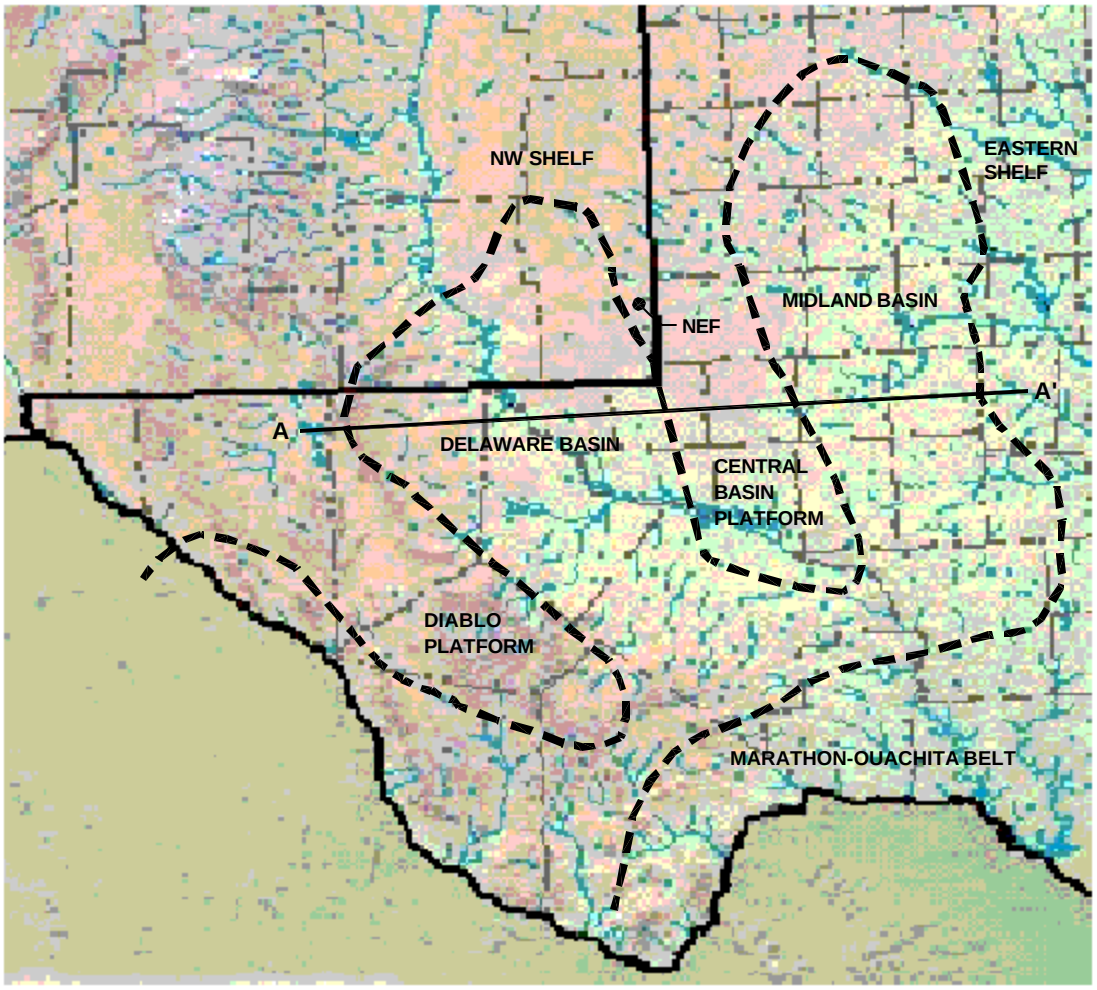

Permian Basin Geologic Profile

(Generalized from UTPB, 2003)

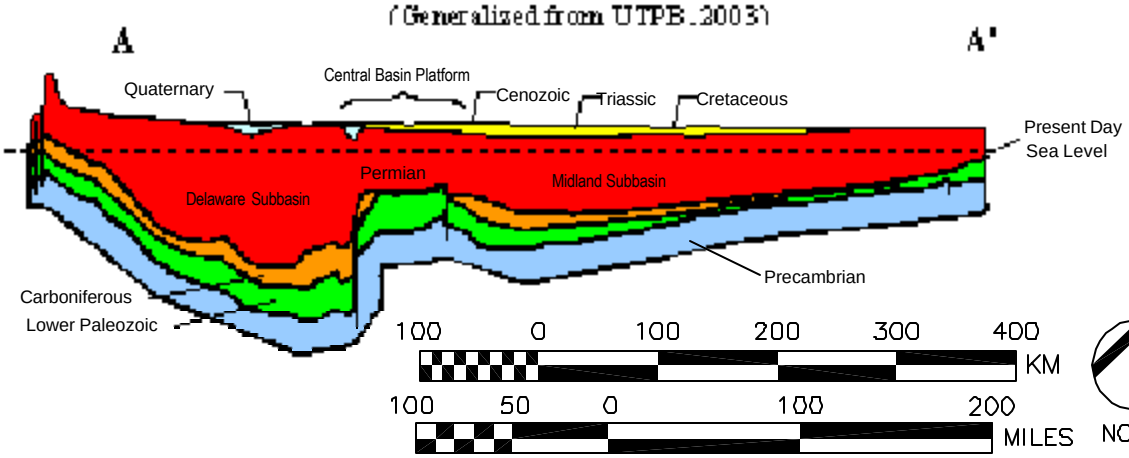

FIGURE 3.2-7

PERMIAN BASIN GEOLOGIC STRUCTURES AND PROFILE

REFERENCE NUMBER

1Figures 3.2.dwg

REVISION DATE: DECEMBER 2003

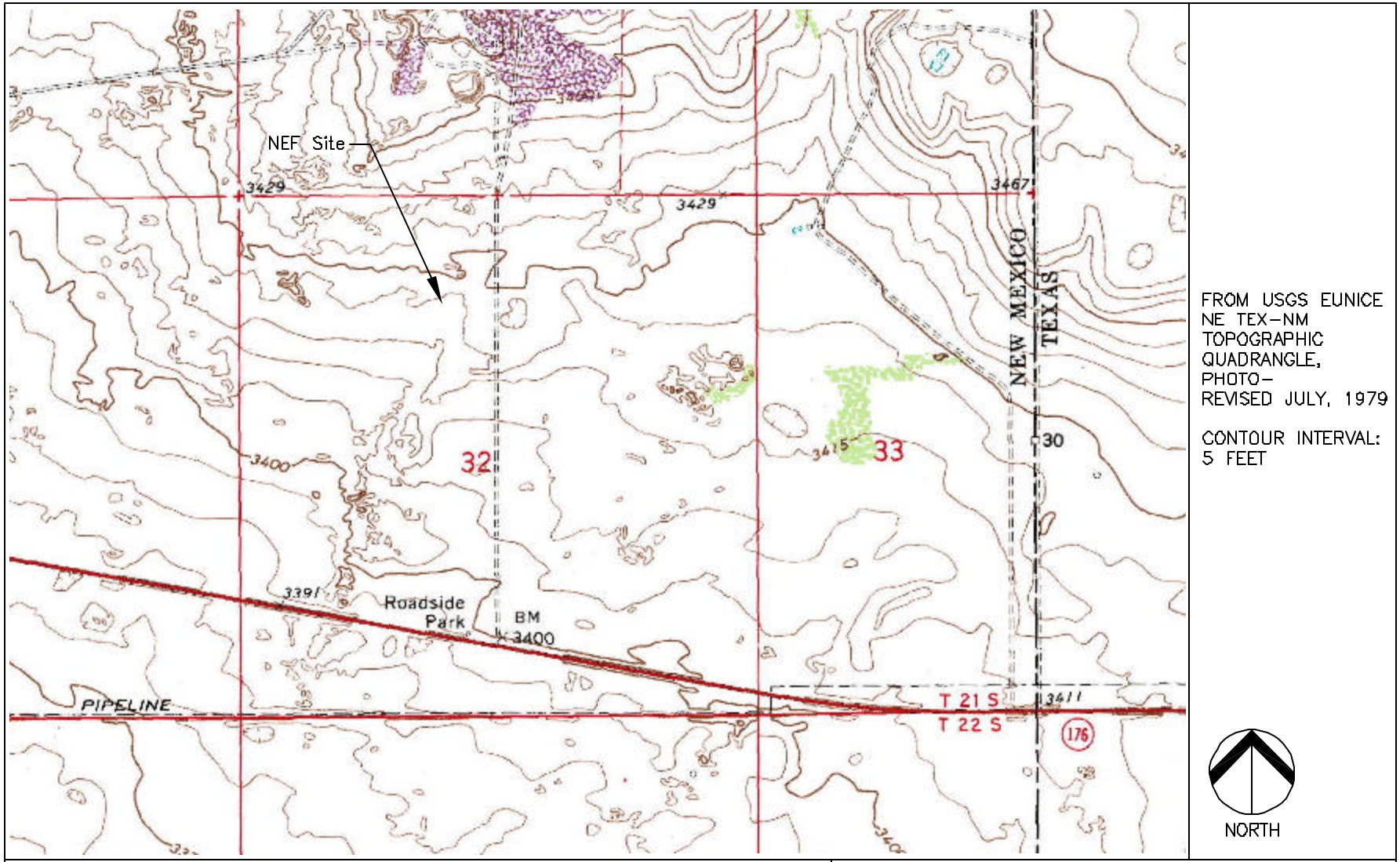

0.25 0 0.25 0.5 0.75 1 MILES

Modified from: http://mrdata.usgs.gov.

REFERENCE NUMBER
Figure 3.2-8.dwg

FIGURE 3.2-8
SITE TOPOGRAPHY

REVISION DATE: DECEMBER 2003

LEGEND

ca — CALICHE — *Partly indurated zone of calcium carbonate accumulation formed in upper layers of surficial deposits; 2 to 10 ft thick; commonly overlain by windblown sand. Much caliche shown on the map consists of tough, slabby surface layers underlain by calcium carbonate nodules that grade downward to fibers and veinlets. Especially well developed in Basin and Range and Great Plains parts of the state. Thick caliches (locally >20 ft) associated with undissected High Plains surfaces of the Great Plains commonly comprise an upper sequence of several carbonate-cemented zones interlayered with reddish loamy paleosol horizons over a basal caprock zone developed on Ogallala (To) sediments. Forms on various types of parent formations, indicated by subscripts. The extensive caliche along Rio Salado northwest of Socorro is partly a travertine deposit. Where buried by sand, the caliche is identified by subscript ca. A distinctive unit; boundaries are well defined where the caliche forms rimrock and approximate where exposed in deflation hollows. Where thick and well indurated, caliche is quarried for road metal and other aggregate, subject to minimal erosion*

al_2 — FLOODPLAIN AND CHANNEL DEPOSITS ALONG GENERALLY DRY ARROYOS AND WASHES — *Includes deposits along some perennial mountain streams. Extent exaggerated to emphasize drainage patterns. Sandier than al_1, gradients 5 to 15 percent. Arroyos 10 ft deep common. Surface flat where deposit was formed by stream overflowing its banks; hummocky where built of coalescing fans at mouths of tributaries that crowd the main stream against its far bank; or V-shaped where alluvium grades laterally into fan sand washed from adjoining hillsides. Ephemeral perched water tables under some deposits. Width of deposits represented has been exaggerated but total area probably about right because small deposits had to be omitted*

fs — SAND FACIES — *Sandy alluvium with subordinate amounts of fine gravel, silt, and clay. Forms at least four kinds of ground: 1) On short, steep fans sloping from the mountains of granitic or gneissic rock (e.g., parts of the Florida Mountains), this facies may form a smooth sandy layer a few feet thick covering gravel below; slopes 5 to 20 percent; washes 1 to 10 ft deep may expose underlying gravel. 2) On other short fans, sand facies may form arcuate belt at toe of fan with slopes averaging 10 percent, commonly reworked into coppice dunes 3 to 7 ft high (sm). 3) Other belts of smooth sandy ground commonly slope 5 percent or less and consist of sand mounds approximately 1 ft high over caliche (fs_2). 4) Gypsiferous sand (fs_3), especially in the Jornada del Muerto, Tularosa Valley and east side of the Pecos Valley. Sand facies absent on the broad Las Palomas surface. Thin fan sand covering pediments is denoted by fs over subscript that identifies underlying formation. Boundary with residual sand, fan gravel, and fan silt is approximate*

s_2/ca/To — MODERATELY THICK SAND ON CALICHE ON OGALLALA FORMATION — *Sand 1 to 3 ft thick. Surface layers noncalcareous over reddish loam. Local sand mounds. Ground favored for farming. Boundaries approximate*

s_3/ca/To — THICK SAND ON CALICHE ON OGALLALA FORMATION — *Sand 3 to 5 ft thick. Local mounds. Brownish-red, fine sandy loam over reddish-brown, sandy clay loam; noncalcareous to depths of 3 ft; calcareous subsoil contains filaments of lime carbonate. Where farmed, ground is subject to wind erosion. Boundaries approximate*

sm — LOOSE SAND IN MOUNDS — *Coppice dunes, commonly 3 to 7 ft high and 25 to 50 ft in diameter; generally elongated north of east but a local exception lies east of Columbus where elongation is south of east. Age is Holocene. Boundaries fairly accurate*

ps — SANDY LAKE OR PLAYA DEPOSITS — *Gypsiferous deposits labeled ps_2*

R — OTHER BEDROCK — *Colluvium or other cover amounts to less than half the area. Only extensive areas are shown; age and rock type keyed by symbol to State geologic map (e.g., Kd, Cretaceous Dakota Sandstone, Rs, Triassic Santa Rosa Sandstone). Many small areas omitted; indicated boundaries are approximate.* R – *Triassic, undifferentiated*

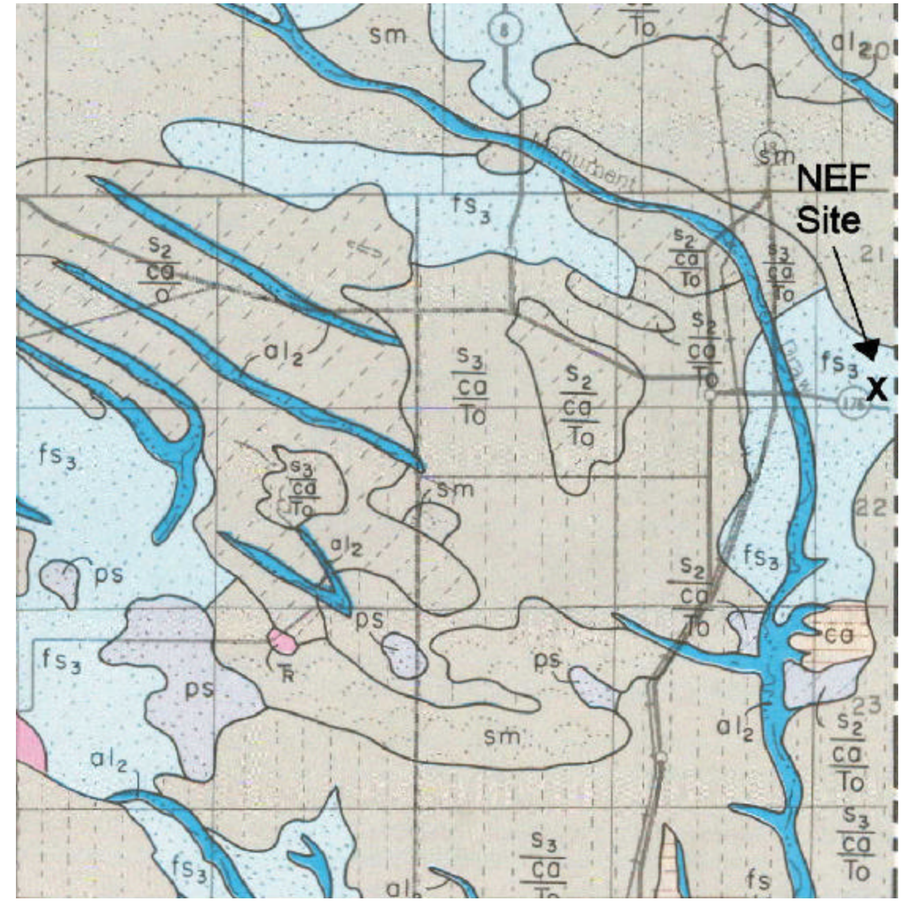

REFERENCE: (NMIMT, 1977)

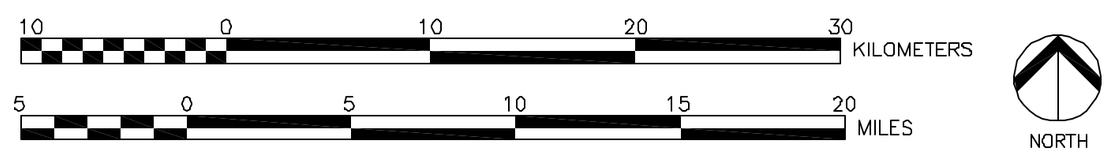

REFERENCE NUMBER
Figure 3.2-9.dwg

FIGURE 3.2-9
SURFICIAL GEOLOGIC MAP OF THE NEF SITE AREA

REVISION DATE: DECEMBER 2003

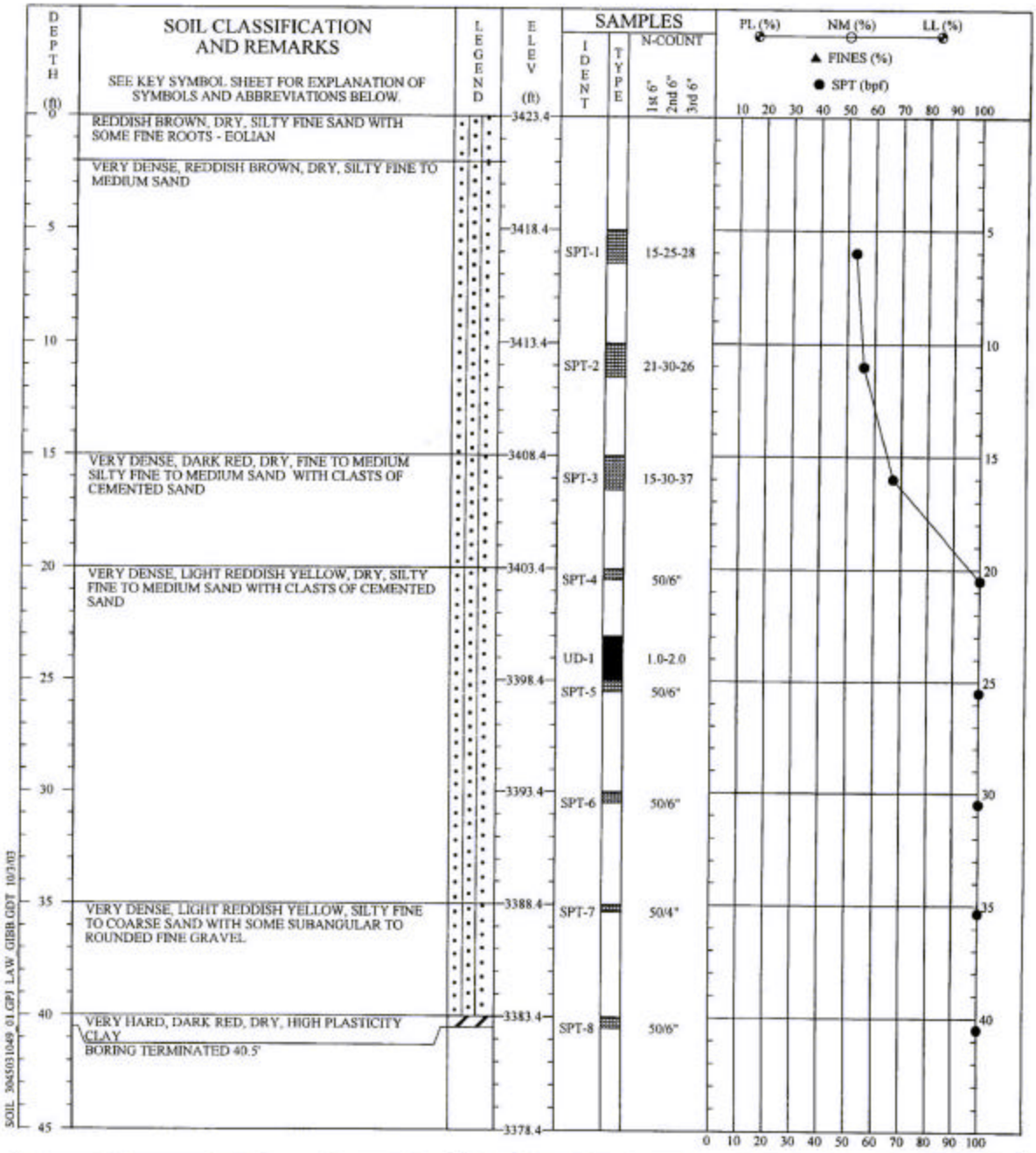

REMARKS: STANDARD PENETRATION RESISTANCE TESTING PERFORMED USING A SAFETY HAMMER. NO GROUND WATER ENCOUNTERED AT TIME OF EXPLORATION. BACK FILLED ON 9/9/2003.

SOIL TEST BORING RECORD

PROJECT: NEF - Lea County, New Mexico

DRILLED: September 9, 2003 **BORING NO.:** B-1

FIGURE 3.2-10

SOIL TEST BORING RECORD B-1

REFERENCE NUMBER BORINGS.DWG

REVISION DATE: DECEMBER 2003

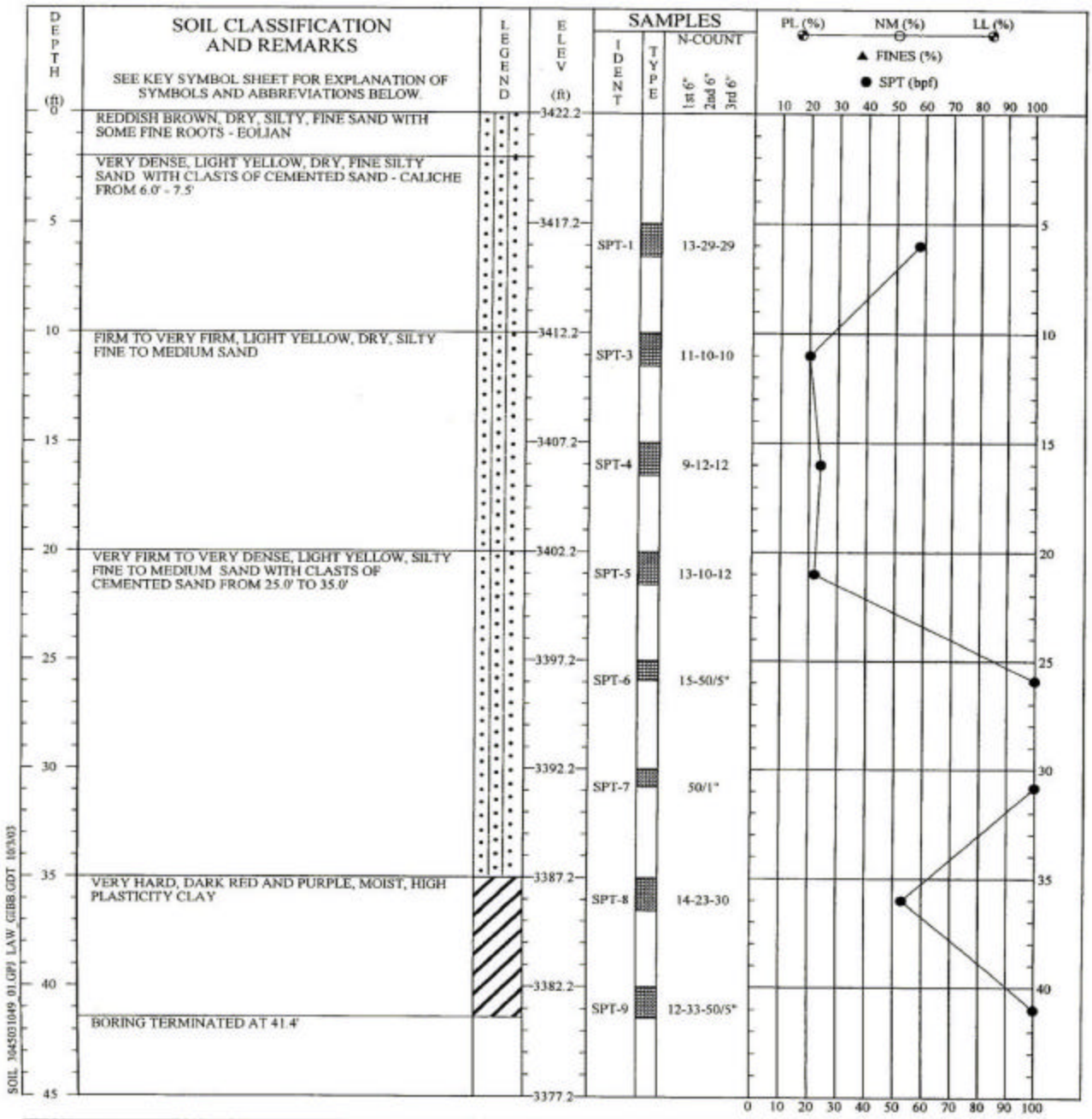

REMARKS: STANDARD PENETRATION RESISTANCE TESTING PERFORMED USING A SAFETY HAMMER. NO GROUND WATER ENCOUNTERED AT TIME OF EXPLORATION. BACK FILLED ON 9/9/2003.

SOIL TEST BORING RECORD

PROJECT: NEF - Lea County, New Mexico

DRILLED: September 9, 2003 **BORING NO.:** B-2

FIGURE 3.2-11

SOIL TEST BORING RECORD B-2

REFERENCE NUMBER BORINGS.DWG

REVISION DATE: DECEMBER 2003

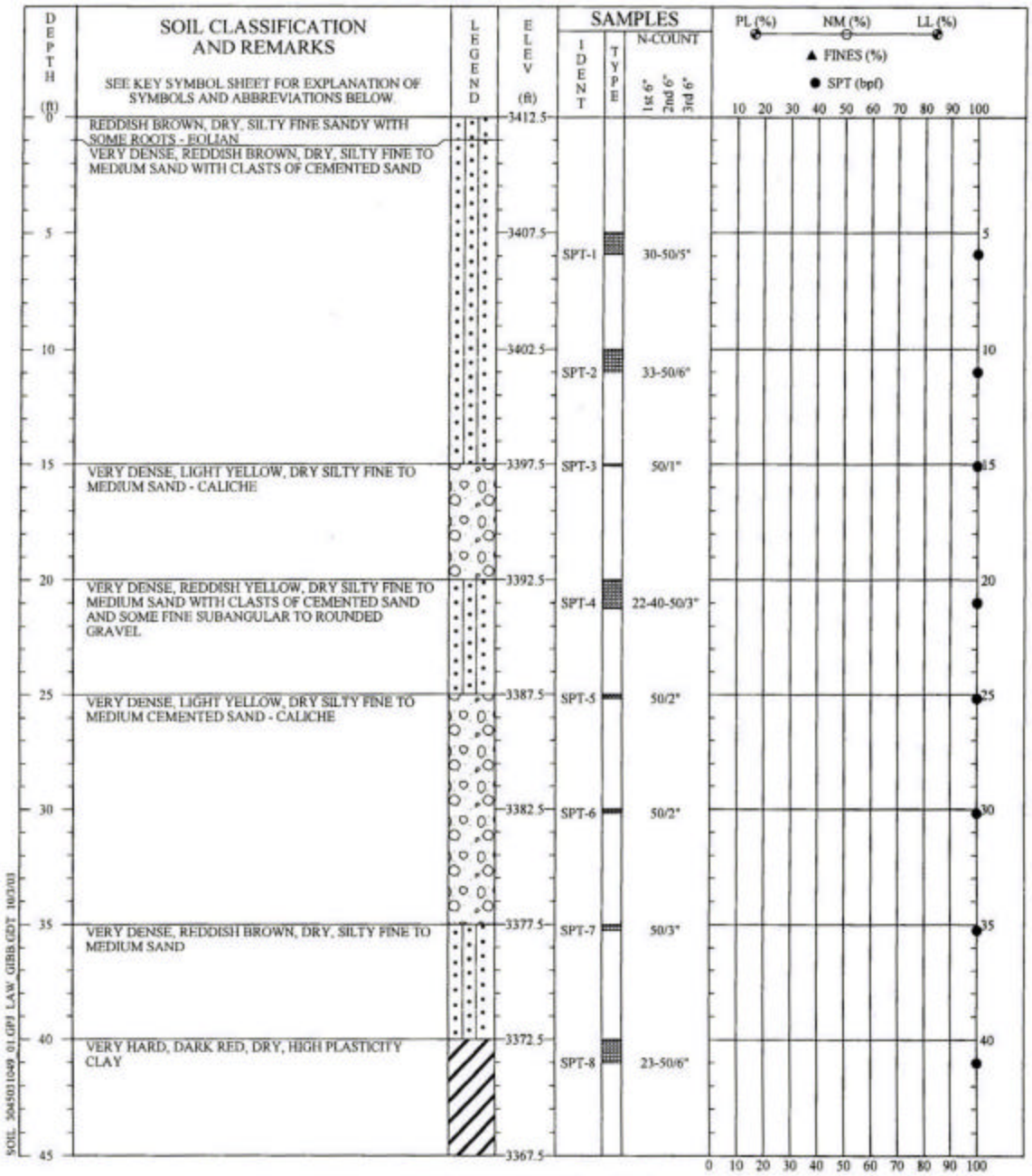

REMARKS: STANDARD PENETRATION RESISTANCE TESTING PERFORMED USING A SAFETY HAMMER. NO GROUND WATER ENCOUNTERED AT TIME OF EXPLORATION. BACK FILLED ON 9/10/2003.

SOIL TEST BORING RECORD

PROJECT: NEF - Lea County, New Mexico

DRILLED: September 10, 2003 **BORING NO.:** B-3

SHEET 1 OF 3

REFERENCE NUMBER BORINGS.DWG

FIGURE 3.2-12

SOIL TEST BORING RECORD B-3

REVISION DATE: DECEMBER 2003

DEPTH (ft)	SOIL CLASSIFICATION AND REMARKS SEE KEY SYMBOL SHEET FOR EXPLANATION OF SYMBOLS AND ABBREVIATIONS BELOW.	LEGEND	ELEV (ft)	SAMPLES IDENT	TYPE	N-COUNT 1st 6" 2nd 6" 3rd 6"	Pl. (%) NM (%) LL (%) ▲ FINES (%) ● SPT (bpf)
45	VERY HARD, DARK RED, DRY, HIGH PLASTICITY CLAY		3367.5	SPT-9		27-50/5"	
50			3362.5	SPT-10		39-50/2"	
55	VERY HARD, DARK RED AND PURPLE, DRY, HIGH PLASTICITY CLAY		3357.5	SPT-11		35-50/4"	
60			3352.5	SPT-12		31-50/5"	
65			3347.5	SPT-13		32-50/4"	
70			3342.5	SPT-14		22-50/5"	
75			3337.5	SPT-15		39-50/4"	
80	VERY HARD, DARK RED AND PURPLE, DRY, HIGH PLASTICITY CLAY WITH OCCASIONAL THIN CEMENTED LAYERS OF GREENISH GRAY		3332.5	SPT-16		50/4"	
85	VERY HARD, REDDISH PURPLE WITH GRAY MOTTLING, DRY HIGH PLASTICITY CLAY		3327.5	SPT-17		50/6"	
90			3322.5				

SOIL 704503 1049 01.GPJ LAW GIBB GDT 10/3/03

REMARKS: STANDARD PENETRATION RESISTANCE TESTING PERFORMED USING A SAFETY HAMMER. NO GROUND WATER ENCOUNTERED AT TIME OF EXPLORATION. BACK FILLED ON 9/10/2003.

SOIL TEST BORING RECORD

PROJECT: NEF - Lea County, New Mexico

DRILLED: September 10, 2003 **BORING NO.:** B-3

SHEET 2 OF 3

REFERENCE NUMBER BORINGS.DWG

FIGURE 3.2-12

SOIL TEST BORING RECORD B-3

REVISION DATE: DECEMBER 2003

DEPTH (ft)	SOIL CLASSIFICATION AND REMARKS	LEGEND	ELEV (ft)	SAMPLES IDENT	TYPE	N-COUNT 1st 6" 2nd 6" 3rd 6"	PL (%) NM (%) LL (%) ▲ FINES (%) ● SPT (bpf)
90	SEE KEY SYMBOL SHEET FOR EXPLANATION OF SYMBOLS AND ABBREVIATIONS BELOW.						
	VERY HARD, RED AND PURPLE, DRY, HIGH PLASTICITY CLAY		3322.5	SPT-18		50/5"	
95			3317.5	SPT-19		50/6"	
100			3312.5	SPT-20		50/6"	
	BORING TERMINATED AT 100.5'						
105			3307.5				
110			3302.5				
115			3297.5				
120			3292.5				
125			3287.5				
130			3282.5				
135			3277.5				

SOIL 3045951049.01.GPJ LAW GIBB.GDT 10/3/03

REMARKS: STANDARD PENETRATION RESISTANCE TESTING PERFORMED USING A SAFETY HAMMER. NO GROUND WATER ENCOUNTERED AT TIME OF EXPLORATION. BACK FILLED ON 9/10/2003.

SOIL TEST BORING RECORD

PROJECT: NEF - Lea County, New Mexico

DRILLED: September 10, 2003 **BORING NO.:** B-3

SHEET 3 OF 3

REFERENCE NUMBER BORINGS.DWG

FIGURE 3.2-12

SOIL TEST BORING RECORD B-3

REVISION DATE: DECEMBER 2003

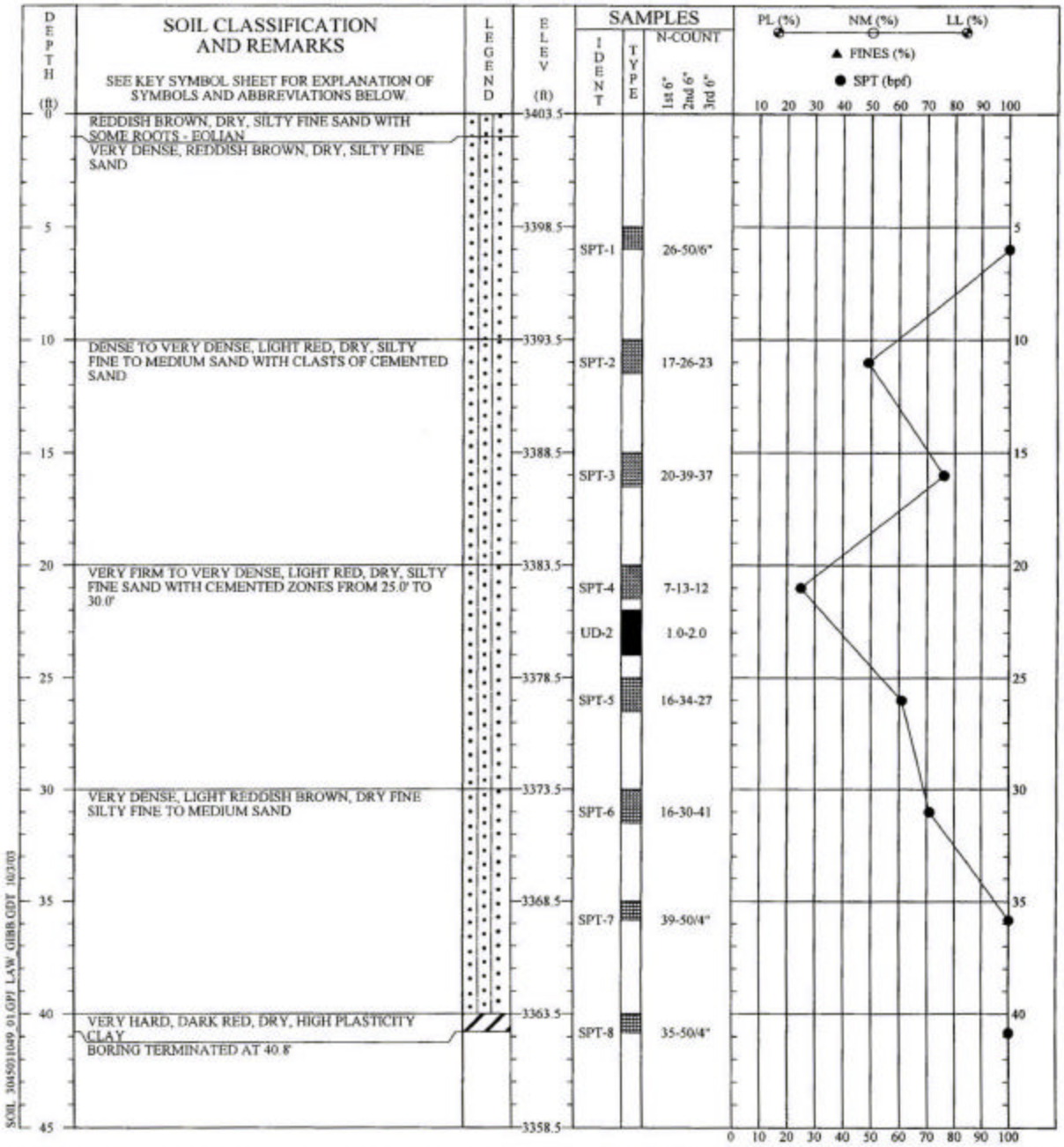

REMARKS: STANDARD PENETRATION RESISTANCE TESTING PERFORMED USING A SAFETY HAMMER. NO GROUND WATER ENCOUNTERED AT TIME OF EXPLORATION. BACK FILLED ON 9/9/2003.

SOIL TEST BORING RECORD

PROJECT: NEF - Lea County, New Mexico

DRILLED: September 9, 2003 **BORING NO.:** B-4

FIGURE 3.2-13

SOIL TEST BORING RECORD B-4

REFERENCE NUMBER

BORINGS.DWG

REVISION DATE: DECEMBER 2003

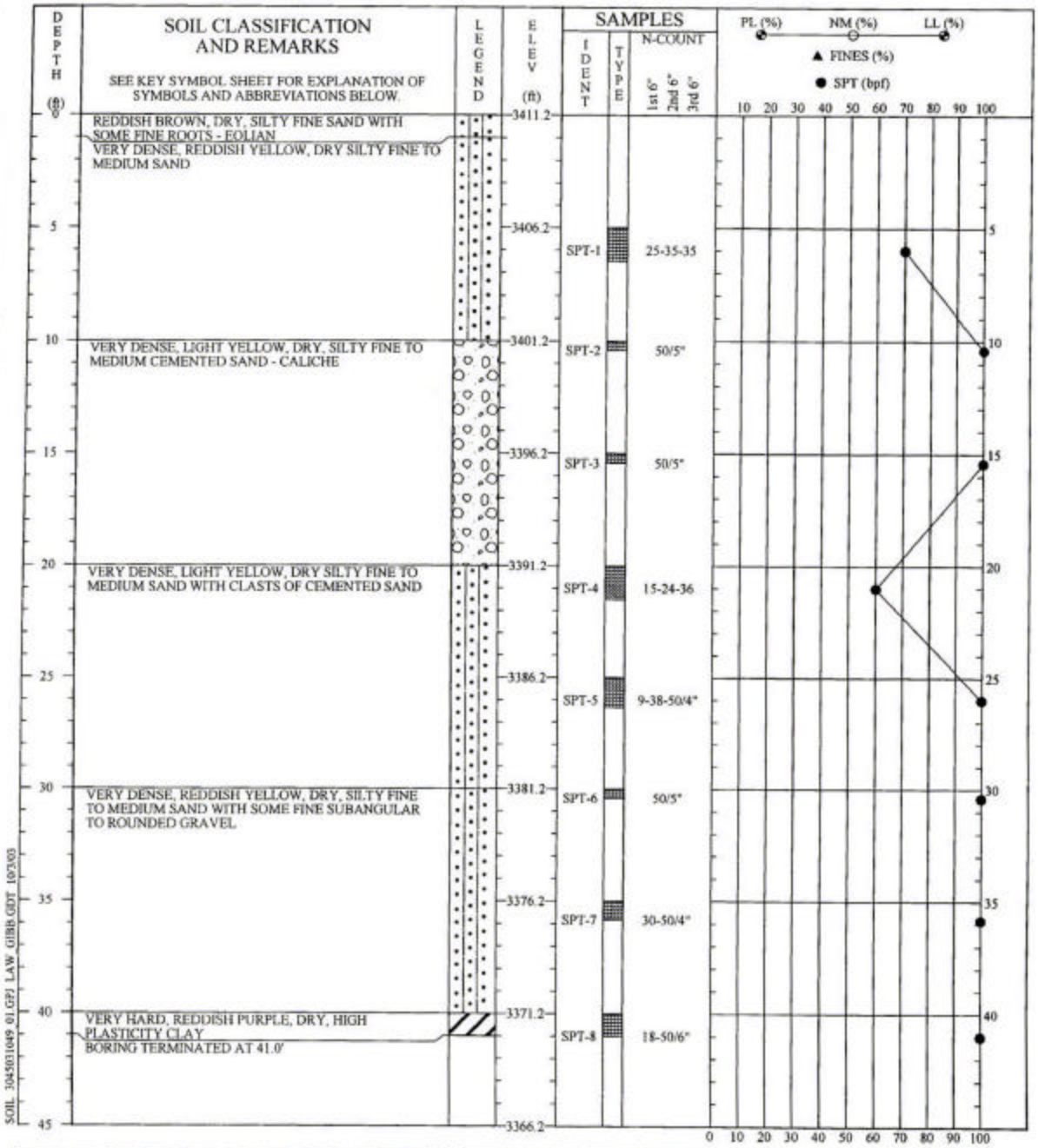

REMARKS: STANDARD PENETRATION RESISTANCE TESTING PERFORMED USING A SAFETY HAMMER. NO GROUND WATER ENCOUNTERED AT TIME OF EXPLORATION. BACK FILLED ON 9/10/2003.

SOIL TEST BORING RECORD

PROJECT: NEF - Lea County, New Mexico

DRILLED: September 10, 2003 **BORING NO.:** B-5

FIGURE 3.2-14

SOIL TEST BORING RECORD B-5

REFERENCE NUMBER

BORINGS.DWG

REVISION DATE: DECEMBER 2003

GROUP SYMBOLS	TYPICAL NAMES	GROUP SYMBOLS	TYPICAL NAMES
	TOPSOIL		CONCRETE
	ASPHALT		DOLOMITE
	GRAVEL		LIMESTONE
	FILL		SHALE
	SUBSOIL		LIMESTONE/SHALE - Limestone with shale laminate
	ALLUVIUM		SANDSTONE
	COLLUVIUM		SILTSTONE
	RESIDUUM - Soft to firm		AUGER BORING
	RESIDUUM - Stiff to very hard		UNDISTURBED SAMPLE ATTEMPT

BOUNDARY CLASSIFICATIONS: Soils possessing characteristics of two groups are designated by combinations of group symbols.

SILT OR CLAY	SAND			GRAVEL		Cobbles	Boulders
	Fine	Medium	Coarse	Fine	Coarse		

No.200 No.40 No.10 No.4 3/4" 3" 12"

U.S. STANDARD SIEVE SIZE

Reference: The Unified Soil Classification System, Corps of Engineers, U.S. Army Technical Memorandum No. 3-357, Vol. 1, March, 1953 (Revised April, 1960)

Undisturbed Sample 1.5-2.0 = Recovered (ft) / Pushed (ft)	
Split Spoon Sample	Auger Cuttings
Rock Core 60-100 = RQD / Recovery	Dilatometer
No Sample	Crandall Sampler
Rotary Drill	Pressure Meter
Water Table at time of drilling	No Recovery
	Water Table after 24 hours

Correlation of Penetration Resistance with Relative Density and Consistency

SAND & GRAVEL		SILT & CLAY	
No. of Blows	Relative Density	No. of Blows	Consistency
0 - 4	Very Loose	0 - 2	Very Soft
5 - 10	Loose	3 - 4	Soft
11 - 20	Firm	5 - 8	Firm
21 - 30	Very Firm	9 - 15	Stiff
31 - 50	Dense	16 - 30	Very Stiff
Over 50	Very Dense	31 - 50	Hard
		Over 50	Very Hard

boringlkey.dwg
BORINGFIGURES.dwg

FIGURE 3.2-15

SOIL TEST BORING KEY TO SYMBOLS AND DESCRIPTIONS

REVISION DATE: DECEMBER 2003

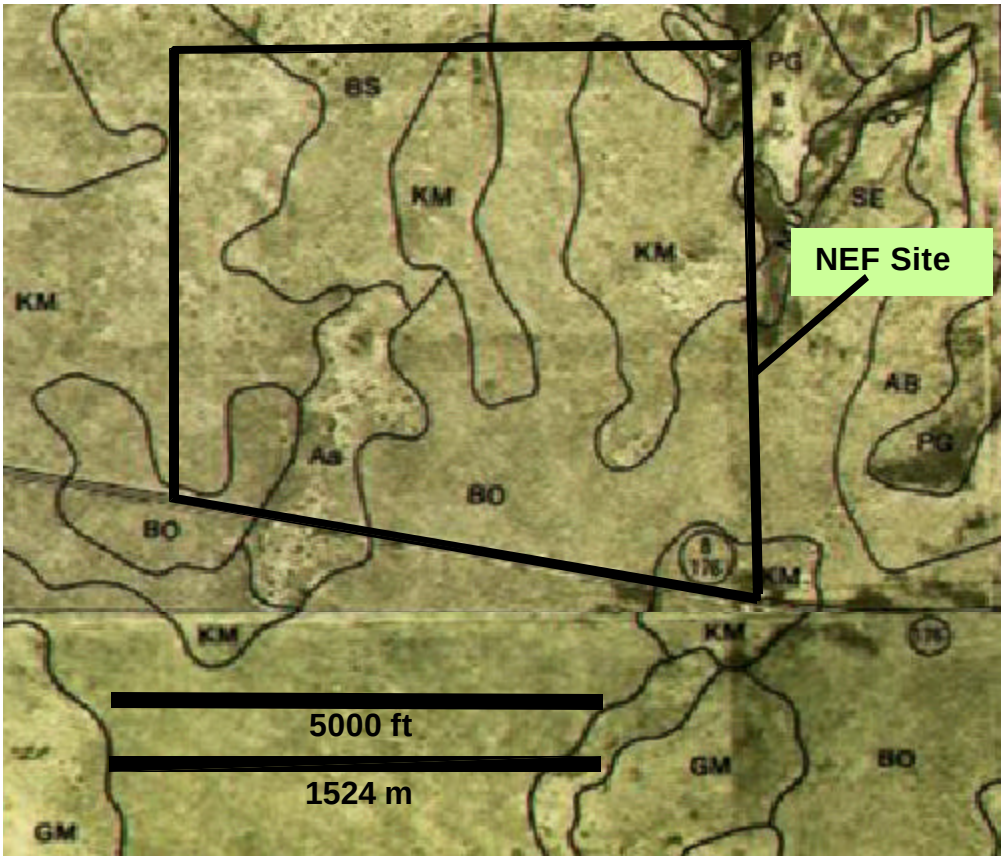

USDA SOIL DESIGNATION	SOIL NAME/DESCRIPTION	UNIFIED SOIL CLASSIFICATION DESIGNATION(S)
Aa	ACTIVE (SAND) DUNE LAND.	SP
BO	BROWNFIELD-SPRINGER ASSOCIATION: MOSTLY FINE SAND WITH LOAM FINE SAND; LEVEL TO UNDULATING TOPOGRAPHY; MODERATELY RAPID PERMEABLILITY AND SLOW RUNOFF.	SM
BS	BROWNFIELD-SPRINGER ASSOCIATION: MOSTLY FINE SAND WITH LOAM FINE SAND; DUNES AND HUMMOCKS FOR CONCAVE AND CONVEX ROLLING TERRAIN; DRAINAGE SIMILAR TO BO.	SM
KM	KERMIT SOILS AND DUNE LAND: EXCESSIVELY-DRAINED NON-CALCAREOUS SOILS; HUMMOCKY AND UNDULATING TOPOGRAPHY DUE TO EOLIAN PROCESSES.	SP-SM OR SM
MU	MIXED ALLUVIAL LANDS: UNCONSOLIDATED, STRATIFIED ALLUVIUM WITH VARIED TEXTURES OCCURRING INTERMITTENTLY IN DRAINAGE-WAYS A FEW FEET IN THICKNESS; MODERATE TO RAPID PERMEABILITY WITH SLOW RUNOFF.	VARIABLE
PG	PORTALES AND GOMEZ FINE SANDY LOAMS: LIGHT CLAY LOAM, WELL-DRAINED.	VARIABLE

SOURCE: (USDA, 1974)

NORTH

REFERENCE NUMBER
Figure 3.2–16.dwg

FIGURE 3.2-16
SITE SOILS MAP
(USDA, 1974)

REVISION DATE: DECEMBER 2003

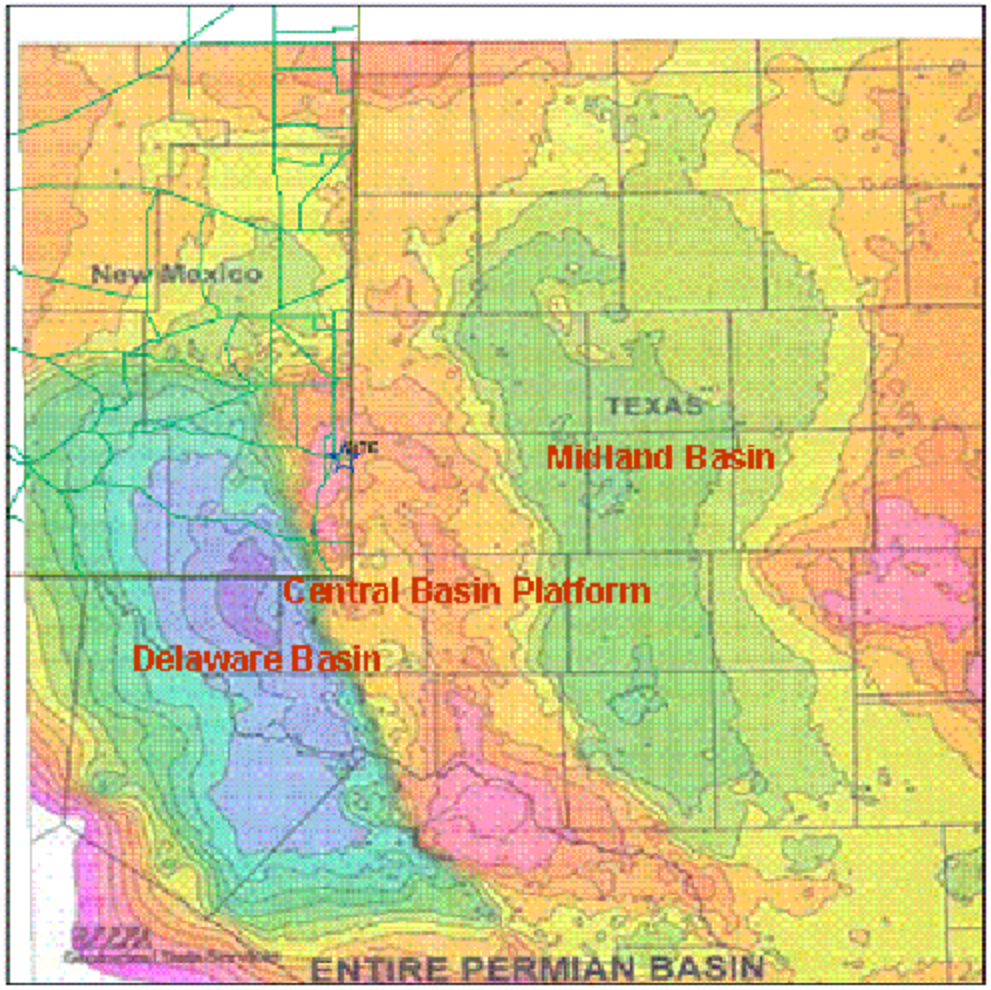

LEGEND

NEF SITE

REFERENCE:

TALLEY, D.J., 1997, CHARACTERIZATION OF A SAN ANDRES CARBONATE RESERVOIR USING FOUR DIMENSIONAL, MULTICOMPONENT ATTRIBUTE ANALYSIS, MASTER OF SCIENCE THESIS, COLORADO SCHOOL OF MINES.

NORTH

60 0 60 120 180 KM

30 0 30 60 90 120 MILES

REFERENCE NUMBER
1Figures 3.2.dwg

FIGURE 3.2-17

TECTONIC SUBDIVISIONS OF THE PERMIAN BASIN

REVISION DATE: DECEMBER 2003

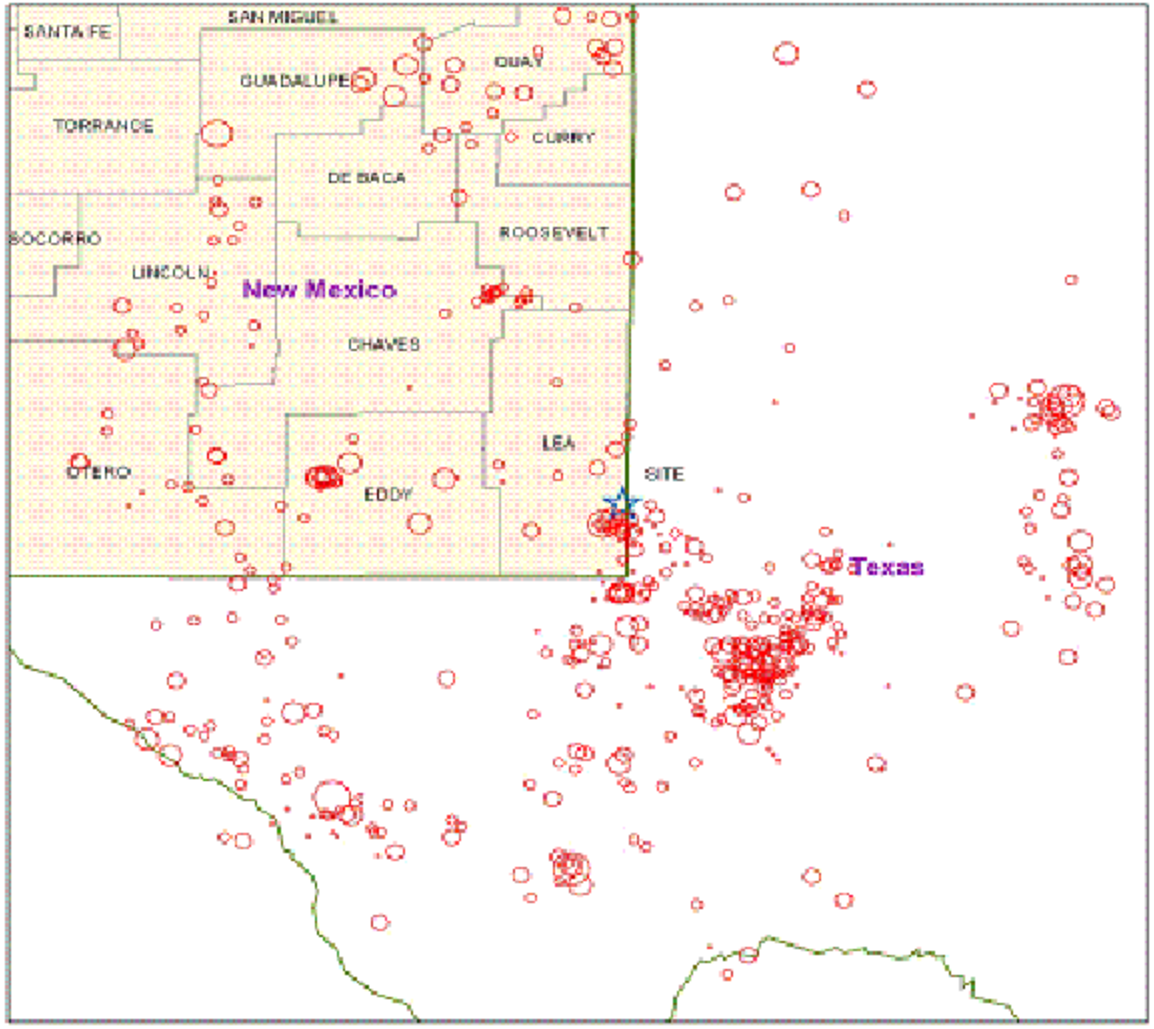

LEGEND

NEF SITE

MAGNITUDE

- 0 - 1
- 1.1 - 2.0
- 2.1 - 3.0
- 3.1 - 4.0
- 4.1 - 5.0
- 5.1 - 6.0

NORTH

0 100 200 300 400 KM

0 50 100 150 200 MILES

REFERENCE NUMBER
1Figures 3.2.dwg

FIGURE 3.2-18

SEISMICITY MAP FOR 322 KILOMETERS (200 MILE) RADIUS OF THE NEF SITE

REVISION DATE: DECEMBER 2003

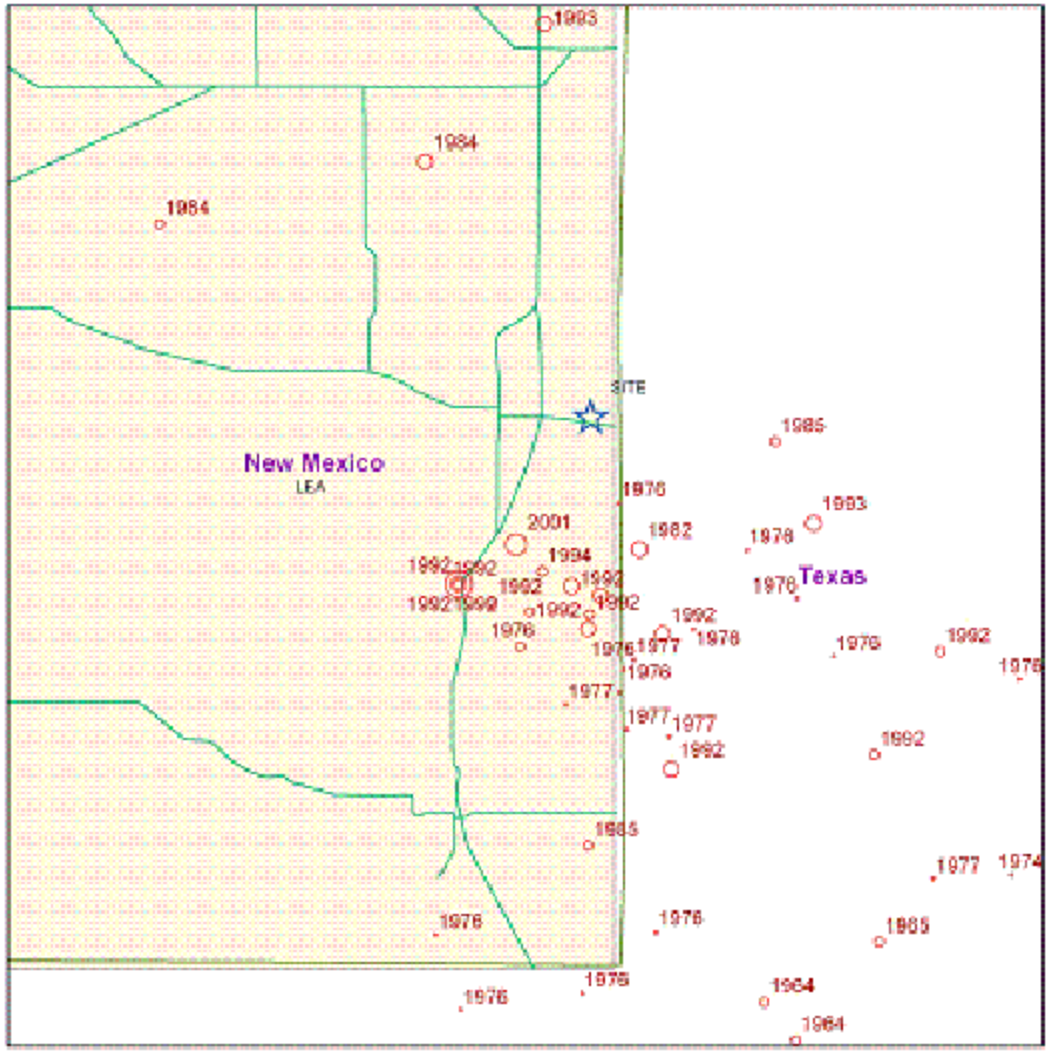
New Mexico
LEA
Texas
SITE
1993
1984
1984
1985
1976
1983
2001
1982
1978
1994
1992
1992
1992

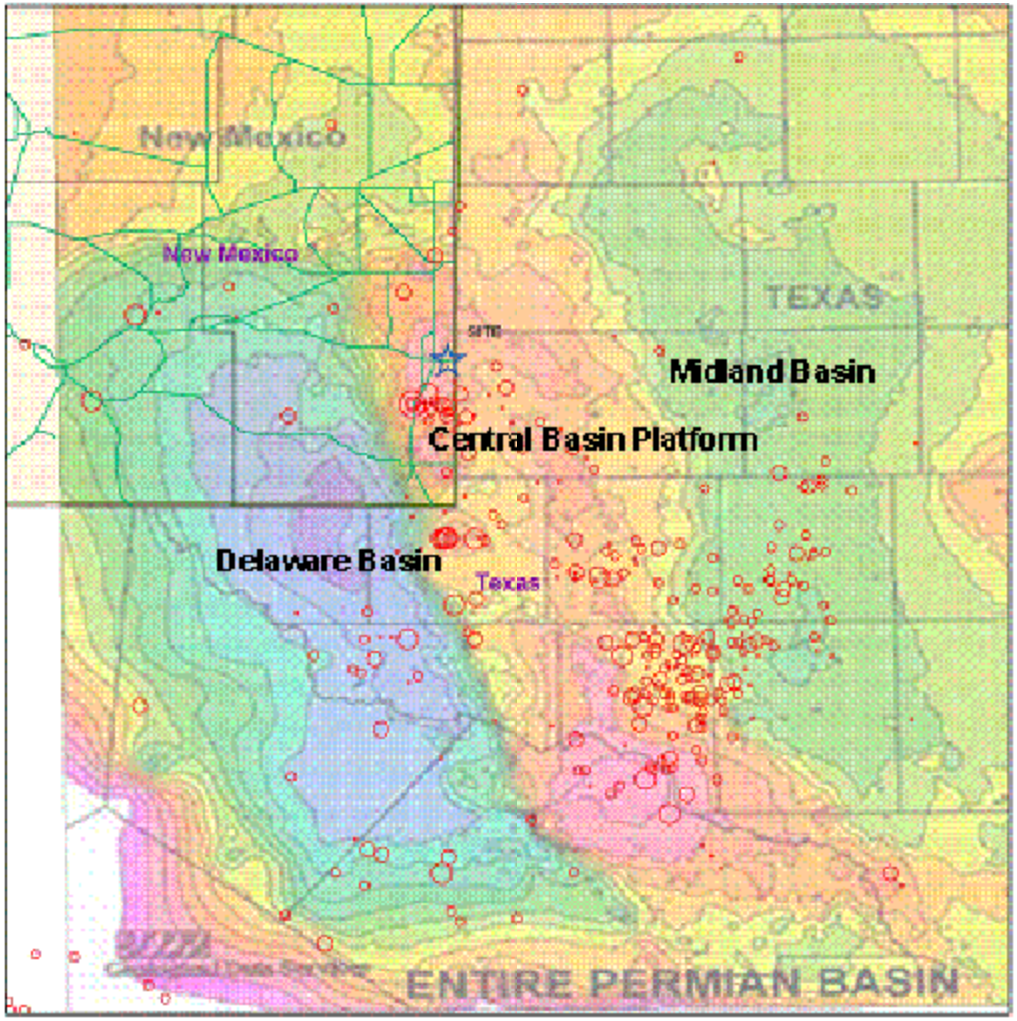

LEGEND

NEF SITE

MAGNITUDE

- 0 - 1
- 1.1 - 2.0
- 2.1 - 3.0
- 3.1 - 4.0
- 4.1 - 5.0
- 5.1 - 6.0

NORTH

40 0 40 80 120 160 KM

20 0 20 40 60 80 MILES

REFERENCE NUMBER
Figures 3.2.dwg

FIGURE 3.2-20

REGIONAL SEISMICITY AND TECTONIC ELEMENTS OF THE PERMIAN BASIN

REVISION DATE: DECEMBER 2003

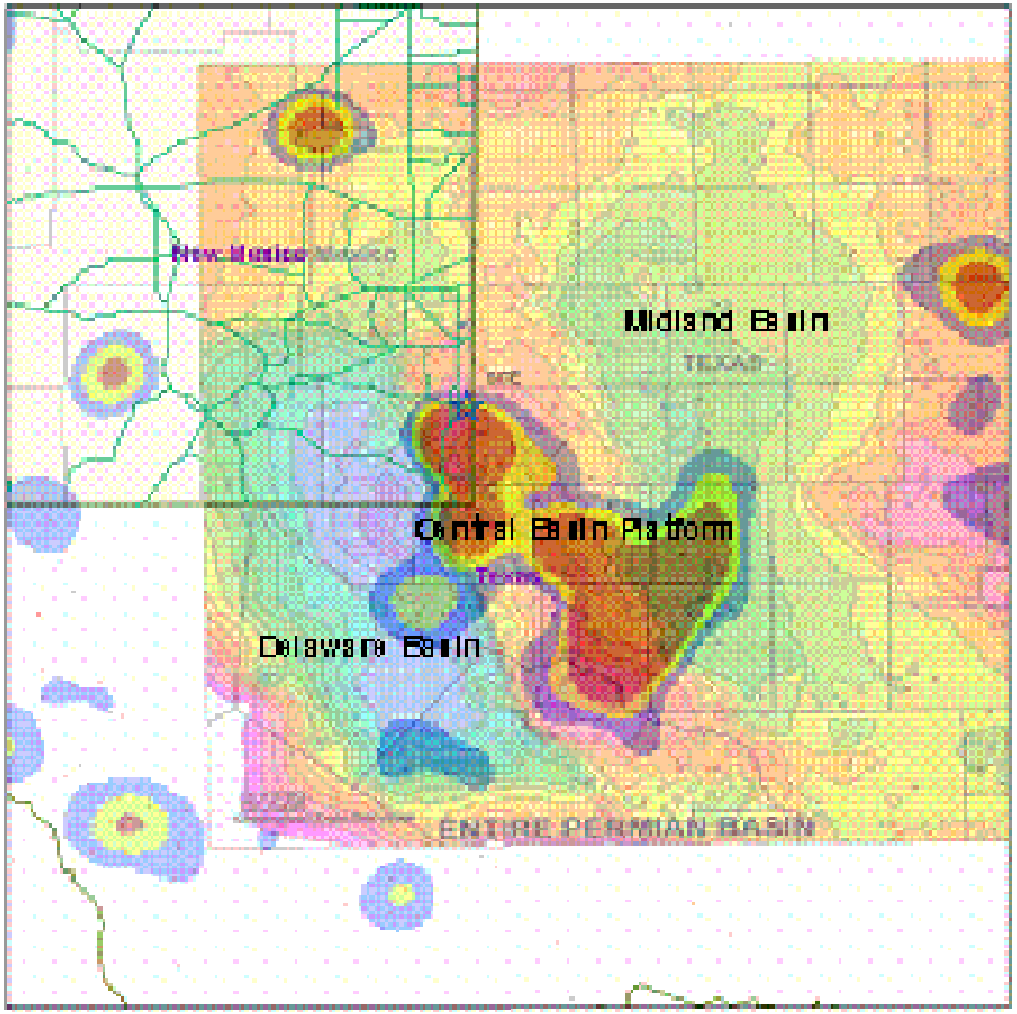

LEGEND

NEF SITE

epicenters

EARTHQUAKE DENSITY

0 - 40

40 - 86

86 - 133

133 - 705

NOTE:
THE EARTHQUAKE FREQUENCY CONTOURS SHOWN PROVIDE A VISUAL PORTRAYAL OF THE AREAS WITH SIMILAR EARTHQUAKE COUNTS PER AREA, i.e., EARTHQUAKE DENSITY. THE DENSITY UNITS THEMSELVES ARE NOT ABSOLUTE, BUT A RELATIVE REPRESENTATION OF EARTHQUAKE FREQUENCY FROM ONE LOCATION TO ANOTHER LOCATION.

2

NORTH

60 0 60 120 180 240 KM

30 0 30 60 90 120 150 MILES

REFERENCE NUMBER
Figures 3.2.dwg

FIGURE 3.2-21

EARTHQUAKE FREQUENCY CONTOURS AND TECTONIC ELEMENTS OF THE PERMIAN BASIN

REVISION 2 DATE: JULY 2004

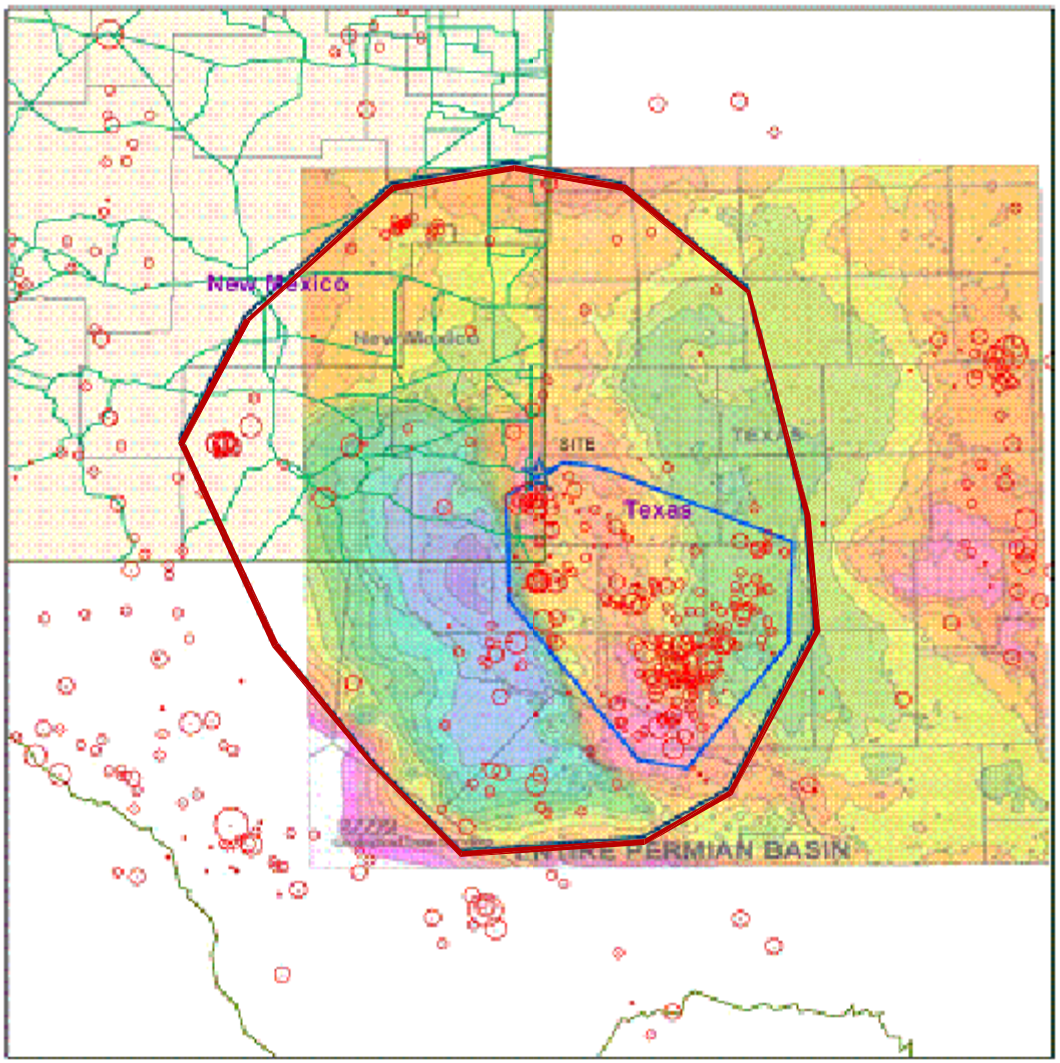

LEGEND

NEF SITE

MAGNITUDE

- 0 - 1
- 1.1 - 2.0
- 2.1 - 3.0
- 3.1 - 4.0
- 4.1 - 5.0
- 5.1 - 6.0
- epicenters

CENTRAL BASIN PLATFORM EARTHQUAKE CLUSTER

REGION 1

NORTH

0 100 200 300 KM

0 50 100 150 200 MILES

REFERENCE NUMBER
2Figures3.2.dwg

FIGURE 3.2-22

SEISMIC SOURCE AREAS FOR EARTHQUAKE FREQUENCY STATISTICAL ANALYSES

REVISION 1 DATE: FEBRUARY 2004

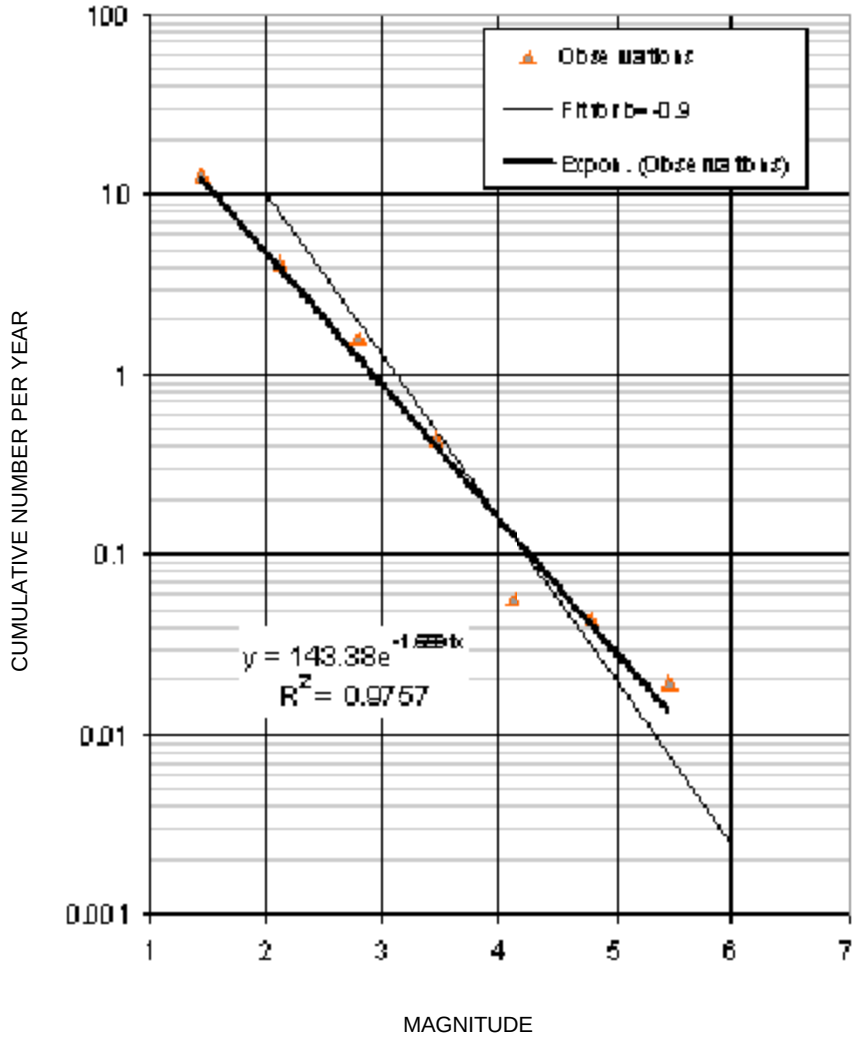

Exponential Best Fit

Log(Nc) = 2.15 – 0.74(M)

Fit assuming b = -0.90

Log(Nc) = 2.80 – 0.90(M)

M IS MAGNITUDE SCALED TO DURATION
MAGNITUDE AS DESCRIBED IN
NEW MEXICO TECH CATALOGS
CIRULAR 210, 2002

REFERENCE NUMBER
2Figures3.2.dwg

FIGURE 3.2-23

EARTHQUAKE RECURRENCE MODELS FOR THE 322 KM (200 MILE) RADIUS COMPOSITE CATALOG

REVISION DATE: DECEMBER 2003

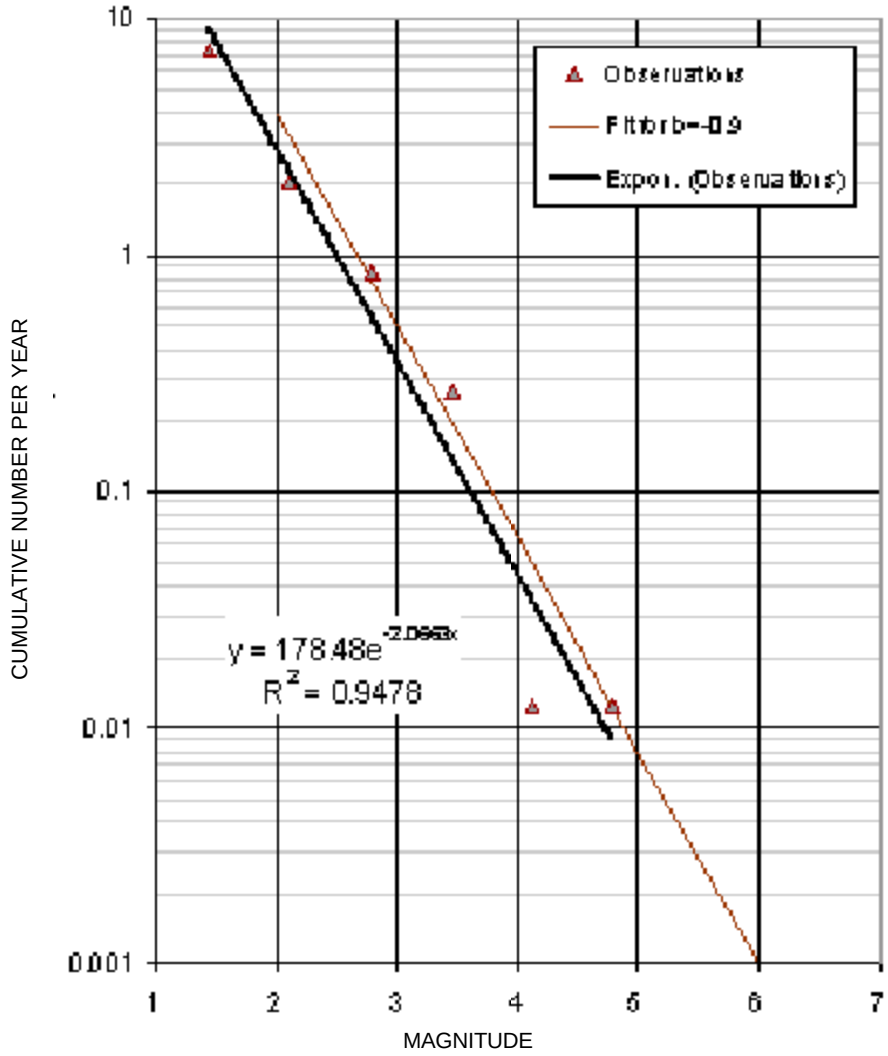

Exponential Best Fit

Log(Nc) = 2.25 – 0.89(M)

Fit assuming b = -0.90

Log(Nc) = 2.40 – 0.90(M)

M IS MAGNITUDE SCALED TO DURATION MAGNITUDE AS DESCRIBED IN NEW MEXICO TECH CATALOGS CIRULAR 210, 2002

REFERENCE NUMBER
2Figures3.2.dwg

FIGURE 3.2-24

EARTHQUAKE RECURRENCE MODELS FOR REGION 1 (161 KM (100 MILE) RADIUS OF NEF SITE)

REVISION DATE: DECEMBER 2003

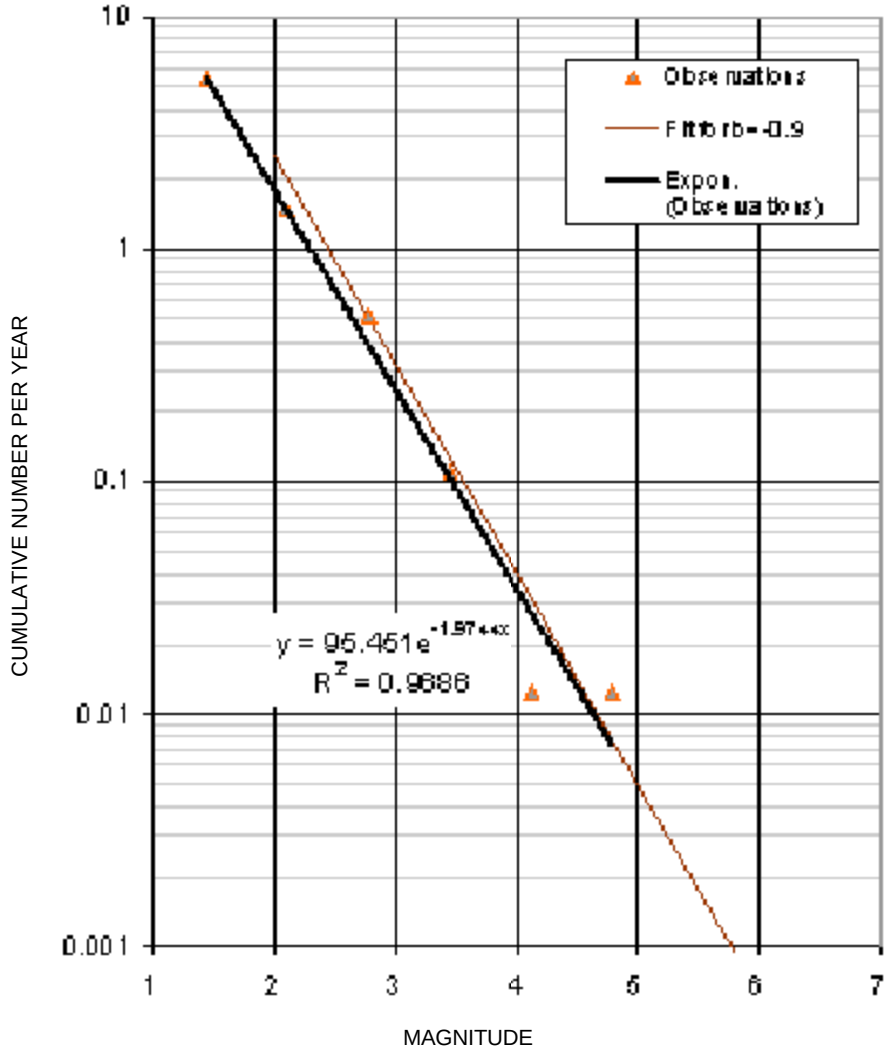

Exponential Best Fit

Log(Nc) = 1.98 – 0.86(M)

Fit assuming b = -0.90

Log(Nc) = 2.20 – 0.90(M)

M IS MAGNITUDE SCALED TO DURATION MAGNITUDE AS DESCRIBED IN NEW MEXICO TECH CATALOGS CIRULAR 210, 2002

REFERENCE NUMBER
2Figures3.2.dwg

FIGURE 3.2-25

EARTHQUAKE RECURRENCE MODELS FOR REGION 2 (CBP HIGHER DENSITY EARTHQUAKE CLUSTER)

REVISION DATE: DECEMBER 2003

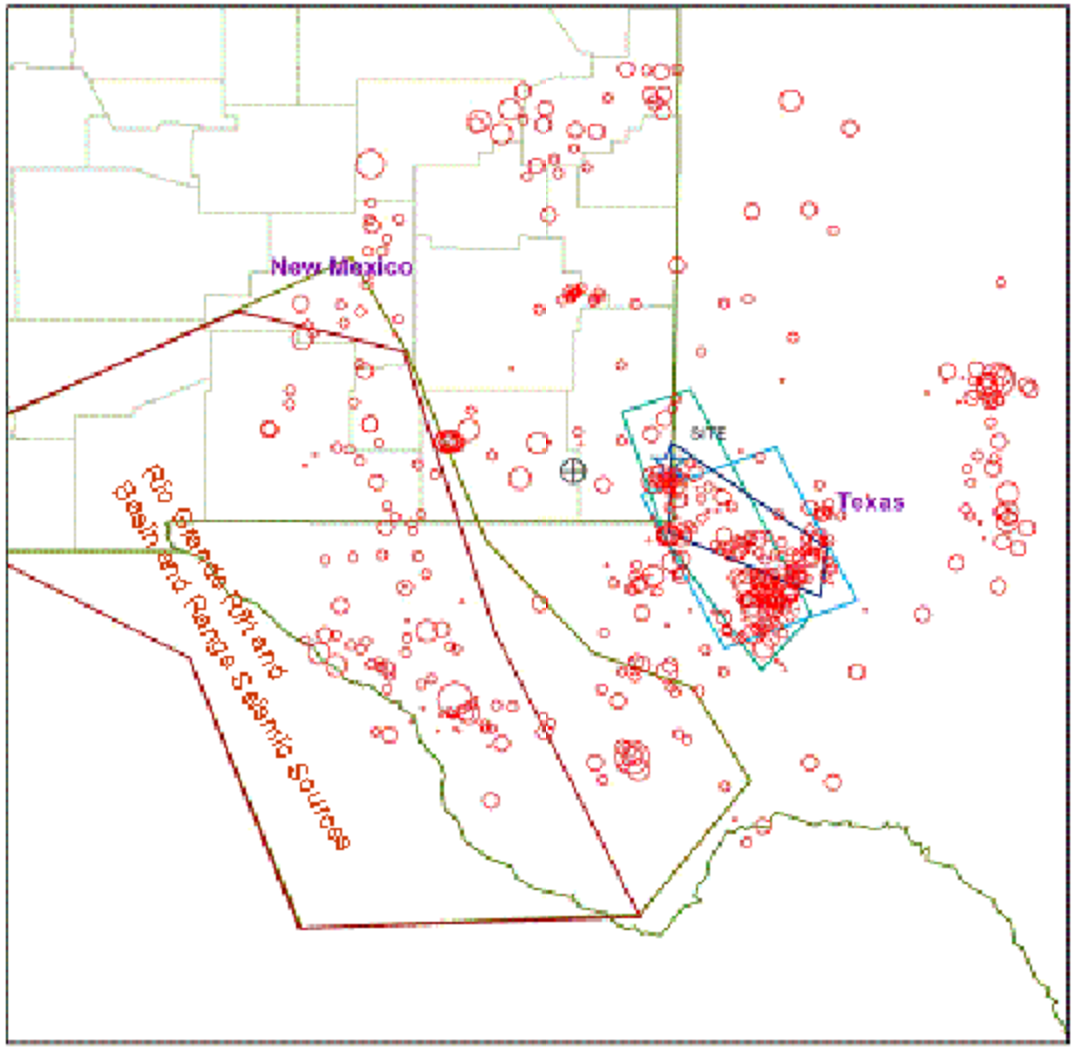

LEGEND

NEF SITE

MAGNITUDE

- 0 - 1
- 1.1 - 2.0
- 2.1 - 3.0
- 3.1 - 4.0
- 4.1 - 5.0
- 5.1 - 6.0

BASIN AND RANGE Sub A

BASIN AND RANGE Sub B

CENTRAL BASIN PLATFORM A

CENTRAL BASIN PLATFORM B

CENTRAL BASIN PLATFORM C

WIPP SITE

REFERENCE:

DOE/WIPP-95-2065 REV. 7
SAFETY ANALYSIS REPORT FOR THE WASTE ISOLATION PILOT PLANT, FIG. 2.5-26

NORTH

100 0 100 200 300 400 KM

50 0 50 100 150 200 MILES

REFERENCE NUMBER
2Figures3.2.dwg

FIGURE 3.2-26

ALTERNATE SEISMIC SOURCE GEOMETRIES USED IN THE WIPP SEISMIC HAZARD STUDY

REVISION DATE: DECEMBER 2003

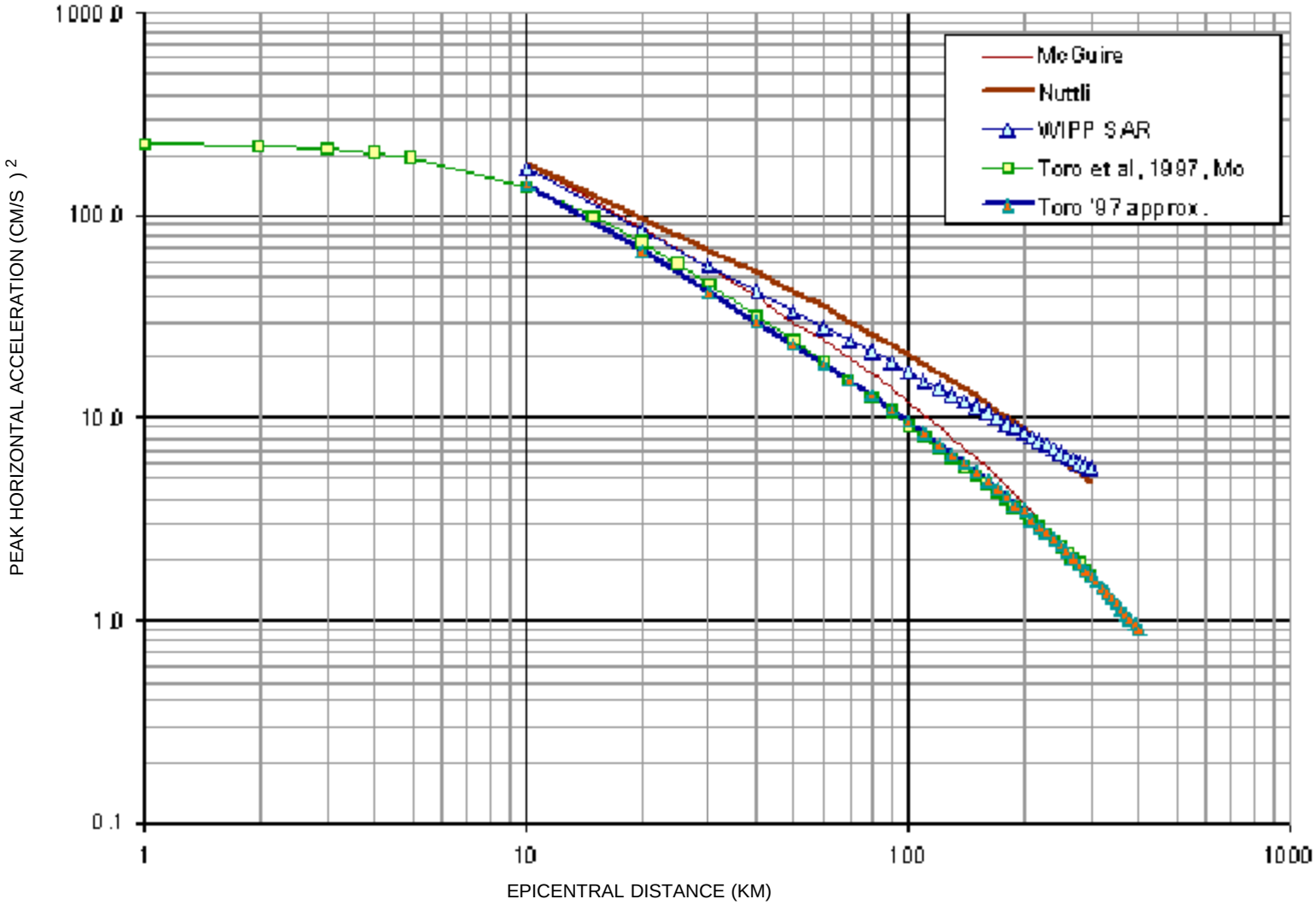

FIGURE 3.2-27

COMPARISION OF PGA ATTENUATION
FOR A MAGNITUDE 5.0 EARTHQUAKE

REFERENCE NUMBER
2Figures3.2.dwg

REVISION DATE: DECEMBER 2003

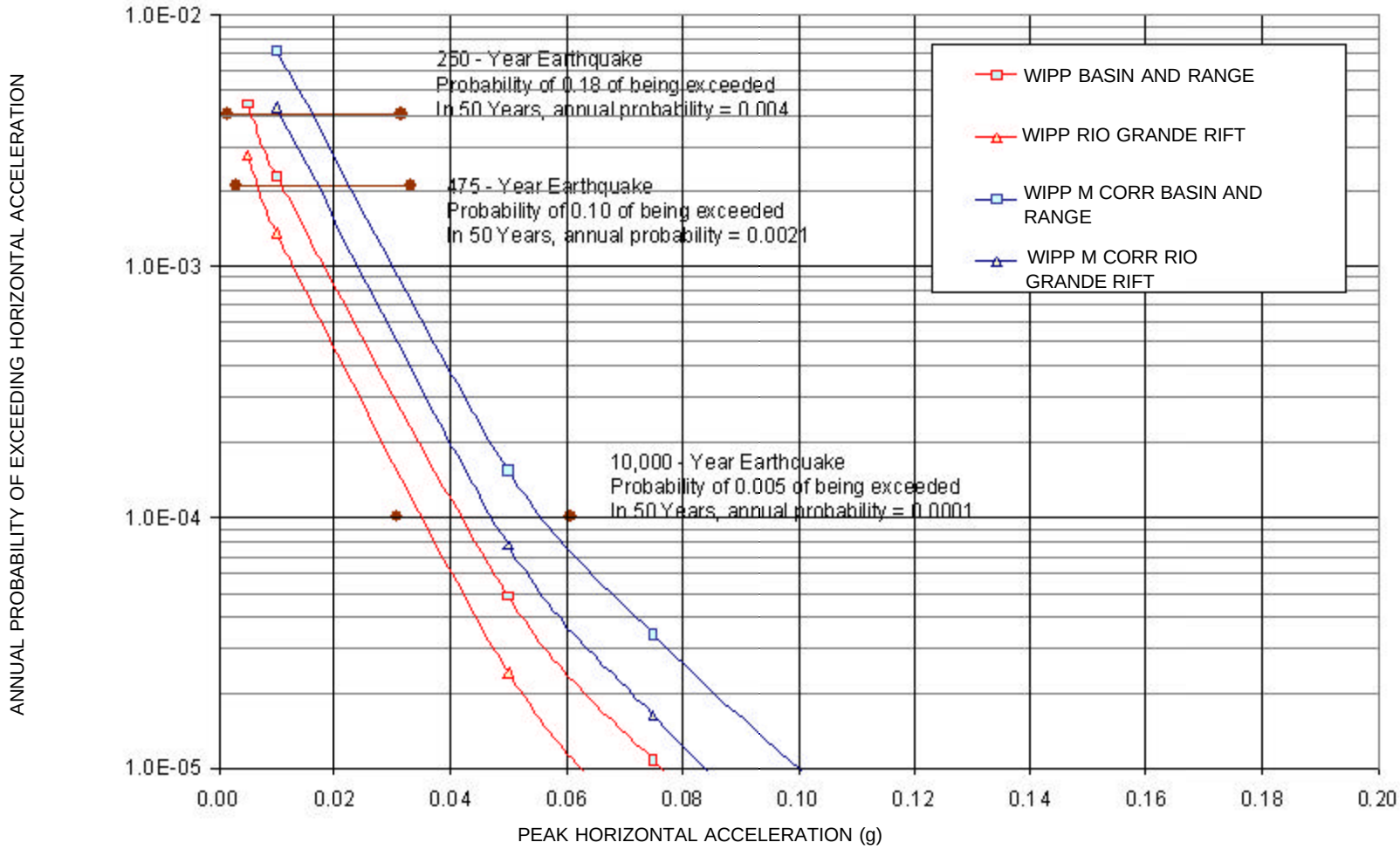

REFERENCE NUMBER
2Figures3.2.dwg

FIGURE 3.2-28

SEISMIC HAZARD AT THE NEF SITE FROM RIO GRANDE RIFT SEISMIC SOURCES

REVISION DATE: DECEMBER 2003

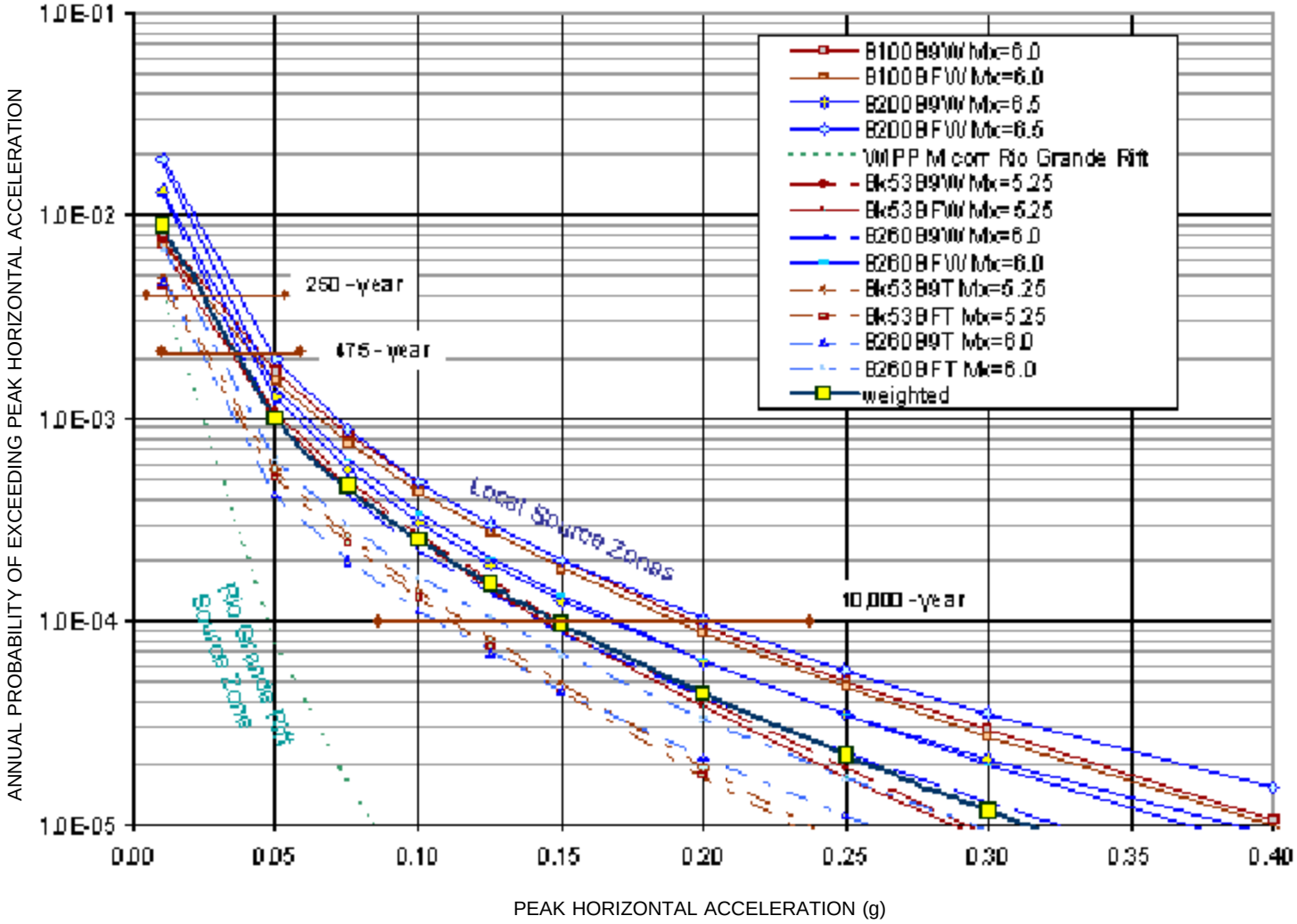

FIGURE 3.2-29

SEISMIC HAZARD AT THE NEF SITE FROM LOCAL SEISMIC SOURCE ZONES

REFERENCE NUMBER
2Figures3.2.dwg

REVISION DATE: DECEMBER 2003

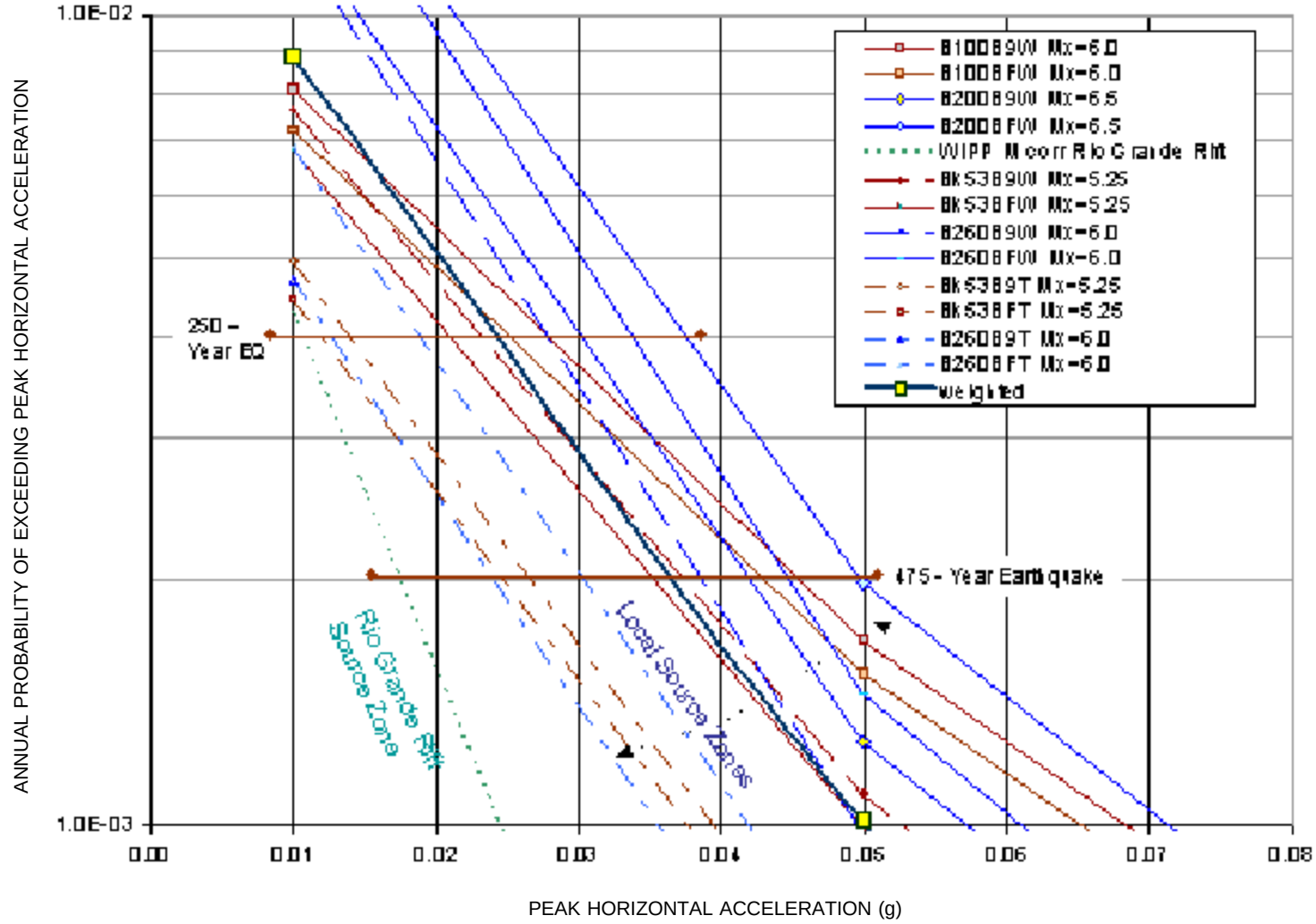

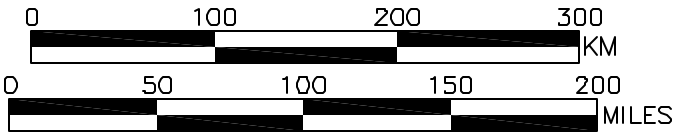

REFERENCE NUMBER
2Figures3.2.dwg

FIGURE 3.2-30

ZOOM OF SEISMIC HAZARD AT THE NEF SITE FROM LOCAL SEISMIC SOURCE ZONES

REVISION DATE: DECEMBER 2003

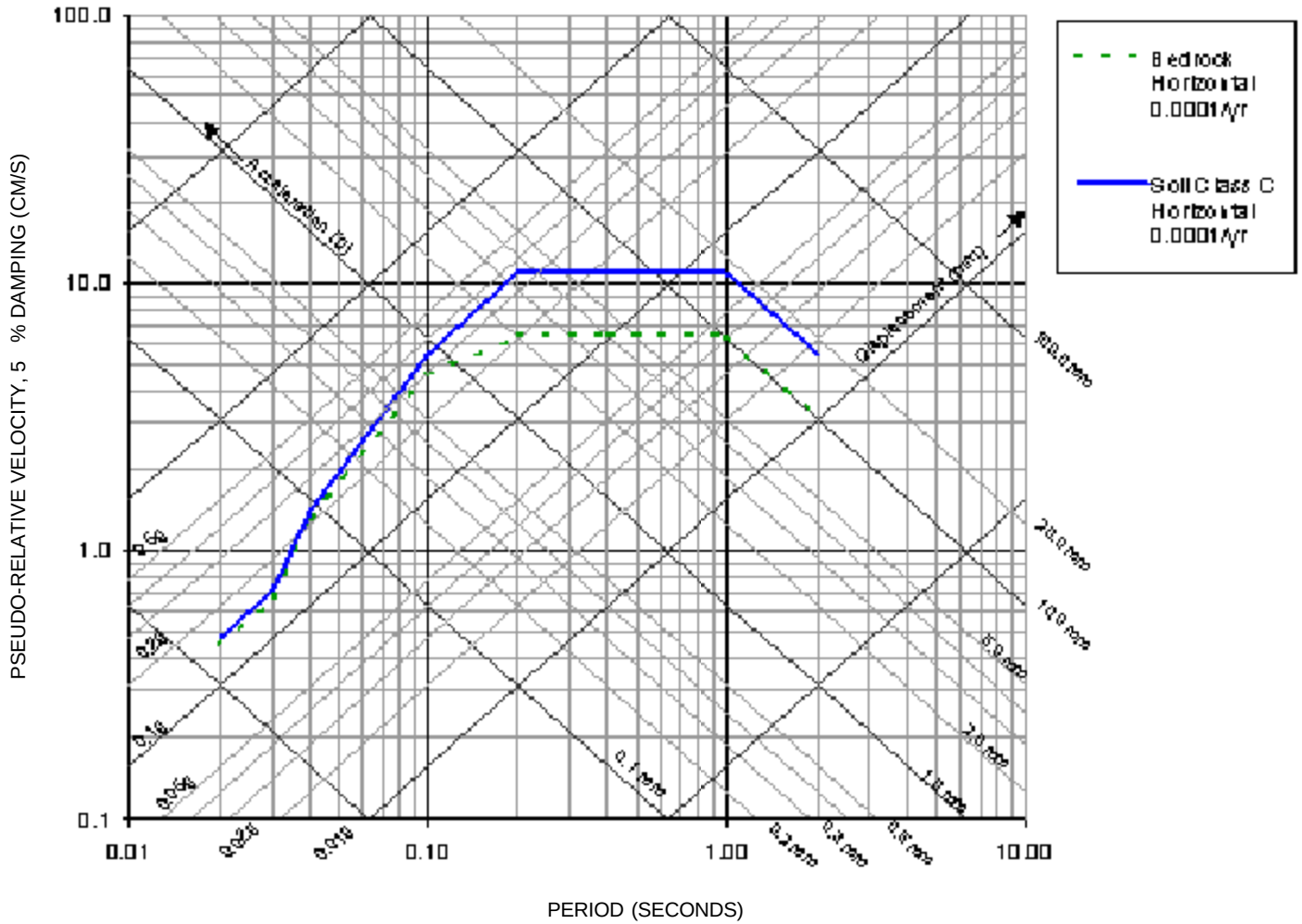

REFERENCE NUMBER
2Figures3.2.dwg

FIGURE 3.2-31
HORIZONTAL RESPONSE SPECTRA FOR THE 10,000-YEAR EARTHQUAKE – BEDROCK AND SOIL CLASS C FOR THE NEF SITE

REVISION DATE: DECEMBER 2003

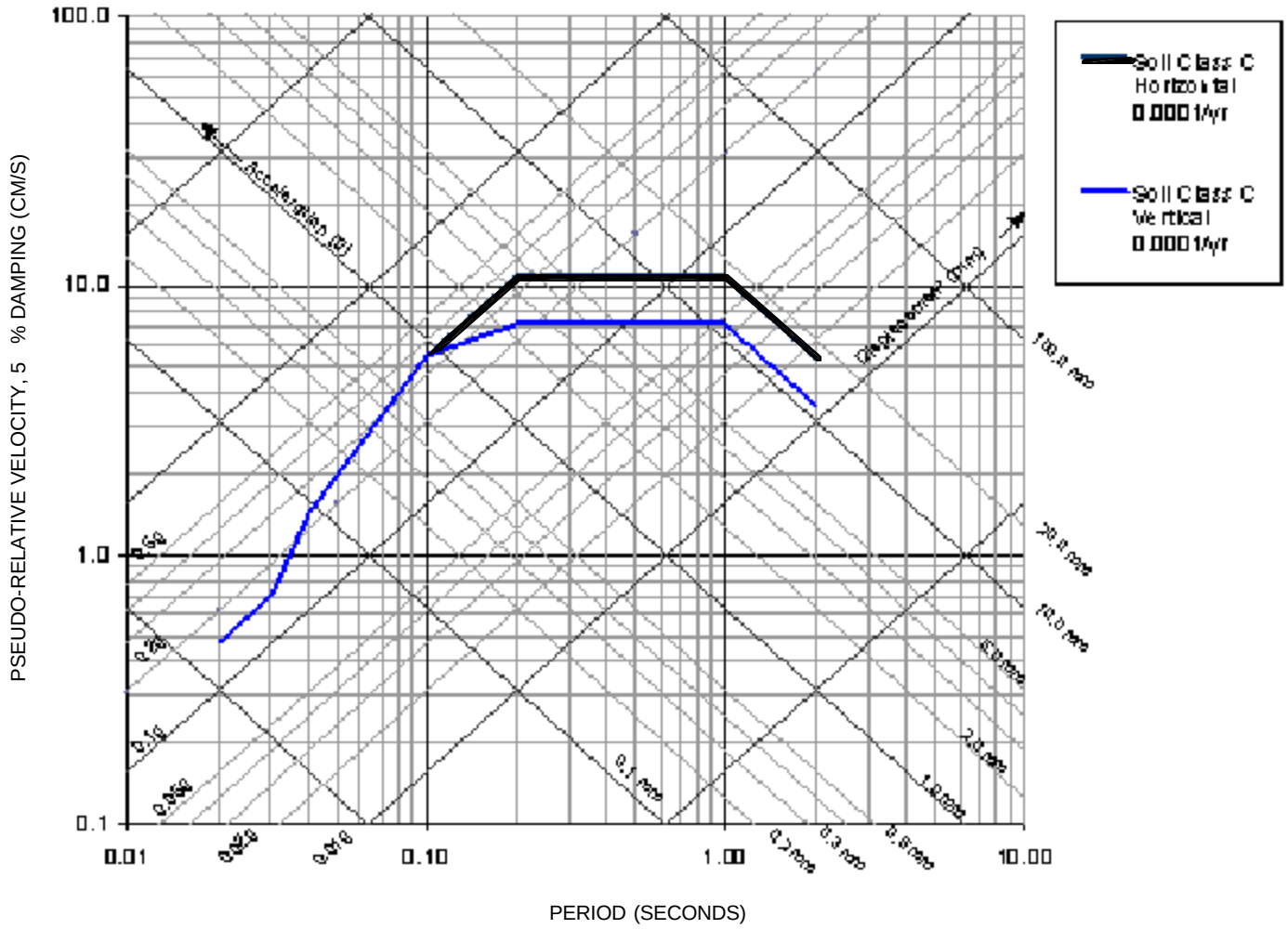

REFERENCE NUMBER
2Figures3.2.dwg

FIGURE 3.2-32
HORIZONTAL AND VERTICAL RESPONSE SPECTRA
FOR THE 10,000-YEAR EARTHQUAKE
SOIL CLASS C FOR THE NEF SITE

REVISION DATE: DECEMBER 2003

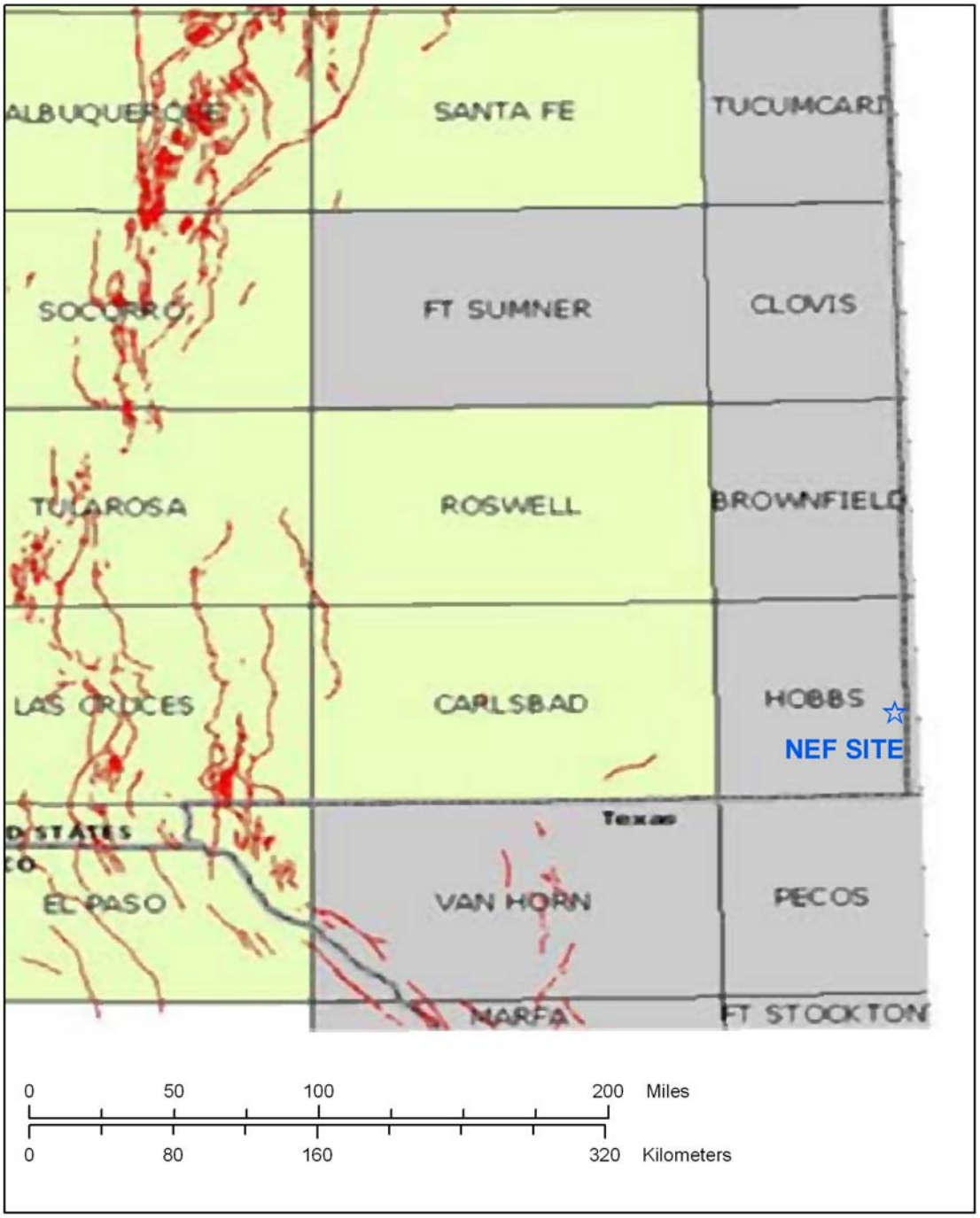

2

SOURCE: Earthquake Hazards Program
Quaternary Fault and Fold Database
(USGS, 2004)

FIGURE 3.2-33

QUATERNARY FAULTS
IN NEW MEXICO

REVISION 2 DATE: JULY 2004

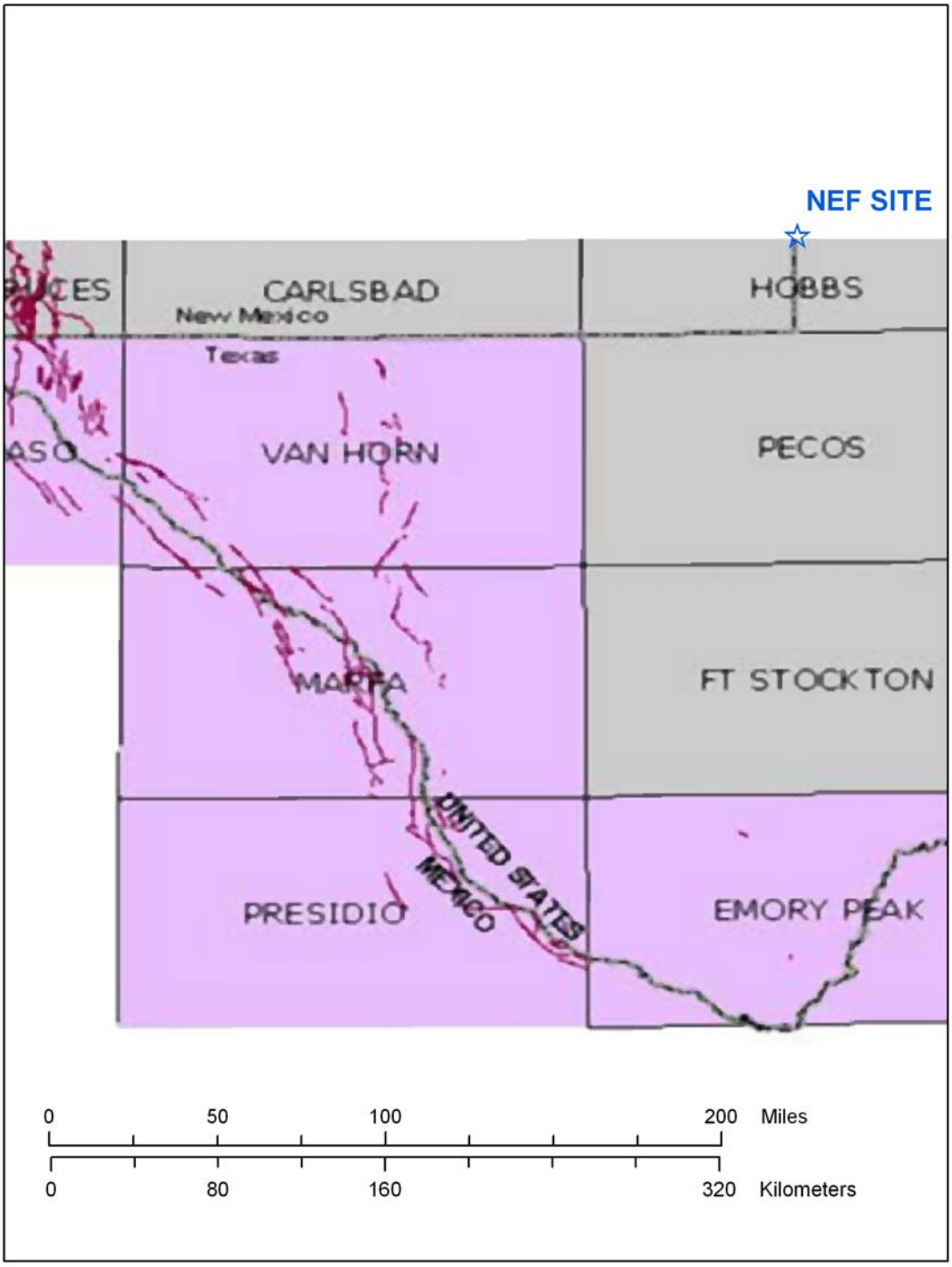

2

SOURCE: Earthquake Hazards Program Quaternary Fault and Fold Database (USGS, 2004)

FIGURE 3.2-34

QUATERNARY FAULTS IN TEXAS

REVISION 2 DATE: JULY 2004

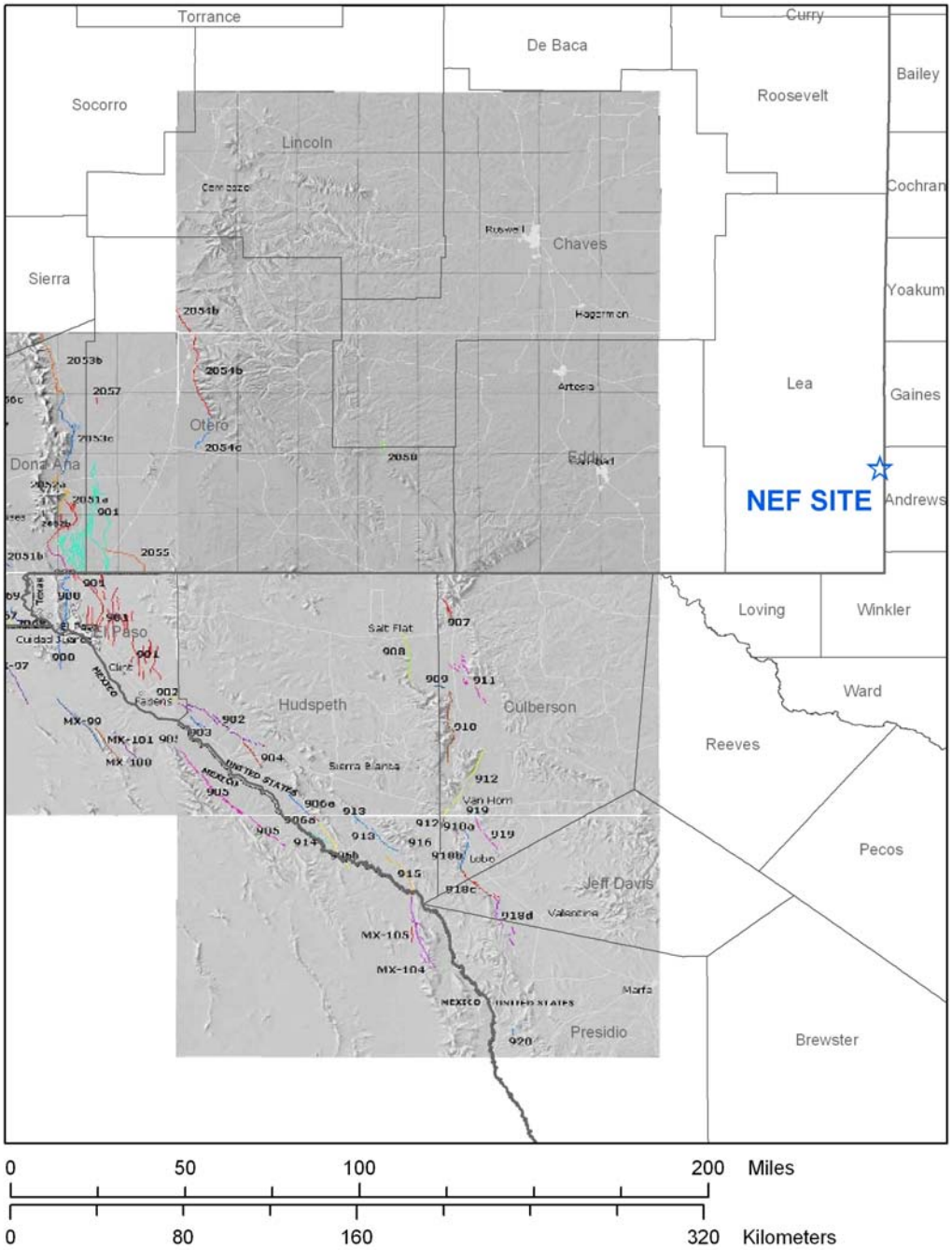

2

SOURCE: USGS, 2004; Machette, 2000

FIGURE 3.2-35

QUATERNARY FAULTS
WITHIN 322 km (200 mi) OF NEF SITE

REVISION 2 DATE: JULY 2004

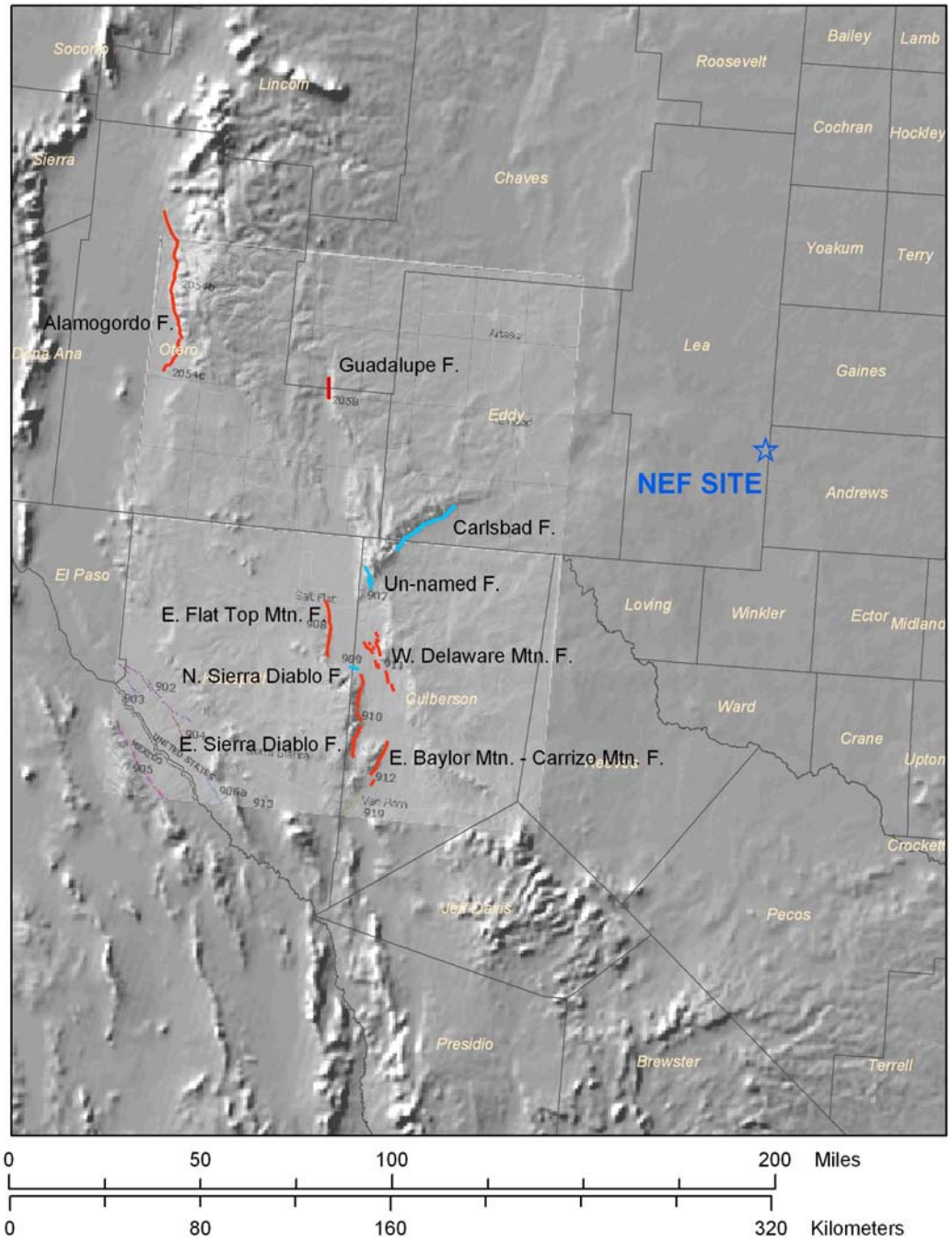

2

NOTE: Locations of nearest capable faults (red traces) and older faults (blue traces)

FIGURE 3.2-36

LOCATIONS OF NEAREST FAULTS TO THE NEF SITE

REVISION 2 DATE: JULY 2004